

## **INFORMATION TO USERS**

**This manuscript has been reproduced from the microfilm master. UMI films the text directly from the original or copy submitted. Thus, some thesis and dissertation copies are in typewriter face, while others may be from any type of computer printer.**

**The quality of this reproduction is dependent upon the quality of the copy submitted. Broken or indistinct print, colored or poor quality illustrations and photographs, print bleedthrough, substandard margins, and improper alignment can adversely affect reproduction.**

**In the unlikely event that the author did not send UMI a complete manuscript and there are missing pages, these will be noted. Also, if unauthorized copyright material had to be removed, a note will indicate the deletion.**

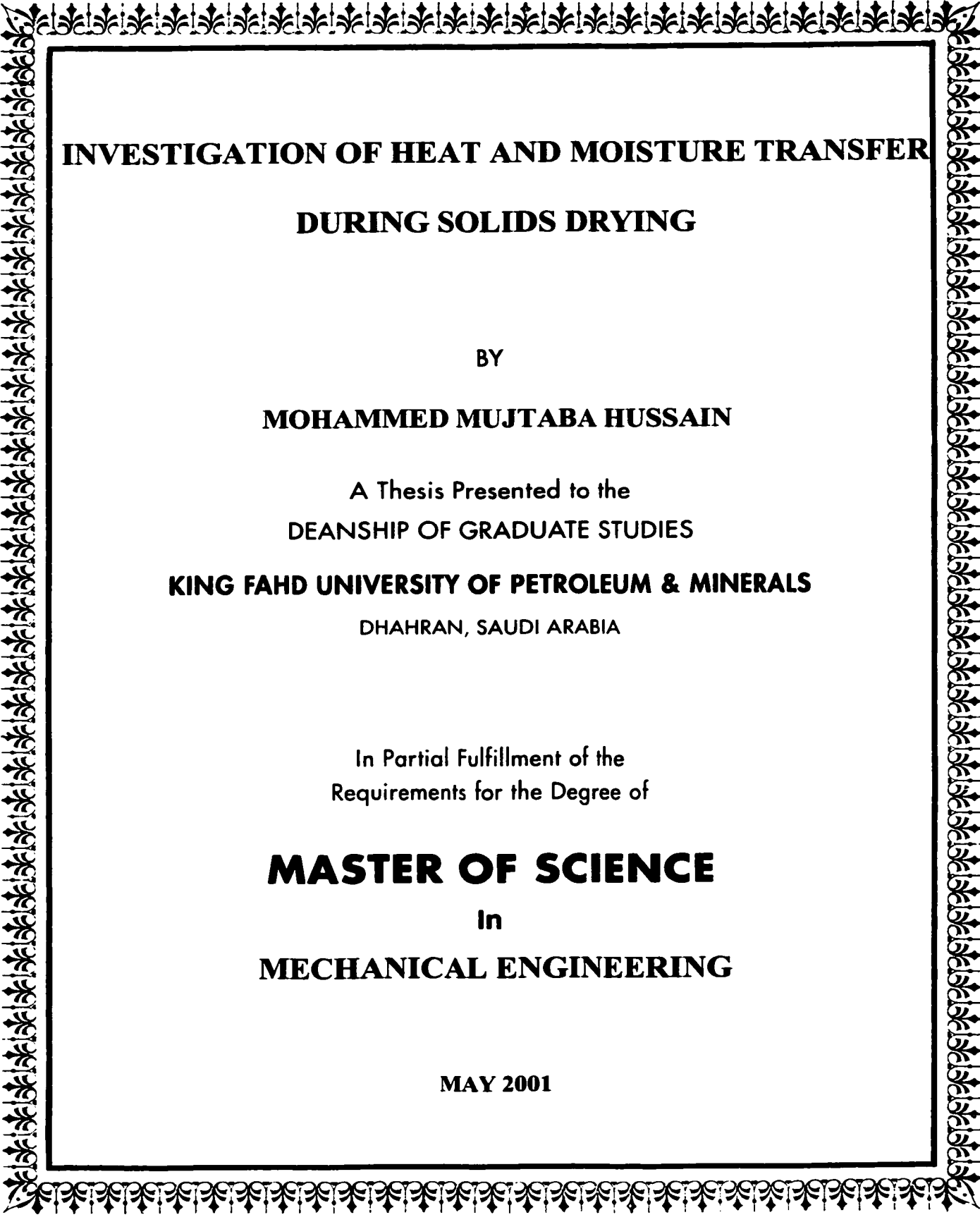
**Oversize materials (e.g., maps, drawings, charts) are reproduced by sectioning the original, beginning at the upper left-hand corner and continuing from left to right in equal sections with small overlaps.**

**Photographs included in the original manuscript have been reproduced xerographically in this copy. Higher quality 6" x 9" black and white photographic prints are available for any photographs or illustrations appearing in this copy for an additional charge. Contact UMI directly to order.**

**ProQuest Information and Learning  
300 North Zeeb Road, Ann Arbor, MI 48106-1346 USA  
800-521-0600**

**UMI<sup>®</sup>**





**INVESTIGATION OF HEAT AND MOISTURE TRANSFER  
DURING SOLIDS DRYING**

BY

**MOHAMMED MUJTABA HUSSAIN**

A Thesis Presented to the  
DEANSHIP OF GRADUATE STUDIES

**KING FAHD UNIVERSITY OF PETROLEUM & MINERALS**

DHAHRAN, SAUDI ARABIA

In Partial Fulfillment of the  
Requirements for the Degree of

**MASTER OF SCIENCE**  
In  
**MECHANICAL ENGINEERING**

**MAY 2001**

**UMI Number: 1407213**

**UMI<sup>®</sup>**

---

**UMI Microform 1407213**

**Copyright 2002 by ProQuest Information and Learning Company.  
All rights reserved. This microform edition is protected against  
unauthorized copying under Title 17, United States Code.**

---


**ProQuest Information and Learning Company  
300 North Zeeb Road  
P.O. Box 1346  
Ann Arbor, MI 48106-1346**


**KING FAHD UNIVERSITY OF PETROLEUM AND MINERALS  
DHAHRAN 31261, SAUDI ARABIA**

**DEANSHIP OF GRADUATE STUDIES**

*This thesis, written by **MOHAMMED MUJTABA HUSSAIN** under the direction of his Thesis Advisor and approved by his Thesis Committee, has been presented to and accepted by the Dean, College of Graduate Studies, in partial fulfillment of the requirements for the degree of **MASTER OF SCIENCE** in **MECHANICAL ENGINEERING**.*

**Thesis Committee**


29/08/2001   
Dr. Ibrahim Dincer (Chairman)

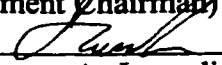
1/09/2001   
Dr. Bekir S. Yilbas (Member)

13/6/1422   
Dr. Abdulghani A. Al-Farayedhi (Member)

1/5/2001   
Dr. P. Gandhidasan (Member)

1-09   
Dr. M. A. M. Antar (Member)

  
Dr. Abdulghani A. Al-Farayedhi  
(Department Chairman)

  
Prof. Osama A. Jannadi  
(Dean of Graduate Studies)

Date: 14/6/1422



***Dedicated to***

***My Beloved Parents***

***Whose constant prayers, sacrifice, and inspiration***

***Led to this accomplishment.***

## **Acknowledgements**

**In the name of ALLAH, the Most Gracious and the Most Merciful.**

*Read in the name of thy Lord and Cherisher, Who created. Created man from a {leech-like} clot. Read and thy Lord is Most Bountiful. He Who taught {the use of} the pen. Taught man that which he knew not. Nay, but man doth transgress all bounds. In that he looketh upon himself as self-sufficient. Verily, to thy Lord is the return {of all}.*

**(The Holy Quran, Surah 96)**

All praises are for ALLAH subhanahu wa ta'ala, the Most Compassionate, the Most Merciful. May peace and blessings be upon our beloved Prophet Muhammad (S.A.W), and his family and his companions. I thank Almighty ALLAH subhanahu wa ta'ala for giving me the knowledge and patience to complete this work.

I acknowledge the support and facilities provided by the King Fahd University of Petroleum and Minerals for this work.

I would like to express my profound gratitude and appreciation to my thesis advisor Dr. Ibrahim Dincer, for his constant help, encouragement, suggestions and guidance throughout the course of this work. I am also greatly indebted to one of my committee member, Dr. Bekir Sami Yilbas for his continuous and endless help, valuable guidance and encouragement in the numerical part of my work.

Thanks are also due to my other thesis committee members Dr. Abdulghani Al-Farayedhi, Dr. Palanichamy Gandhidasan, and Dr. Mohamed Abdelkarim Mohamed Antar for their interest, cooperation, advice and constructive criticisms.

I also wish to acknowledge my friends at KFUPM especially Salman, Baseer, Saif, Imran, Anwar and others for their moral support, good wishes and the memorable days we shared together.

Finally, I thank my parents, brother, and grandmother for their prayers, encouragement, sacrifices and understanding during the course of this work.



# Contents

<b>Acknowledgements</b>	<b>i</b>
<b>List of Tables</b>	<b>vi</b>
<b>List of Figures</b>	<b>viii</b>
<b>Nomenclature</b>	<b>xiv</b>
<b>Abstract (English)</b>	<b>xviii</b>
<b>Abstract (Arabic)</b>	<b>xix</b>
<b>1 INTRODUCTION</b>	<b>1</b>
1.1 Definition of Drying	1
1.2 Background	2
1.3 Periods of Drying	4
1.4 Drying Systems	5
1.4.1 Classifications of Dryers Based on Heat Transfer Method	5
1.4.2 Classifications of Dryers Based on Handling Characteristics and Physical Properties of Wet Material	10
1.5 Objectives of the Present Study	11
1.6 Scope of the Present Work	12
<b>2 LITERATURE REVIEW</b>	<b>14</b>
2.1 Drying Kinetics	14

2.2	Heat and Moisture Transfer Analyses	17
<b>3</b>	<b>MATHEMATICAL ANALYSIS</b>	<b>21</b>
3.1	Analytical Modeling of Heat and Moisture Transfer	21
3.1.1	1-D Slab Object	22
3.1.2	1-D Cylindrical Object	25
3.1.3	1-D Spherical Object	27
3.2	Numerical Modeling of Heat and Moisture Transfer	28
3.2.1	2-D Slab Object	29
3.2.2	2-D Cylindrical Object	35
3.2.3	2-D Spherical Object	39
3.3	Development of New Drying Correlations	43
<b>4</b>	<b>RESULTS AND DISCUSSION</b>	<b>48</b>
4.1	Results of Analytical Heat and Moisture Transfer Analyses	48
4.1.1	1-D Slab Object	48
4.1.2	1-D Cylindrical Object	53
4.1.3	1-D Spherical Object	55
4.2	Results of Numerical Heat and Moisture Transfer Analyses	57
4.2.1	2-D Rectangular Slab	57
4.2.2	2-D Cylindrical Object	70
4.2.3	2-D Spherical Object	82
4.3	Results of New Drying Correlations	90
4.3.1	Biot Number-Reynolds Number ( $Bi_m$ -Re) Correlation	90

4.3.2	Verification of Biot Number-Reynolds Number ( $Bi_m-Re$ )	
	Correlation	90
4.3.3	Biot Number-Dincer Number ( $Bi_m-Di$ ) Correlation	94
4.3.4	Verification of Biot Number-Dincer Number ( $Bi_m-Di$ )	
	Correlation	95
4.3.5	Biot Number-Lag Factor ( $Bi_m-G$ ) Correlation	98
4.3.6	Verification of Biot Number-Lag Factor ( $Bi_m-G$ )	
	Correlation	98
4.3.7	Biot Number-Drying Coefficient ( $Bi_m-S$ ) Correlation	102
4.3.8	Verification of Biot Number-Drying Coefficient ( $Bi_m-S$ )	
	Correlation	103
<b>5</b>	<b>CONCLUSIONS AND RECOMMENDATIONS</b>	<b>107</b>
5.1	Conclusions	107
5.2	Recommendations	109
	<b>REFERENCES</b>	<b>110</b>
	<b>VITA</b>	<b>115</b>

## List of Tables

4.1	Drying conditions and properties of apple slab used in the simulation	49
4.2	Thermophysical properties and drying conditions used in the simulation of rectangular slab	57
4.3	Experimental drying conditions and product properties	69
4.4	Thermophysical properties and drying conditions used in the simulation of cylindrical object	71
4.5	Thermophysical properties and drying conditions used in the simulation of spherical object	82
4.6	Drying conditions of the experiments used for validation in $Bi_m$ -Re correlation development	91
4.7	Obtained drying process and moisture transfer parameters for the samples used in $Bi_m$ -Re correlation development	91
4.8	Drying conditions of the experiments used for validation in $Bi_m$ -Di correlation development	95
4.9	Obtained drying process and moisture transfer parameters for the samples used in $Bi_m$ -Di correlation development	96
4.10	Drying conditions of the experiments used for validation in $Bi_m$ -G correlation development	99

<b>4.11</b>	<b>Obtained drying process and moisture transfer parameters for the samples used in <math>Bi_m</math>-G correlation development</b>	<b>99</b>
<b>4.12</b>	<b>Drying conditions of the experiments used for validation in <math>Bi_m</math>-S correlation development</b>	<b>103</b>
<b>4.13</b>	<b>Obtained drying process and moisture transfer parameters for the samples used in <math>Bi_m</math>-S correlation development</b>	<b>104</b>

# List of Figures

1.1	Periods of drying	4
3.1	Numerical grid for a slab object	32
3.2	Numerical grid for an axisymmetric cylindrical object	37
3.3	Numerical grid for a spherical object	41
4.1	Temperature distribution within a slab object at different locations	50
4.2	Temperature gradient with respect to time in a slab object	50
4.3	Temperature distributions inside a slab object at different drying periods	51
4.4	Temperature gradient inside a slab object at different drying periods	51
4.5	Moisture content distribution within a slab object at different locations	52
4.6	Moisture gradient with respect to time in a slab object	53
4.7	Dimensionless temperature distribution inside the cylindrical object of different radii	54
4.8	Dimensionless moisture distribution inside the cylindrical object of different radii	54
4.9	Dimensionless temperature distribution inside the spherical object of different radii	55
4.10	Dimensionless moisture distribution inside the spherical object of different radii	56
4.11	Temperature distribution inside a slab object after 100 s	59
4.12	3-D plot showing temperature distribution inside a slab object after 100 s	59
4.13	Temperature distribution inside a slab object after 200 s	60

4.14	3-D plot showing temperature distribution inside a slab object after 200 s	60
4.15	Temperature distribution inside a slab object after 300 s	61
4.16	3-D plot showing temperature distribution inside a slab object after 300 s	61
4.17	Variation of reduced center temperature in a slab object for different heat transfer coefficients	62
4.18	Variation of reduced surface temperature in a slab object for different heat transfer coefficients	62
4.19	Variation of reduced center temperature gradient in a slab object for different heat transfer coefficients	63
4.20	Variation of reduced surface temperature gradient in a slab object for different heat transfer coefficients	63
4.21	Moisture distribution inside a slab object after 100 s	65
4.22	3-D plot showing moisture distribution inside a slab object after 100 s	65
4.23	Moisture distribution inside a slab object after 200 s	66
4.24	3-D plot showing moisture distribution inside a slab object after 200 s	66
4.25	Moisture distribution inside a slab object after 300 s	67
4.26	3-D plot showing moisture distribution inside a slab object after 300 s	67
4.27	Variation of reduced center and surface moisture content in a slab object with time	68
4.28	Drying rate variation with time in a slab object	68
4.29	Measured and calculated center temperature distribution in a slab object	69
4.30	Measured and calculated center moisture content distribution in a slab object	70

4.31	Temperature distribution inside a cylindrical object after 100 s	72
4.32	3-D plot showing temperature distribution inside a cylindrical object after 100 s	73
4.33	Temperature distribution inside a cylindrical object after 200 s	73
4.34	3-D plot showing temperature distribution inside a cylindrical object after 200 s	74
4.35	Temperature distribution inside a cylindrical object after 300 s	74
4.36	3-D plot showing temperature distribution inside a cylindrical object after 300 s	75
4.37	Variation of reduced center temperature in a cylindrical object for different heat transfer coefficients	75
4.38	Variation of reduced surface temperature in a cylindrical object for different heat transfer coefficients	76
4.39	Variation of reduced center temperature gradient in a cylindrical object for different heat transfer coefficients	76
4.40	Variation of reduced surface temperature gradient in a cylindrical object for different heat transfer coefficients	77
4.41	Moisture distribution inside a cylindrical object after 100 s	78
4.42	Moisture distribution inside a cylindrical object after 200 s	78
4.43	Moisture distribution inside a cylindrical object after 300 s	79
4.44	Variation of reduced center and surface moisture content in a cylindrical object with time	79
4.45	Drying rate variation with time in a cylindrical object	80



4.46	Comparison between the measured and calculated dimensionless temperature distribution in a cylindrical object	80
4.47	Comparison between the measured and calculated dimensionless moisture content in a cylindrical object	81
4.48	Variation of reduced center temperature in a spherical object for different heat transfer coefficients	84
4.49	Variation of reduced surface temperature in a spherical object for different heat transfer coefficients	84
4.50	Variation of reduced center temperature gradient in a spherical object for different heat transfer coefficients	85
4.51	Variation of reduced surface temperature gradient in a spherical object for different heat transfer coefficients	85
4.52	Variation of reduced temperature along radius in a spherical object for different drying periods	86
4.53	Reduced moisture distribution at the center and surface of a sphere object	86
4.54	Drying rate variation with time in a spherical object	87
4.55	Variation of reduced moisture content along radius in a spherical object at different time periods	88
4.56	Comparison between the calculated and measured dimensionless temperature distribution in a spherical object	88
4.57	Comparison between the calculated and measured dimensionless moisture content in a spherical object	89

4.58	<b>Bi<sub>m</sub>-Re diagram for food products subjected to drying</b>	90
4.59	<b>Measured and predicted dimensionless moisture distributions using Bi<sub>m</sub>-Re correlation for a slab object</b>	92
4.60	<b>Measured and predicted dimensionless moisture distributions using Bi<sub>m</sub>-Re correlation for a cylindrical object</b>	93
4.61	<b>Measured and predicted dimensionless moisture distributions using Bi<sub>m</sub>-Re correlation for a spherical object</b>	93
4.62	<b>Bi<sub>m</sub>-Di diagram for food products subjected to drying</b>	94
4.63	<b>Measured and predicted dimensionless moisture distributions using Bi<sub>m</sub>-Di correlation for a slab object</b>	96
4.64	<b>Measured and predicted dimensionless moisture distributions using Bi<sub>m</sub>-Di correlation for a cylindrical object</b>	97
4.65	<b>Measured and predicted dimensionless moisture distributions using Bi<sub>m</sub>-Di correlation for a spherical object</b>	97
4.66	<b>Bi-G diagram for food products subjected to drying</b>	98
4.67	<b>Measured and predicted dimensionless moisture distributions using Bi<sub>m</sub>-G correlation for a slab object</b>	100
4.68	<b>Measured and predicted dimensionless moisture distributions using Bi<sub>m</sub>-G correlation for a cylindrical object</b>	101
4.69	<b>Measured and predicted dimensionless moisture distributions using Bi<sub>m</sub>-G correlation for a spherical object</b>	101
4.70	<b>Bi<sub>m</sub>-S diagram for food products subjected to drying</b>	102
4.71	<b>Measured and predicted dimensionless moisture distributions</b>	

	<b>using <math>Bi_m</math>-S correlation for a slab object</b>	<b>104</b>
<b>4.72</b>	<b>Measured and predicted dimensionless moisture distributions</b>	
	<b>using <math>Bi_m</math>-S correlation for a cylindrical object</b>	<b>105</b>
<b>4.73</b>	<b>Measured and predicted dimensionless moisture distributions</b>	
	<b>using <math>Bi_m</math>-S correlation for a spherical object</b>	<b>105</b>

## NOMENCLATURE

<b>a</b>	constant
<b>A<sub>1</sub></b>	constant ( $\exp((0.2533Bi_m)/(1.3 + Bi_m))$ )
<b>A<sub>mn</sub></b>	constant
<b>A<sub>n</sub></b>	constant
<b>b</b>	constant
<b>B<sub>1</sub></b>	constant ( $\exp(-\mu_1^2 Fo_m)$ )
<b>B<sub>mn</sub></b>	constant
<b>B<sub>n</sub></b>	constant
<b>Bi</b>	Biot number for heat transfer, $\frac{h Y}{k}$ (dimensionless)
<b>Bi<sub>m</sub></b>	Biot number for moisture transfer, $\frac{h_m Y}{D}$ (dimensionless)
<b>c</b>	constant
<b>c<sub>p</sub></b>	specific heat capacity at constant pressure (J/kg K)
<b>d</b>	constant
<b>D</b>	moisture diffusivity (m <sup>2</sup> /s)
<b>D<sub>o</sub></b>	pre-exponential factor of Arr-henius equation (m <sup>2</sup> /s)
<b>Di</b>	Dincer number, $\frac{U}{SY}$ (dimensionless)
<b>e</b>	constant
<b>erfc</b>	complimentary error function
<b>f</b>	constant

- Fo** Fourier number for heat transfer,  $\frac{\alpha t}{Y^2}$  (dimensionless)
- Fo** Fourier number for moisture transfer,  $\frac{Dt}{Y^2}$  (dimensionless)
- g** constant
- G** lag factor (dimensionless)
- h** heat transfer coefficient (W/m<sup>2</sup>K); constant
- h<sub>m</sub>** moisture transfer coefficient (m/s)
- J<sub>0</sub>** Bessel function of zero order
- k** thermal conductivity (W/mK)
- l** half thickness (m)
- m** number of mesh points of the numerical grid in x- direction for slab, in z-direction for cylinder and in r-direction for sphere
- M** moisture content (kg/kg, db)
- $\overline{M}$  laplace of M ( $\ell(M)$ )
- M\*** reduced (dimensionless) moisture content,  $\frac{M - M_d}{M_i - M_d}$
- n** number of mesh points of the numerical grid in y-direction for slab, in r-direction for cylinder and in  $\phi$ -direction for sphere
- r** radial coordinate
- RH** relative humidity (kg/kg, db or %)
- R** radius of cylinder & sphere (m)
- Re** Reynolds number,  $\frac{2UY}{\nu}$  (dimensionless)
- S** drying coefficient (1/s)

<b>t</b>	<b>time (s)</b>
<b>T</b>	<b>temperature (K)</b>
$\bar{T}$	<b>laplace of T (<math>\ell(T)</math>)</b>
<b>T*</b>	<b>reduced (dimensionless) temperature, <math>\frac{T - T_i}{T_d - T_i}</math></b>
<b>U</b>	<b>velocity of the drying air (m/s)</b>
<b>x</b>	<b>coordinate</b>
<b>y</b>	<b>coordinate</b>
<b>Y</b>	<b>characteristic dimension (l for slab, r for cylinder and sphere) (m)</b>
<b>z</b>	<b>coordinate</b>

### **Greek Symbols**

$\alpha$	<b>thermal diffusivity (<math>\text{m}^2/\text{s}</math>)</b>
$\beta$	<b>ratio of heat transfer coefficient to thermal conductivity (h/k)</b>
$\beta_m$	<b>ratio of moisture transfer coefficient to moisture diffusivity (<math>\text{h}_m/D</math>)</b>
$\mu_1$	<b>first characteristic root (dimensionless)</b>
$\nu$	<b>dynamic viscosity (<math>\text{m}^2/\text{s}</math>)</b>
$\rho$	<b>density (<math>\text{kg}/\text{m}^3</math>)</b>
$\varphi$	<b>spherical polar coordinate; moisture difference <math>M - M_d</math> (kg/kg, db)</b>
$\phi$	<b>temperature difference <math>T - T_d</math> (K)</b>
$\Phi$	<b>dimensionless moisture distribution, <math>\frac{M - M_e}{M_i - M_e}</math></b>
$\theta$	<b>dimensionless temperature distribution, <math>\frac{T - T_i}{T_d - T_i}</math></b>

**Subscripts**

- d**     **drying air**
- e**     **equilibrium**
- i**     **initial**
- n**     **1,2,3...**

## THESIS ABSTRACT

**Name:** MOHAMMED MUJTABA HUSSAIN

**Title:** INVESTIGATION OF HEAT AND MOISTURE  
TRANSFER DURING SOLIDS DRYING

**Major Field:** MECHANICAL ENGINEERING

**Date of Degree:** May 2001

*In the present study, analytical and numerical analysis of the heat and moisture transfer during drying of food products of regular geometries is carried out. The analysis is based on fundamental laws of heat conduction and moisture diffusion. Analytical models of heat conduction and moisture diffusion for one-dimensional rectangular slab, cylinder and sphere are examined for drying applications. Two-dimensional analysis of heat and moisture transfer of regular shaped products subjected to drying is carried out using explicit finite-difference scheme. Computer programs are developed to determine the temperature and moisture distributions inside the products subjected to drying. Moreover, the results predicted are compared with the experimental data obtained from the literature and it is found that they are in good agreement.*

*New drying correlations in terms of drying process parameters and moisture transfers parameters are developed. The development of new correlations is based on experimental drying data taken from various sources in the literature. In addition, the moisture distribution profiles obtained from the correlations developed are validated using the experimental drying profiles available in the literature.*

Master of Science Degree

King Fahd University of Petroleum and Minerals  
Dhahran, Saudi Arabia.

Rabi'I 1422.

May 2001.



## خلاصة الرسالة

الإسم	:	محمد مجتبی حسین
العنوان	:	دراسة انتقال الحرارة والرطوبة خلال عمليات تجفيف الجوامد
التخصص	:	هندسة ميكانيكية
تاريخ الشهادة	:	ربيع الأول ١٤٢٢

هذا البحث يتناول تحليليا وعدديا توصيل الحرارة وانتشار الرطوبة في اثناء عمليات تجفيف المنتجات

الغذائية منتظمة الأشكال . يعتمد البحث على القوانين الأساسية لتوصيل الحرارة وانتشار الرطوبة .

تم اختيار نماذج توصيل الحرارة وانتشار الرطوبة لصفحة أحادية البعد واسطوانة وكرة في تطبيقات التجفيف . تم

التحليل ثنائي البعد لتوصيل الحرارة وانتشار الرطوبة لمنتجات منتظمة الأشكال عرضت للتجفيف باستخدام طريقة

الفرق الثابت . تم تطوير برامج حاسوبية لإيجاد درجة الحرارة وتوزيع الرطوبة داخل المنتجات المعرضة للتجفيف .

علاوة على ذلك تمت مقارنة النتائج مع البيانات التجريبية الموجودة في بعض مانشر حيث وجد أنها متوافقة .

تم تطوير علاقة ارتباط جديدة للتجفيف بالنسبة لعوامل عملية التجفيف وانتقال الرطوبة حيث اعتمد في ذلك على

البيانات التجريبية التي أخذت من مصادر مختلفة . بالإضافة إلى ذلك تم التحقق من صحة توزيع الرطوبة المتحصل

عليه من علاقة الارتباط باستخدام النتائج التجريبية في البحوث المنشورة .

ماجستير في العلوم

جامعة الملك فهد للبترول والمعادن

الظهران / المملكة العربية السعودية

# **CHAPTER 1**

## **INTRODUCTION**

### **1.1. Definition of Drying**

Drying is a process of thermally removing volatile substances such as moisture to yield a solid product. Mechanical methods of separating a liquid from a solid are not considered to be drying. When a wet solid is subjected to drying, two processes occur simultaneously:

**Process I:** Transfer of energy in the form of heat from the surrounding environment to evaporate the surface moisture.

**Process II:** Transfer of internal moisture to the surface of the solid and its subsequent evaporation due to process I

The rate at which drying is accomplished is governed by the rate at which the two processes proceed. In the first process, energy (heat) transfer from the surrounding to the wet solid can be due to convection, conduction, radiation or combination of any of these mechanisms. In common practice, heat is transferred to the surface of the wet solid and then to the interior. However, in di-electric, radio frequency or microwave freeze-drying, heat is supplied internally within the solid and flows to the exterior surfaces.

Process I depends on the external conditions such as temperature, air humidity and flow conditions, area of exposed surface, and pressure. Whereas, process II, i.e., the movement of internal moisture within the solid is a function of physical nature of the

solid, the temperature, and its moisture content. The parameters on which process I and II depends, act as the limiting factors governing the rate and total time of drying.

## **1.2. Background**

Drying is considered as one of the most widely used energy intensive unit operations in the industry. No other unit operation exists capable of handling such a large variety of products ranging from paper through textiles to food. It accounts for about 25% of the total national industrial energy consumption in the developed countries (Mujumdar, 1999). The diversity and diffusivity problems related to drying in combination with its complexity resulted in a greater scientific interest over the last decade with more emphasis on minimizing energy consumption and maximizing product quality.

The dehydration of fruits and vegetables prevents the growth and reproduction of micro-organisms causing decay and minimizes many of the moisture mediated deteriorative reactions. The micro-organisms are almost inactive, when the moisture content is reduced to about 10%. And in food products, it is essential to reduce the moisture content below 5% in order to preserve flavor and nutrition. Drying also brings about substantial reduction in weight and volume minimizing packing, storage, and transportation costs and enables storability and shipment of products under ambient conditions.

Sharp rise in energy costs has promoted a dramatic upsurge in interest in drying worldwide over the last few years. Advances in techniques and development of novel drying methods have made available a wide range of dehydrated products, especially instantly re-constitutable ingredients, from fruits and vegetables with properties that could

not have been foreseen some years ago and the growth of fast foods have fueled the need for such ingredients. Due to changing life styles especially in the developed world, there is now a great demand for a wide variety of dried products with high quality and freshness. This calls for sustained basic research on drying process, operating conditions and dryers and their influence on energy consumption and food quality.

One of the major concerns in the drying process is the provision of optimum processing conditions for good quality products, which can be made possible by analyzing the internal moisture transfer and moisture transfer parameters in terms of moisture diffusivity and moisture transfer coefficient. Accurate determination of moisture transfer parameters is important in order to attain a good quality dried products leading to energy savings. Decreasing energy consumption in the drying process will decrease the environmental impact in terms of pollutants and hence protect the environment (Dincer, 1998).

The most important aspect of drying technology is the mathematical modeling of the drying processes and equipment. Its purpose is to allow design engineers to choose the most suitable operating conditions and then size the drying equipment and drying chamber accordingly to meet desired operating conditions. The principle of modeling is based on having a set of mathematical equations, which can adequately characterize the system. The solution of these equations must allow the prediction of the process parameters as a function of time at any point in the dryer based on initial conditions.

### 1.3. Periods of Drying

When a wet solid is subjected to drying, it loses moisture in stages, first by evaporation from a saturated surface of the solid, followed by a period of evaporation from a saturated surface of gradually decreasing area, and finally evaporates in the interior of the solid. These stages (shown in Figure 1.1) are in general referred to as constant rate period and falling rate period, which are summarized as follows:

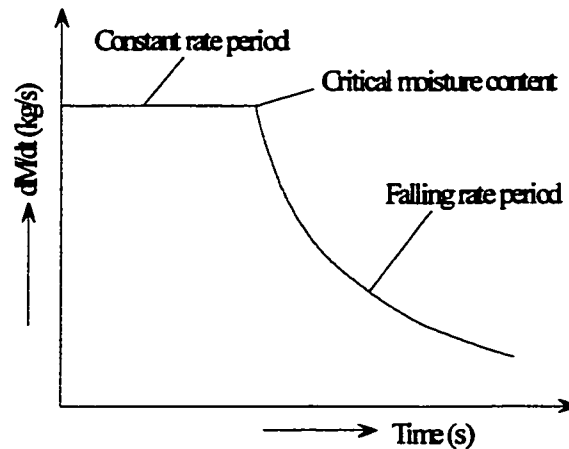


Figure 1.1: Periods of drying

**Constant-rate Period:** It is the drying period during which the rate of water removal per unit drying surface is constant. In this period moisture movement within the solid is rapid enough to maintain a saturated condition at the surface, and the rate of drying is controlled by the rate of heat transferred to the evaporating surface. Drying progresses by means of diffusion of vapor from the saturated surface of the solid across a stagnant air film into the surroundings. This period is highly influenced by the heat and moisture transfer coefficients, area exposed to drying medium, and temperature difference and relative humidity between the gas stream and the wet surface of the solid.

**Falling-rate Period:** It is the drying period during which the instantaneous drying rate continuously decreases. It starts at the critical moisture content when the constant-rate period ends. It is an indication of increased resistance to both heat and moisture transfer. When the initial moisture content is above the critical moisture content, the entire drying process occurs in the constant-rate period. If it is below the critical moisture content, the entire drying process occurs in the falling-rate period. This period is dependent on the factors affecting the diffusion of moisture away from the evaporating surface and those affecting the rate of internal moisture movement.

## **1.4. Drying Systems**

Drying systems can be classified in several ways; but the two most useful classifications are based on:

- i. The method of transferring heat to the wet solids and
- ii. The handling characteristics and physical properties of the wet material.

The first method of classification reveals the differences in dryer design and operation, while the second method is most useful in the selection of a group of dryers for preliminary consideration in a given drying problem.

### **1.4.1. Classification of Dryers Based on Heat Transfer Method**

- **Direct Dryers**

In these dryers heat transfer for drying is obtained by direct contact between the wet solid and hot gases. The vaporized liquid is carried away by the drying medium; i.e., the hot gases. They are also termed as convection dryers. They can be sub-classified as:

- ***Continuous direct dryers***

Operation in these dryers is continued without interruption as long as wet feed is supplied.

They have the following types:

- ***Continuous-tray dryers*** such as continuous metal belts, vibrating trays utilizing hot gases, vertical turbo-dryers.
- ***Continuous sheet dryers***, in which continuous sheet of wet solid passes through the dryer either as festoons or as taut sheet stretched on a fin frame.
- ***Pneumatic conveying dryers***. In this type, drying is performed in conjunction with grinding. Wet solid is conveyed in high temperature high velocity gases to a cyclone collector.
- ***Rotary dryers***. Wet solid in this dryer is conveyed and showered inside a rotating cylinder through which hot gases flow.
- ***Spray dryers***. In this type, fluid is atomized using a rotating wheel or a nozzle, and the spray of droplets comes immediately in contact with a flow of hot drying medium, usually air.
- ***Through-circulation dryers***. Wet solid in this dryer is held on a continuous conveying screen, and hot air is blown through it.
- ***Tunnel dryers***. Wet solid on trucks is moved through a tunnel in contact with hot gases.
- ***Fluid beds***. Solid products are fluidized in a stationary tank and dried while suspended in the upward-moving drying gas.

- ***Batch direct dryers***

They are designed to operate on a definite size of batch of wet feed for given time cycles. In these dryers, the conditions of moisture content and temperature continuously change at any point in the dryer. They have following types:

- *Batch through-circulation dryers.* In this dryer, wet solid is held on screen bottom trays and through which hot air is blown.
- *Tray and compartment dryers.* Solid in this dryer is supported on trays that may or may not be on removable trucks and air is blown across the solid on trays.
- *Fluid beds.* Solid products are fluidized in a stationary cart with filter mounted above.

- **Indirect Dryers**

In this type of dryers, heat for drying is transmitted to the wet solid through a retaining wall. The vaporized liquid is removed independently from the heating medium. Rate of drying depends on the contacting of the wet material with hot surfaces. They are also called as conduction or contact dryers. They are sub-classified as:

- ***Continuous indirect dryers***

In these types of dryers, drying is accomplished by passing the wet solid through the dryer continuously in contact with the hot surface. They have following types:

- *Cylinder dryers.* It is applicable for continuous sheets such as paper, cellophane, and textile piece goods. The cylinders are generally steam-heated and rotate.



- *Drum dryers.* In this dryer, the product to be dried is usually in fluid, slurry, or pastelike form, with the solids in either solution or suspension. The drum surface is heated with steam or hot water.
- *Screw-conveyor dryers.* Although these dryers are continuous, operation under a vacuum is feasible.
- *Steam-tube rotary dryers.* Steam or hot water is used to heat the cylinder and the wet solid is fed into one end of the cylinder and discharge as finished product at the other end.
- *Vibrating-tray dryers.* Heating is accomplished by steam or hot water.
- *Special types* such as a continuous fabric belt moving in close contact with a steam-heated platen. Solid to be dried lies on the belt and receives heat by contact.
- *Batch indirect dryers*

These are generally well suited to operate under vacuum and are divided into agitated and non-agitated types.

- *Agitated-pan dryers.* They can operate under atmosphere or under vacuum, and can handle small production of nearly any form of wet solid, i.e., liquids, slurries, pastes, or granular solids.
- *Freeze dryers.* In these dryers, wet solid is frozen prior to drying and then water is removed as a vapor by sublimation from the frozen solid in a vacuum chamber.
- *Vacuum rotary dryers.* These dryers are heated by condensing steam or by circulating a suitable heating medium through a jacket around the shell and the wet solid is agitated in a horizontal stationary shell. Agitator is also steam heated in addition to the shell. They are used for relatively low temperature operation.

- *Vacuum tray dryers.* Heating in these dryers is accomplished by contact with steam-heated or hot-water-heated shelves on which solid lies.

- **Infrared or Radiant-Heat Dryers**

They consists of a bank of infrared heaters combined side by side in such a way to provide high-density heating of the sheet and the rate of drying depends on the generation, transmission, and absorption of infrared rays. An infrared heater can be electric infrared or gas infrared. The electric infrared is a metal filament in a sealed enclosure whereas gas infrared are gas generating burners consisting of a perforated special ceramic tile, set in a rugged cast iron or ceramic housing, with a special alloy screen grid which protects the tile and also serves as a reradiator and air deflector. The application of infrared heaters are limited to the drying of coatings, owing to high operating costs, i.e., the cost of electrical energy or gas.

- **Dielectric-Heat Dryers**

They operate on the principle of heat generation within the solid by placing the latter in a high frequency electric field. Since the dielectric constants of liquids are much higher than those of solids, the heat developed rises rapidly with increasing moisture content. This property provides a convenient means of attaining a uniform dry product. Dielectric drying systems are used in various industries like textile, paper, food, lumber, automobile tyre etc. due to its characteristics such as reduce drying times, uniformity of drying reduced handling and so on. But due to high capital costs they are used judiciously in conjunction with conventional dryers.

### **1.4.2. Classification of Dryers Based on Handling Characteristics and Physical Properties of Wet Material**

- **Batch Tray Dryers**

A tray or compartment dryer consists of an enclosed, insulated housing in which solids are placed upon tiers of trays in the case of particulate solids or stacked in piles or upon shelves in the case of large objects. Heat transfer can be direct from gas to solids by circulation of large volumes of hot gas or indirect by use of heated shelves, radiator coils, or refractory walls inside the housing. Due to high labor requirements associated with loading and unloading of compartments, batch compartment equipment is often considered to be economical. Moreover, due to the nature of solid gas contacting, which is usually by parallel flow and occasionally by through circulation, heat and moisture transfer are comparatively inefficient. Because of these reasons, the application of tray and compartment dryers is limited to ordinary drying and heat-treating operations.

- **Batch Through-Circulation Dryers**

This type is similar to a standard tray dryer except that hot air passes through the wet solid instead of across it. Heated air passes through a stationary permeable bed of the wet solid placed on removable screen-bottom trays suitably supported in the dryer. In some models, deep perforated bottom trays are placed on top of plenum chambers in a closed-circuit hot-air circulation system.

- **Continuous Tunnel Dryers**

They consist of batch truck or tray compartments operated in series. The solid to be dried is placed in trays or on trucks, which moves through the tunnel in contact with hot gases.

Operation is often semi-continuous; when the tunnel is filled, one truck is removed from the discharge end as each new truck is fed into the inlet end. Continuous tunnel dryers are applicable for all forms of particulate solids and large solid objects, but they are more suitable for large quantity production representing investment and installation savings over multiple batch compartments.

- **Rotary Dryers**

A rotary dryer consists of a cylinder, rotated upon suitable bearings and usually slightly inclined to the horizontal. The length of the cylinder may range from 4 to more than 10 times its diameter, which may vary from less than 0.3 to 3 m. Feed solids fed into one end of the cylinder progress through it by virtue of rotation, head effect, and slope of the cylinder and discharge as finished product at the other end. Gases flowing through the cylinder may retard or increase the rate of solids flow, depending upon whether gas flow is countercurrent or concurrent with solids flow. Rotary dryer is applicable to batch or continuous processing solids which are relatively free flowing and granular when discharged.

## **1.5. Objectives of the Present Study**

The objectives of the present study are:

- Application of one-dimensional analytical models of heat conduction and moisture diffusion during drying of products with regular geometries such as slab, cylinder and sphere.
- Two-dimensional numerical analysis of heat and moisture transfer of regular shaped products subjected to drying using finite-difference method. Analysis

involved development of computer programs to calculate the transient temperature and moisture distribution inside the products.

- Development of new drying correlations to determine the moisture transfer parameters involved in the drying process. The development involves the regression analysis of experimental data available in the literature.

## **1.6. Scope of the Present Work**

In the present study, application of one-dimensional analytical models of heat conduction and moisture diffusion during drying of products with regular geometries is carried out for drying problems. The product geometries studied are slab, cylinder and sphere. The governing equations consist of Fourier heat conduction and Fick's diffusion equations with convective conditions at the free boundaries. Numerical analysis of two-dimensional heat and moisture transfer during drying of products with regular geometries is based on finite-difference approach. The determination of heat and moisture transfer during drying is important for process design, handling practices, quality control and energy savings. Theoretical models and analysis describing the drying process can enhance the understanding of the physical phenomena and moisture transfer distributions and parameters. Temperature dependence moisture diffusivity is used as an Arr-henius like equation. This is because moisture diffusivity varies with time and space, since temperature varies with time and space.

Development of new drying correlations helps in calculating the two important moisture transfer parameters (i.e., moisture diffusivity and moisture transfer coefficient) required in the analysis, design and optimization of drying process. There is little amount

of published data available in the literature for these parameters with a wide variation due to structural complexity of foods and different methods of estimation. An accurate prediction of diffusion parameters is possible by developing new models and methods representing the physical characteristics of the substrates subjected to drying, as it is essential for efficient moisture transfer analysis, leading to optimized energy use and operating conditions, hence efficient drying (Dincer and Dost, 1996). Thus in the present work, we intend to develop new correlations or models which helps in calculating the drying process and moisture transfer parameters in a simple and accurate manner.

## **CHAPTER 2**

### **LITERATURE REVIEW**

This chapter deals with the literature available in the field of drying. The literature in this multi-disciplinary field of drying is very diverse and can be classified into following categories:

1. Drying kinetics
2. Heat and moisture transfer analysis
3. Drying systems and process optimization
4. Solar drying
5. Energy and exergy analyses of drying systems

However, in the present study the first two categories of the above classifications is essential and therefore we will discuss the works carried out by various researchers in the following sections.

#### **2.1. Drying Kinetics**

Drying kinetics is one of the most important aspects of drying process. It describes the mechanism of heat and moisture transport phenomena and investigates the influence of certain process variables on moisture removal process. It is known as the rate at which water can be removed from the initially moist or wet substance. The basic parameters, which influence the kinetics of drying, are temperature and airflow velocity. It forms the

most essential part of the actual mathematical model of any dehydration operation, which seeks a proper estimation of drying time involved as well as the related behavior of all corresponding operational factors playing an important role in the design and optimization of dryers (Krokida et al., 2000).

The kinetics of apricot dehydration was examined by Vagenas et al. (1991) using a  $2^3$  factorial experimental design to evaluate the effect of three parameters such as air temperature, air velocity, and pretreatment of the sample on the drying time and the transport coefficients of apricots at two different levels of temperature, velocity, and pretreatment. They also used finite element method to solve the governing differential equations describing the moisture transfer in the apricot and found the moisture transfer in apricots to be entirely controlled by the external resistance to mass transfer during drying.

Kiranoudis et al. (1992) examined the drying kinetics of onion and green pepper by using the one-parameter empirical mass transfer model, where the characteristic parameter (drying constant) was a function of process variables. They reported that the characteristic dimension of the sample and air temperature influenced the drying kinetics in a negative and positive way, respectively.

Experimental investigation of the drying kinetics was a subject of considerable interest to many researchers in the last decade. Estrada and Litchfield (1993) studied the drying rates of corn at high and low humidity conditions using a thin-layer dryer and found out that high humidity drying reduced the drying rate by up to 44 % as compared to low humidity drying. Jumah et al. (1996) investigated the batch drying kinetics of a corn in a novel rotating jet spouted bed using both continuous and intermittent spouting and heating schemes. The parameters investigated include inlet air temperature, bed height,



superficial air velocity, nozzle diameter, distributor rotational speed and intermittency of spouting and heat input. The results indicated that the inlet temperature was the parameter which most significantly affected the drying rate and distributor rotational speed, air flow rate, bed height and nozzle diameter had little effect on the drying kinetics of slow drying materials. McMinn and Magee (1996) investigated the kinetics of moisture transport in potato cylinders by using an experimental air tunnel dryer. Two series of experiments were carried out to study the influence of air velocity and temperature on drying behavior. The first series were performed at constant air temperature ( $60^{\circ}\text{C}$ ) and air velocities of 0.5, 1.0 and 1.5 m/s and in the second series, the experiments were carried out at different air temperatures 30, 40, 50 and  $60^{\circ}\text{C}$  and at constant air velocity (1.5 m/s). They found that drying of potato was completely controlled by internal moisture mass transfer and temperature was the principal factor in determination of drying rate. They also concluded that airflow rate had a limited effect within the range studied.

Piotrowski and Lenart (1998) conducted the experiments to examine the influence of constant and variable temperatures or velocities on apple's drying kinetics. The experiments were carried out in a cabinet convective dryer. During the experiments, inlet temperature was kept or changed from 50 to  $90^{\circ}\text{C}$  and air velocity was set or changed from 0.7 to 3 m/s. The results showed the influence of temperature and velocity of air on the drying kinetics. They concluded that the step change of  $\pm 20^{\circ}\text{C}$  in the inlet air temperature caused sudden changes in the product temperature while the step change of  $\pm 0.8$  or  $\pm 1.5$  m/s in the velocity of airflow caused moderate, time elongation temperature changes in the product. Chua et al. (2000) studied the drying kinetics of three different agricultural products namely banana, guava and potato dried in a two-stage

heat pump dryer by varying the inlet temperature. They found that varying temperature drying produced intermediate drying rates between constant inlet air temperatures. They also found that drying rate of banana was approximately one order smaller than that for guava and potato under similar drying conditions.

Recently, Tsami and Katsioti (2000) studied the drying kinetics of four fruits (prune, quince, fig and strawberry) by using a simple mass transfer mathematical model involving a characteristic parameter ( $K$ ) as a function of process variables. The investigation involved three values of sample thickness (5, 10, and 15 mm) and three different air temperatures (50, 60, and 70°C). They found that the parameters of the model were greatly affected by sample thickness and air temperatures.

## **2.2. Heat and Moisture Transfer Analyses**

Drying involves the application of heat to vaporize moisture and some means of removing water vapor from the products surface. Hence, it is a process of simultaneous heat and moisture transfer, whereby moisture is vaporized and swept away from the surface by means of a carrier fluid passing through or over the moist object. Two important aspects of mass transfer are the transfer of water to the surface of the material being dried and the removal of water vapor from the surface. Knowledge of temperature and moisture distributions within the product during the drying process is essential for process design, handling practices, quality control, and energy savings.

In order to achieve dried products of high quality at a reasonable cost, drying must occur fairly rapidly. Four main factors affect the rate and total time of drying are properties of the product in terms of its size and geometry, geometrical arrangement in

relation to heat transfer medium, physical properties of drying medium and characteristics of the drying system (Holdsworth, 1971).

It is generally observed in many products that the initial rate of drying is constant which then decreases, sometimes at two different rates (Chung and Chung, 1982). Although several internal mechanisms of moisture have been suggested, owing to the complexity of the process no generalized theory currently exists to explain the mechanism of internal moisture transfer (Rizvi, 1986), which is generally accepted to be the major rate limiting step (King, 1977).

Luikov (1973) proposed the first theoretical model of heat and moisture transfer describing the drying phenomena in moist materials. He found that it was not just the moisture content but also the mass transfer potential, which is the most effective variable of moisture movement in porous materials.

Chiang (1988) evaluated the heat and mass transfer coefficients and formulated a mathematical model for forced convective air-drying of apples. He found air humidity to have the greatest influence on time period of first falling rate period and the temperature dependence of the drying rate to follow Arr-henius type of equation. Zhao and Poulsenk (1988) observed only falling rate period during potato dehydration. A semi empirical equation was developed to extrapolate the diffusivities for other drying conditions and it was concluded that dehydration of potato was completely by internal mass transfer and dry bulb temperature and relative humidity greatly influenced the drying rate.

Later Dincer and Dost (1996) developed an analytical model for determining the moisture diffusivities and moisture transfer coefficients for solid objects (namely, infinite slab, infinite cylinder and sphere) subjected to drying. The drying coefficients and lag

factors were employed in the model. The results showed that the method was useful in determining the moisture transfer parameters for solid objects in a simple and accurate manner for variety of drying applications. Ruiz-Cabrera et al. (1997) evaluated the effect of path diffusion on the average moisture diffusivity in carrot for different shapes (slices and cylinders) using non-linear regression analysis. The result showed significant differences between radial and axial average diffusivities and also between core and annular diffusivity.

Recently Jia et al. (2000) developed a model for two dimensional heat and mass transfer within a single grain kernel during drying. In this model, the moisture was assumed to diffuse to the outer boundary of the kernel in liquid form and evaporate on the surface of the kernel. The governing equations were solved using the finite element method and simulation data were verified on a thin layer dryer for wheat kernels. They conclude that some technical drying processes such as tempering and intermittence drying should be adopted to avoid kernel cracking due to thermal and moisture stresses results in improved grain quality after drying. Kechaou and Maalej (2000) conducted an experiment for Tunisia Deglet Nour dates in a laboratory dryer under different drying conditions. The air temperature was verified from 30°C to 69°C, relative humidity from 11.6 to 47.1% and air velocity from 0.9 to 2.7 m/s. They have found an empirical equation for the diffusivity of moisture in the date by comparing drying curves obtained experimentally with the predicted drying curves.

A careful review of the literature reveals the need of detailed information on the mechanism of the internal moisture transfer during drying and the influence of moisture transfer parameters on the rate of drying. Only few studies have been devoted to calculate

the moisture transfer parameters such as moisture diffusivity and moisture transfer coefficient for the products subjected to drying and there is wide variation in the calculated values of these parameters due to different methods of estimation and complexity of food structure. Hence there is urgent need to develop models or correlations to calculate the moisture transfer parameters in a simple and accurate manner.

In the classification of heat and moisture transfer analysis during drying, a large number of models, varying from simple models based on physical and engineering principles, to more rigorous mathematical analyses have been proposed. However, there is need to analyze it using the fundamental models of heat conduction and moisture diffusion and compare it with experimental results available in the literature so as to propose new design improvements and optimization techniques.

## **CHAPTER 3**

### **MATHEMATICAL ANALYSIS**

This chapter is devoted to the mathematical formulation pertinent to the analytical and numerical analyses of heat and moisture transfer during solids drying. The methodology or procedure employed in the development of new drying correlations is also presented. It is divided into three sections:

1. Analytical modeling of heat and moisture transfer
2. Numerical modeling of heat and moisture transfer
3. Development of new drying correlations

#### **3.1. ANALYTICAL MODELING OF HEAT AND MOISTURE TRANSFER**

In this section, analytical analysis of heat and moisture transfer during solids drying is presented for three regular shaped objects (slab object, cylindrical object, and spherical object). The assumptions considered in the analysis are as follows:

- Thermophysical properties are constant.
- There is no heat generation inside the objects.
- There is negligible shrinkage or deformation of objects during drying

- The temperature of the drying air is constant.
- The variation of temperature and moisture is in 'x' direction through thickness for slab and in 'r' direction through radius for cylinder and sphere.

In the following subsections, each object is discussed in detail.

### 3.1.1. 1-D Slab Object

#### Governing Equations

The mathematical analysis pertinent to drying process is based on Fourier law of heat conduction and Fick's law of mass diffusion. The governing Fickian equation is exactly in the form of the Fourier equation of heat transfer, in which temperature and thermal diffusivity are replaced with concentration and moisture diffusivity, respectively. The governing equations representing the drying process in one dimension are:

- Heat Transfer

$$\frac{\partial^2 T}{\partial x^2} = \frac{1}{\alpha} \frac{\partial T}{\partial t} \quad (3.1)$$

where

$$\alpha = \frac{k}{\rho c_p} \quad (3.2)$$

The initial condition and boundary conditions are:

$$T = T_i \quad \text{at } t = 0 \quad (3.3a)$$

$$\left. \frac{\partial T}{\partial x} \right|_{x=0} = \frac{h}{k} (T - T_d) \quad \text{at } x = 0 \quad (3.3b)$$

and

$$T = T_i \quad \text{at } x = \infty \quad (3.3c)$$

- **Moisture Transfer**

The governing equation of moisture transfer is:

$$\frac{\partial M}{\partial t} = D \frac{\partial^2 M}{\partial x^2} \quad (3.4)$$

where  $D$  is the moisture diffusivity, whose dependence on temperature is of the form of Arr-henius equation (Ruiz-Cabrera et al., 1997):

$$D = D_o \exp\left(\frac{-1119}{T}\right) \quad (3.5)$$

Initial and boundary conditions are:

$$M = M_i \quad \text{at } t = 0 \quad (3.6a)$$

$$\left. \frac{\partial M}{\partial x} \right|_{x=0} = \frac{h_m}{D} (M - M_d) \quad \text{at } x = 0 \quad (3.6b)$$

$$M = M_i \quad \text{at } x = \infty \quad (3.6c)$$

### **Solution Technique**

Applying Laplace transformation to the equation (3.1) and (3.4) results in:

$$\frac{\partial^2 \bar{T}}{\partial x^2} - \frac{s}{\alpha} \left( \bar{T} - \frac{1}{s} T_i \right) = 0 \quad (3.7)$$

$$\frac{\partial^2 \bar{M}}{\partial x^2} - \frac{s}{D} \left( \bar{M} - \frac{1}{s} M_i \right) = 0 \quad (3.8)$$

The boundary condition at the surface becomes:

$$\frac{d\bar{T}}{dx} = -\frac{h}{k} (\bar{T} - T_d) \quad (3.9)$$

$$\frac{d\bar{M}}{dx} = -\frac{h_m}{D} (\bar{M} - \bar{M}_d) \quad (3.10)$$

where  $\bar{T} = \ell(T)$ ; and  $\bar{M} = \ell(M)$



The solution of equations (3.7) and (3.8), satisfying the conditions (3.9) and (3.10) at the surface and the condition that

$$\overline{T}(\infty, t) = T_i; \quad \overline{M}(\infty, t) = M_i \quad (3.11)$$

are obtained as:

$$\overline{T} - \frac{1}{s}T_i = \frac{\beta(T_d - T_i)e^{-\beta\sqrt{\frac{\rho}{\alpha}}}}{s\left(\beta + \sqrt{\frac{s}{\alpha}}\right)} \quad (3.12)$$

$$\overline{M} - \frac{1}{s}M_i = \frac{\beta_m(M_d - M_i)e^{-\beta_m\sqrt{\frac{\rho_m}{D}}}}{s\left(\beta_m + \sqrt{\frac{s}{D}}\right)} \quad (3.13)$$

where

$$\beta = \frac{h}{k}; \quad \beta_m = \frac{h_m}{D}$$

Using the partial fraction technique and the Laplace inversion of equation (3.12) and (3.13) yields the temperature and moisture distribution inside the slab as:

$$T - T_i = (T_d - T_i) \left[ \operatorname{erfc}\left(\frac{x}{2\sqrt{\alpha t}}\right) - e^{\beta x + \beta^2 \alpha t} \operatorname{erfc}\left(\frac{x}{2\sqrt{\alpha t}} + \beta\sqrt{\alpha t}\right) \right] \quad (3.14)$$

$$M - M_d = (M_i - M_d) \left[ \operatorname{erfc}\left(\frac{x}{2\sqrt{Dt}}\right) - e^{\beta_m x + \beta_m^2 Dt} \operatorname{erfc}\left(\frac{x}{2\sqrt{Dt}} + \beta_m\sqrt{Dt}\right) \right] \quad (3.15)$$

The above equations represent the closed form solution to the temperature and moisture distribution inside the slab object subjected to drying. For the given initial temperature and moisture content of the slab object, the above expressions can be easily used to determine the temperature and moisture distribution inside the slab object for different heating periods.

### 3.1.2. 1-D Cylindrical Object

#### Governing Equations

The governing equations of heat and moisture transfer in one dimension for a cylindrical object subjected to drying are:

- Heat Transfer

$$\frac{1}{r} \frac{\partial}{\partial r} \left( r \frac{\partial \phi}{\partial r} \right) = \frac{1}{\alpha} \frac{\partial \phi}{\partial t} \quad (3.16)$$

where  $\phi = T - T_d$

The initial and boundary conditions are:

$$\phi(r,0) = \phi_i = T_i - T_d \quad (3.17a)$$

$$\frac{\partial \phi}{\partial r}(0,t) = 0 \quad (3.17b)$$

$$-k \frac{\partial \phi}{\partial r}(R,t) = h\phi(R,t) \quad (3.17c)$$

- Moisture Transfer

$$\frac{1}{r} \frac{\partial}{\partial r} \left( r \frac{\partial \varphi}{\partial r} \right) = \frac{1}{D} \frac{\partial \varphi}{\partial t} \quad (3.18)$$

where D is the moisture diffusivity given by equation (3.5) and  $\varphi = M - M_d$

Initial and boundary conditions are:

$$\varphi(r,0) = \varphi_i = M_i - M_d \quad (3.19a)$$

$$\frac{\partial \varphi}{\partial r}(0,t) = 0 \quad (3.19b)$$

$$-D \frac{\partial \varphi}{\partial r}(R,t) = h_m \varphi(R,t) \quad (3.19c)$$

where  $R$  is the radius of the cylinder

The temperature and moisture content at any point of the solid object is non-dimensionalized using the following equations:

$$\theta = \frac{T - T_i}{T_d - T_i} \quad (3.20)$$

$$\Phi = \frac{M - M_d}{M_i - M_d} \quad (3.21)$$

The solution to the governing equations (3.16) and (3.18) under the conditions given in equations (3.17) and (3.19) yields dimensionless center temperature and moisture distributions inside the cylindrical object in the following forms:

$$\theta = \sum_{n=1}^{\infty} A_n B_n \quad (3.22)$$

$$\Phi = \sum_{n=1}^{\infty} A_{mn} B_{mn} \quad (3.23)$$

where  $A_n = (2Bi) / (\mu_n^2 + Bi^2 + J_0(\mu_n))$  (3.24)

$$A_{mn} = (2Bi_m) / (\mu_n^2 + Bi_m^2 + J_0(\mu_n)) \quad (3.25)$$

and  $B_n = \exp(-\mu_n^2 Fo)$  (3.26)

$$B_{mn} = \exp(-\mu_n^2 Fo_m) \quad (3.27)$$

Biot number for heat and moisture transfer is defined as:

$$Bi = \frac{hY}{k} \quad (3.28)$$

$$Bi_m = \frac{h_m Y}{D} \quad (3.29)$$

and Fourier number for heat and moisture transfer is defined as:

$$Fo = \frac{\alpha t}{Y^2} \quad (3.30)$$

$$Fo_m = \frac{Dt}{Y^2} \quad (3.31)$$

### 3.1.3. 1-D Spherical Object

#### Governing Equations

The governing equations of heat and moisture transfer in one dimension for a spherical object subjected to drying are:

- Heat Transfer

$$\frac{1}{r^2} \frac{\partial}{\partial r} \left( r^2 \frac{\partial \phi}{\partial r} \right) = \frac{1}{\alpha} \frac{\partial \phi}{\partial t} \quad (3.32)$$

where  $\phi = T - T_d$

The initial and boundary conditions are:

$$\phi(r,0) = \phi_i = T_i - T_d \quad (3.33a)$$

$$\frac{\partial \phi}{\partial r}(0,t) = 0 \quad (3.33b)$$

$$-k \frac{\partial \phi}{\partial r}(R,t) = h\phi(R,t) \quad (3.33c)$$

- Moisture Transfer

$$\frac{1}{r^2} \frac{\partial}{\partial r} \left( r^2 \frac{\partial \varphi}{\partial r} \right) = \frac{1}{D} \frac{\partial \varphi}{\partial t} \quad (3.34)$$

where D is the moisture diffusivity given by equation (3.5) and  $\varphi = M - M_d$

Initial and boundary conditions are:

$$\varphi(r,0) = \varphi_i = M_i - M_d \quad (3.35a)$$

$$\frac{\partial \varphi}{\partial r}(0,t) = 0 \quad (3.35b)$$

$$-D \frac{\partial \varphi}{\partial r}(R, t) = h_m \varphi(R, t) \quad (3.35c)$$

where  $R$  is the radius of the sphere

The dimensionless temperature and moisture distribution inside the spherical object is given by equations (3.20) and (3.21). The solution to the governing equations (3.32) and (3.34) under the conditions given in equations (3.33) and (3.35) yields dimensionless center temperature and moisture distributions inside the spherical object in the following forms:

$$\theta = \sum_{n=1}^{\infty} A_n B_n \quad (3.36)$$

$$\Phi = \sum_{n=1}^{\infty} A_{mn} B_{mn} \quad (3.37)$$

where

$$A_n = (2Bi \sin \mu_n) / (\mu_n - \sin \mu_n \cos \mu_n) \quad (3.38)$$

$$A_{mn} = (2Bi_m \sin \mu_n) / (\mu_n - \sin \mu_n \cos \mu_n) \quad (3.39)$$

and

$$B_n = \exp(-\mu_n^2 Fo) \quad (3.40)$$

$$B_{mn} = \exp(-\mu_n^2 Fo_m) \quad (3.41)$$

### 3.2. NUMERICAL MODELING OF HEAT AND MOISTURE TRANSFER

In this section, numerical analysis of heat and moisture transfer during drying is presented for three regular shaped objects. The analysis includes:

- 1) 2-D slab object
- 2) 2-D cylindrical object

### 3) 2-D spherical object

The assumptions considered in the analysis are as follows:

- Thermophysical properties are constant.
- There is negligible shrinkage or deformation of objects during drying.
- There is no heat generation inside the objects.
- The temperature of the drying air is constant.
- Two-dimensional variations of temperature and moisture are considered in slab (i.e., x and y), cylinder (i.e., r and z) and sphere (i.e., r and  $\phi$ )

#### 3.2.1. 2-D Slab Object

##### Governing Equations

The mathematical equations governing the drying process in two-dimensional case with the appropriate boundary conditions are given as:

- Heat transfer

$$\frac{1}{\alpha} \frac{\partial T}{\partial t} = \frac{\partial^2 T}{\partial x^2} + \frac{\partial^2 T}{\partial y^2} \quad (3.42)$$

Initial and boundary conditions are:

$$T(x, y, 0) = T_i \quad (3.43a)$$

$$\text{at } x = 0; \quad -k \frac{\partial T(0, y, t)}{\partial x} = h (T - T_d) \quad (3.43b)$$

$$\text{at } x = l; \quad -k \frac{\partial T(l, y, t)}{\partial x} = h (T - T_d) \quad (3.43c)$$

$$\text{at } y = 0; \quad -k \frac{\partial T(x, 0, t)}{\partial y} = h (T - T_d) \quad (3.43d)$$

$$\text{at } y = h; \quad -k \frac{\partial T(x, h, t)}{\partial y} = h (T - T_d) \quad (3.43e)$$

- **Moisture Transfer**

$$\frac{\partial M}{\partial t} = \frac{\partial}{\partial x} \left( D \frac{\partial M}{\partial x} \right) + \frac{\partial}{\partial y} \left( D \frac{\partial M}{\partial y} \right) \quad (3.44)$$

Initial and boundary conditions are:

$$M(x, y, 0) = M_i \quad (3.45a)$$

$$\text{at } x = 0; \quad -D \frac{\partial M(0, y, t)}{\partial x} = h_m (M - M_d) \quad (3.45b)$$

$$\text{at } x = l; \quad -D \frac{\partial M(l, y, t)}{\partial x} = h_m (M - M_d) \quad (3.45c)$$

$$\text{at } y = 0; \quad -D \frac{\partial M(x, 0, t)}{\partial y} = h_m (M - M_d) \quad (3.45d)$$

$$\text{at } y = h; \quad -D \frac{\partial M(x, h, t)}{\partial y} = h_m (M - M_d) \quad (3.45e)$$

The temperature dependence moisture diffusivity (D) is given by equation (3.5).

The temperature in the heat conduction equation and moisture content in the diffusion equation is non-dimensionalized (reduced) using the following equations

$$T^* = \frac{T - T_i}{T_d - T_i} \quad (3.46)$$

$$M^* = \frac{M - M_d}{M_i - M_d} \quad (3.47)$$

### **Solution Methodology**

The solution of the governing equations presented in the previous section is difficult to obtain using the analytical methods. Moreover, considerable assumptions have to be considered in order to obtain a closed form solution with many inadequacies. Therefore, approximate methods of solution are used to solve them. The method used in the present study is the explicit finite difference approximation where the governing equations are first transformed into difference equations by dividing the domain of solution to a grid of points in the form of mesh and the derivatives are expressed along each mesh point referred to as a node. Knowing the dependent variable at each node initially, it is approximated for the next time step and it continues until the final time step. The numerical grid of the solution domain is shown in Figure 3.1. It consists of two sets of perpendicular lines representing the x-direction and y-direction and the intersection of these lines constitute the nodes where the solution of the governing equations is obtained. The index  $i$  represents the mesh points in the X-direction starting with  $i = 0$  being one boundary and ending at  $i = m$ , the other boundary while index  $j$  represents the mesh points in the Y-direction starting from  $j = 0$ . Thus, the finite difference representation of the mesh points will be as follows:

$$X_i = i\Delta X \quad \text{for } i = 0, 1, 2, \dots, m$$

$$Y_j = j\Delta Y \quad \text{for } j = 0, 1, 2, \dots, n$$



Where  $\Delta X$  and  $\Delta Y$  represents the grid sizes in the X and Y-directions respectively and the subscripts denote the location of the dependent under consideration, i.e.,  $T_{i,j}$  means the temperature at the  $i$ 'th X-location and  $j$ 'th Y-location.

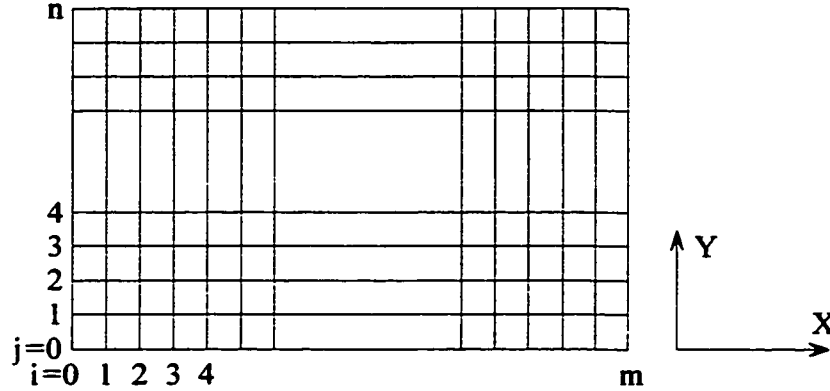


Figure 3.1: Numerical grid for a slab object

The finite difference representation of the various derivatives appear in the governing equations can be written as follows:

$$\frac{\partial T}{\partial t} = \frac{T_{i,j,k+1} - T_{i,j,k}}{\Delta t} \quad (3.48)$$

$$\frac{\partial M}{\partial t} = \frac{M_{i,j,k+1} - M_{i,j,k}}{\Delta t} \quad (3.49)$$

$$\frac{\partial^2 T}{\partial X^2} = \frac{T_{i+1,j,k} - 2T_{i,j,k} + T_{i-1,j,k}}{\Delta X^2} \quad (3.50)$$

$$\frac{\partial^2 M}{\partial X^2} = \frac{M_{i+1,j,k} - 2M_{i,j,k} + M_{i-1,j,k}}{\Delta X^2} \quad (3.51)$$

$$\frac{\partial^2 T}{\partial Y^2} = \frac{T_{i,j+1,k} - 2T_{i,j,k} + T_{i,j-1,k}}{\Delta Y^2} \quad (3.52)$$

$$\frac{\partial^2 M}{\partial Y^2} = \frac{M_{i,j+1,k} - 2M_{i,j,k} + M_{i,j-1,k}}{\Delta Y^2} \quad (3.53)$$

The finite difference representation of the governing equations are written as:

- Heat Transfer

$$T_{i,j,k+1} = r(\Delta Y)^2 T_{i+1,j,k} + [1 - 2r((\Delta X)^2 + (\Delta Y)^2)]T_{i,j,k} + r(\Delta Y)^2 T_{i-1,j,k} + r(\Delta X)^2 T_{i,j+1,k} + r(\Delta X)^2 T_{i,j-1,k} \quad (3.54)$$

where 
$$r = \frac{\alpha \Delta t}{(\Delta X)^2 (\Delta Y)^2}$$

Initial and boundary conditions are:

$$T_{i,j,0} = T_i \quad (3.55a)$$

$$\text{at } x = 0; \quad T_{0,j,k} = \frac{T_{1,j,k} + C_1 \times T_d}{1 + C_1} \quad (3.55b)$$

$$\text{at } x = l; \quad T_{m,j,k} = \frac{T_{m-1,j,k} + C_1 \times T_d}{1 + C_1} \quad (3.55c)$$

$$\text{at } y = 0; \quad T_{i,0,k} = \frac{T_{i,1,k} + C_2 \times T_d}{1 + C_2} \quad (3.55d)$$

$$\text{at } y = h; \quad T_{i,n,k} = \frac{T_{i,n-1,k} + C_2 \times T_d}{1 + C_2} \quad (3.55e)$$

where

$$C_1 = \frac{h \times \Delta X}{k}$$

$$C_2 = \frac{h \times \Delta Y}{k}$$

- Moisture Transfer

$$M_{i,j,k+1} = r_d (\Delta Y)^2 M_{i+1,j,k} + [1 - 2r_d ((\Delta X)^2 + (\Delta Y)^2)]M_{i,j,k} + r_d (\Delta Y)^2 M_{i-1,j,k} + r_d (\Delta X)^2 M_{i,j+1,k} + r_d (\Delta X)^2 M_{i,j-1,k} \quad (3.56)$$

where 
$$r_d = \frac{D\Delta t}{(\Delta X)^2(\Delta Y)^2}$$

Initial and boundary conditions are:

$$M_{i,j,0} = M_i \quad (3.57a)$$

$$\text{at } x = 0; \quad M_{0,j,k} = \frac{M_{1,j,k} + C_3 \times M_d}{1 + C_3} \quad (3.57b)$$

$$\text{at } x = l; \quad M_{m,j,k} = \frac{M_{m-1,j,k} + C_3 \times M_d}{1 + C_3} \quad (3.57c)$$

$$\text{at } y = 0; \quad M_{i,0,k} = \frac{M_{i,1,k} + C_4 \times M_d}{1 + C_4} \quad (3.57d)$$

$$\text{at } y = h; \quad M_{i,n,k} = \frac{M_{i,n-1,k} + C_4 \times M_d}{1 + C_4} \quad (3.57e)$$

where

$$C_3 = \frac{h_m \times \Delta X}{D}$$

$$C_4 = \frac{h_m \times \Delta Y}{D}$$

The above difference equations are solved to obtain temperature and moisture distributions inside the rectangular slab at different time periods. The grid independent tests are conducted to ensure the grid independent results in the simulation. Stability analysis is performed in order to investigate the boundedness of the exact solution of the finite-difference equations using the von Neumann's method. The method introduces an initial line of errors as represented by a finite-Fourier series and applies in a theoretical sense to initial value problem. The stability criterions obtained for the above difference equations are:

for heat transfer 
$$\Delta t \leq \frac{(\Delta X)^2 (\Delta Y)^2}{2\alpha [(\Delta X)^2 + (\Delta Y)^2]} \quad (3.58)$$

for moisture transfer 
$$\Delta t \leq \frac{(\Delta X)^2 (\Delta Y)^2}{2D [(\Delta X)^2 + (\Delta Y)^2]} \quad (3.59)$$

Thus the above criterions have to be satisfied in order to have converged solution.

### 3.2.2. 2-D Cylindrical Object

#### Governing Equations

The mathematical equations governing the drying process in two-dimensional cylindrical object with appropriate boundary conditions are given as:

- Heat transfer

$$\frac{1}{\alpha} \frac{\partial T}{\partial t} = \frac{1}{r} \frac{\partial}{\partial r} \left( r \frac{\partial T}{\partial r} \right) + \frac{\partial^2 T}{\partial z^2} \quad (3.60)$$

Initial and boundary conditions are:

$$T(r, z, 0) = T_i \quad (3.61a)$$

$$\text{at } r = 0; \quad \frac{\partial T(0, z, t)}{\partial r} = 0 \quad (3.62b)$$

$$\text{at } r = R; \quad -k \frac{\partial T(R, y, t)}{\partial r} = h (T - T_d) \quad (3.62c)$$

$$\text{at } z = 0; \quad -k \frac{\partial T(r, 0, t)}{\partial z} = h (T - T_d) \quad (3.62d)$$

$$\text{at } z = L; \quad -k \frac{\partial T(r, L, t)}{\partial z} = h (T - T_d) \quad (3.62e)$$

- **Moisture Transfer**

$$\frac{1}{D} \frac{\partial M}{\partial t} = \frac{1}{r} \frac{\partial}{\partial r} \left( r \frac{\partial M}{\partial r} \right) + \frac{\partial^2 M}{\partial z^2} \quad (3.63)$$

Initial and boundary conditions are:

$$M(r, z, 0) = M_i \quad (3.64a)$$

$$\text{at } r = 0; \quad \frac{\partial M(0, z, t)}{\partial r} = 0 \quad (3.64b)$$

$$\text{at } r = R; \quad -D \frac{\partial M(R, y, t)}{\partial r} = h_m (M - M_d) \quad (3.64c)$$

$$\text{at } z = 0; \quad -D \frac{\partial M(r, 0, t)}{\partial z} = h_m (M - M_d) \quad (3.64d)$$

$$\text{at } z = L; \quad -D \frac{\partial M(r, L, t)}{\partial z} = h_m (M - M_d) \quad (3.64e)$$

### **Solution Methodology**

The above governing equations are discretized using the explicit finite-difference method. Numerical grid of a axisymmetric cylindrical object is shown in Figure 3.2. The index  $i$  represents the mesh points in the  $Z$ -direction starting with  $i = 0$  being one boundary and ending at  $i = m$ , the other boundary while index  $j$  represents the mesh points in the  $R$ -direction starting from  $j = 0$ . Thus, the finite difference representation of the mesh points will be as follows:

$$Z_i = i\Delta Z \quad \text{for } i = 0, 1, 2, \dots, m$$

$$R_j = j\Delta R \quad \text{for } j = 0, 1, 2, \dots, n$$

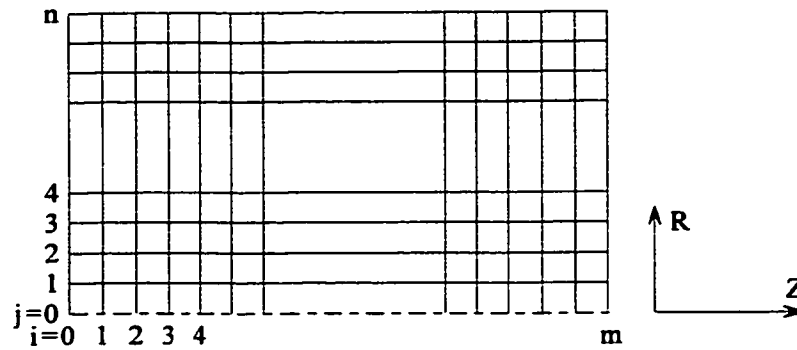


Figure 3.2: Numerical grid for an axisymmetric cylindrical object

Where  $\Delta Z$  and  $\Delta R$  represents the grid sizes in the  $Z$  and  $R$ -directions respectively and the subscripts denote the location of the dependent under consideration, i.e.,  $T_{ij}$  means the temperature at the  $i$ 'th  $Z$ -location and  $j$ 'th  $R$ -location. Knowing the value of dependent variable at the initial time step, unknown values at next time steps are calculated using the finite difference equations. The finite difference representations of the governing equations can be written in the following form:

- Heat Transfer

$$T_{i,j,k+1} = AT_{i+1,j,k} + (1 - 2[A + B])T_{i,j,k} + AT_{i-1,j,k} + B(1 + 0.5j)T_{i,j+1,k} + B(1 - 0.5j)T_{i,j-1,k} \quad (3.65)$$

where  $A = \frac{\alpha \Delta t}{(\Delta Z)^2}$  and  $B = \frac{\alpha \Delta t}{(\Delta R)^2}$

Initial and boundary conditions can be written as:

$$T_{i,j,0} = T_i \quad (3.66a)$$

$$\text{at } r = 0; \quad T_{i,0,k} = T_{i,1,k} \quad (3.66b)$$

$$\text{at } r = R; \quad T_{i,n,k} = \frac{T_{i,n-1,k} + C_5 \times T_d}{1 + C_5} \quad (3.66c)$$

$$\text{at } z = 0; \quad T_{0,j,k} = \frac{T_{1,j,k} + C_6 \times T_d}{1 + C_6} \quad (3.66d)$$

$$\text{at } z = L; \quad T_{m,j,k} = \frac{T_{m-1,j,k} + C_6 T_d}{1 + C_6} \quad (3.66e)$$

where

$$C_5 = \frac{h \Delta R}{k}; \quad C_6 = \frac{h \Delta Z}{k}$$

- Moisture Transfer

$$\begin{aligned} M_{i,j,k+1} = & A_m M_{i+1,j,k} + (1 - 2[A_m + B_m])M_{i,j,k} + A_m M_{i-1,j,k} \\ & + B_m(1 + 0.5j)M_{i,j+1,k} + B_m(1 - 0.5j)M_{i,j-1,k} \end{aligned} \quad (3.67)$$

where

$$A_m = \frac{D\Delta t}{(\Delta Z)^2} \quad \text{and} \quad B_m = \frac{D\Delta t}{(\Delta R)^2}$$

Initial and boundary conditions can be written as:

$$M_{i,j,0} = M_i \quad (3.68a)$$

$$\text{at } r = 0; \quad M_{i,0,k} = M_{i,1,k} \quad (3.68b)$$

$$\text{at } r = R; \quad M_{i,n,k} = \frac{M_{i,n-1,k} + C_7 \times M_d}{1 + C_7} \quad (3.68c)$$

$$\text{at } z = 0; \quad M_{0,j,k} = \frac{M_{1,j,k} + C_8 \times M_d}{1 + C_8} \quad (3.68d)$$

$$\text{at } z = L; \quad M_{m,j,k} = \frac{M_{m-1,j,k} + C_8 \times M_d}{1 + C_8} \quad (3.68e)$$

where

$$C_7 = \frac{h_m \Delta R}{D}; \quad C_8 = \frac{h_m \Delta Z}{D}$$

The above difference equations are used to obtain temperature and moisture distributions inside the cylindrical object at different time periods. Stability analysis is performed in order to investigate the boundedness of the exact solution of the finite-difference equations. The stability criteria obtained for the above difference equations are:

$$\text{for heat transfer} \quad \Delta t \leq \frac{(\Delta Z)^2 (\Delta R)^2}{2\alpha [(\Delta Z)^2 + (\Delta R)^2]} \quad (3.69)$$

$$\text{for moisture transfer} \quad \Delta t \leq \frac{(\Delta Z)^2 (\Delta R)^2}{2D [(\Delta Z)^2 + (\Delta R)^2]} \quad (3.70)$$

Thus the above conditions have to be satisfied in order to have converged solution.

### 3.2.3. 2-D Spherical Object

#### Governing Equations

The mathematical equations governing the drying process in two-dimensional spherical object with appropriate boundary conditions are given as:

- Heat transfer

$$\frac{1}{\alpha} \frac{\partial T}{\partial t} = \frac{1}{r^2} \frac{\partial}{\partial r} \left( r^2 \frac{\partial T}{\partial r} \right) + \frac{1}{r^2 \sin^2 \theta} \frac{\partial^2 T}{\partial \phi^2} \quad (3.71)$$

Initial and boundary conditions are:

$$T(r, \phi, 0) = T_i \quad (3.72a)$$



$$\text{at } r = 0; \quad \frac{\partial T(0, \phi, t)}{\partial r} = 0 \quad (3.72b)$$

$$\text{at } r = R; \quad -k \frac{\partial T(R, \phi, t)}{\partial r} = h (T - T_d) \quad (3.72c)$$

$$T(r, 0, t) = T(r, 2\pi, t) \quad (3.72d)$$

$$\frac{\partial T(r, 0, t)}{\partial \phi} = \frac{\partial T(r, 2\pi, t)}{\partial \phi} \quad (3.72e)$$

- **Moisture Transfer**

$$\frac{1}{D} \frac{\partial M}{\partial t} = \frac{1}{r^2} \frac{\partial}{\partial r} \left( r^2 \frac{\partial M}{\partial r} \right) + \frac{1}{r^2 \sin^2 \theta} \frac{\partial^2 M}{\partial \phi^2} \quad (3.73)$$

Initial and boundary conditions are:

$$M(r, \phi, 0) = M_i \quad (3.74a)$$

$$\text{at } r = 0; \quad \frac{\partial M(0, \phi, t)}{\partial r} = 0 \quad (3.74b)$$

$$\text{at } r = R; \quad -D \frac{\partial M(R, \phi, t)}{\partial r} = h_m (M - M_d) \quad (3.74c)$$

$$M(r, 0, t) = M(r, 2\pi, t) \quad (3.74d)$$

$$\frac{\partial M(r, 0, t)}{\partial \phi} = \frac{\partial M(r, 2\pi, t)}{\partial \phi} \quad (3.74e)$$

### **Solution Methodology**

Explicit finite-difference scheme is used to discretize the above governing equations. The numerical grid of the spherical object is shown in Figure 3.3. The index  $i$  represents the mesh points in the R-direction starting with  $i = 0$  being the center of the sphere and

ending at  $i = m$ , while index  $j$  represents the mesh points in the  $\Phi$ -direction starting from  $j = 0$ . Thus, the finite difference representation of the mesh points will be as follows:

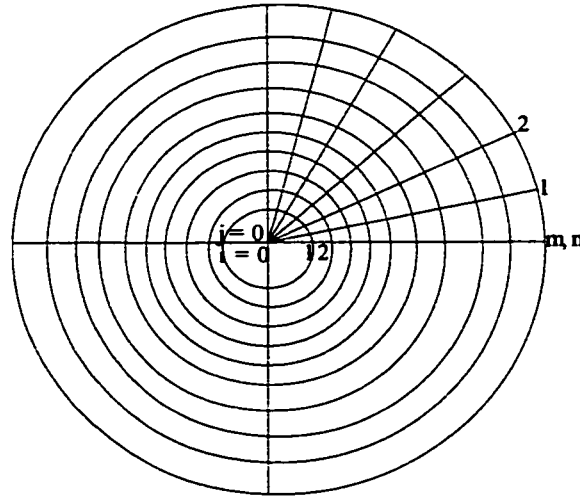


Figure 3.3: Numerical grid for a spherical object

$$R_i = i\Delta R \quad \text{for } i = 0, 1, 2, \dots, m$$

$$\Phi_j = j\Delta\Phi \quad \text{for } j = 0, 1, 2, \dots, n$$

where  $\Delta R$  and  $\Delta\Phi$  represents the grid sizes in the  $R$  and  $\Phi$ -directions respectively and the subscripts denote the location of the dependent under consideration, i.e.,  $T_{ij}$  means the temperature at the  $i$ 'th  $R$ -location and  $j$ 'th  $\Phi$ -location. Knowing the value of dependent variable at the initial time step, unknown values at next time steps are calculated using the finite difference equations. The finite difference representations of the governing equations can be written in the following form:

- Heat Transfer

$$T_{i,j,k+1} = A(1+j)T_{i+1,j,k} + [1-2(A+B)]T_{i,j,k} + A(1-j)T_{i-1,j,k} + BT_{i,j+1,k} + BT_{i,j-1,k} \quad (3.75)$$

where  $A = \frac{\alpha\Delta t}{(\Delta R)^2}$ ;  $B = \frac{\alpha\Delta t}{R^2 \sin^2 \theta (\Delta\Phi)^2}$

Initial and boundary conditions can be written as:

$$T_{i,j,0} = T_i \quad (3.76a)$$

$$\text{at } r = 0; \quad T_{0,j,k} = T_{1,j,k} \quad (3.76b)$$

$$\text{at } r = R; \quad T_{m,j,k} = \frac{T_{m-1,j,k} + C_9 \times T_d}{1 + C_9} \quad (3.76c)$$

$$T_{i,0,k} = T_{i,n,k} \quad (3.76d)$$

$$T_{i,0,k} = 0.5[T_{i,1,k} + T_{i,n-1,k}] \quad (3.76e)$$

where 
$$C_9 = \frac{h \Delta R}{k}$$

- Moisture Transfer

$$\begin{aligned} M_{i,j,k+1} = & A_m(1+j)M_{i+1,j,k} + [1-2(A_m+B_m)]M_{i,j,k} \\ & + A_m(1-j)M_{i-1,j,k} + B_m M_{i,j+1,k} + B_m M_{i,j-1,k} \end{aligned} \quad (3.77)$$

where 
$$A_m = \frac{D\Delta t}{(\Delta R)^2}; \quad B_m = \frac{D\Delta t}{R^2 \sin^2 \theta (\Delta \Phi)^2}$$

Initial and boundary conditions can be written as:

$$M_{i,j,0} = M_i \quad (3.78a)$$

$$\text{at } r = 0; \quad M_{0,j,k} = M_{1,j,k} \quad (3.78b)$$

$$\text{at } r = R; \quad M_{m,j,k} = \frac{M_{m-1,j,k} + C_{10} M_d}{1 + C_{10}} \quad (3.78c)$$

$$M_{i,0,k} = M_{i,n,k} \quad (3.78d)$$

$$M_{i,0,k} = 0.5[M_{i,1,k} + M_{i,n-1,k}] \quad (3.78e)$$

where 
$$C_{10} = \frac{h_m \Delta R}{D}$$

The above difference equations are used to obtain temperature and moisture distributions inside the spherical object at different time periods.

### **3.3. DEVELOPMENT OF NEW DRYING CORRELATIONS**

This section deals with the development of new drying correlations for determining the moisture transfer parameters involved in the drying process. The two important mass transfer parameters needed in the analysis, design and optimization of drying process are moisture diffusivity and moisture transfer coefficient. Moisture diffusivity is an important transport property needed for correct modeling in the food drying process and is generally supposed as an independent of mass transfer path (Pakowski and Mujumdar, 1987; Karathanos et al. 1990). Its accurate determination can lead to better design and optimization of drying process. Numerous theoretical and experimental works have been directed towards moisture diffusivity estimation (Karathanos et al., 1990, Jayas et al., 1991, Zogzas et al., 1996). But limited data is available on moisture diffusivity, with a wide variation due to the structure complexity of foods and different methods of its estimation (Ruiz-Cabrera et al., 1997). An accurate prediction of diffusion parameters is possible by developing new models and methods representing the physical characteristics of the objects subjected to drying, as it is essential for efficient moisture transfer analysis, leading to optimized energy use and operating conditions, hence efficient drying (Dincer and Dost, 1996). Hence in the present study, an attempt has been made to develop new drying correlations to calculate the moisture transfer parameters in a simple and accurate manner.

- **Drying Process Parameters**

Dincer and Dost (1995) proposed two important process parameters used in evaluating and representing a drying process. The parameters are drying coefficient (S, 1/s) and lag factor (G, dimensionless unit). Drying coefficient shows the drying capability of the object or product and lag factor is an indication of internal resistance of object to the moisture transfer during drying. These parameters are called drying process parameters and are related by

$$\Phi = G \exp(-St) \quad (3.79)$$

These parameters can be defined either for an individual product or for a bunch of products. During the drying experiments, drying data in terms of moisture loss vs. drying time are measured for each product or group of products. The dimensionless moisture content values can be found using the following equation

$$\Phi = (M - M_e) / (M_i - M_e) \quad (3.80)$$

The above dimensionless moisture distribution is regressed using a least-square curve fitting method in the exponential form given by equation (5.1). Therefore G and S appear in the correlation and for each product these values are different since there is an intimate connection between the drying process parameters and heat and moisture parameters.

- **Moisture Transfer Parameters**

As already stated, moisture transfer parameters are moisture diffusivity and moisture transfer coefficient. Dincer (1996) developed an analytical model for moisture diffusivity estimation in regular shape products such as slab, cylinder and sphere as:

$$D = (SY^2) / (\mu_1^2) \quad (3.81)$$

The corresponding characteristic root ( $\mu_1$ ) equations for slab, cylinder and sphere have been simplified to the following relations (Dincer et al., 2000)

for slab

$$\mu_1 = -419.24G^4 + 2013.8G^3 - 3615.8G^2 + 2880.3G - 858.94 \quad (3.82)$$

for cylinder

$$\mu_1 = -3.4775G^4 + 25.285G^3 - 68.43G^2 + 82.468G - 35.638 \quad (3.83)$$

for sphere

$$\mu_1 = -8.3256G^4 + 54.842G^3 - 134.01G^2 + 145.83G - 58.124 \quad (3.84)$$

The equation determining the moisture transfer coefficient is given by the following equation

$$h_m = (D \times Bi_m) / Y \quad (3.85)$$

where the Biot number ( $Bi_m$ ) is given by the following relation

$$Bi_m = (\mu_1 / \cot \mu_1) \quad (3.86)$$

The methodology employed in the development of new drying correlations is as follows:

- Experimental moisture content data and drying time for regular geometrical solid products are acquired from various literature sources. Other information related to drying experiments such as air velocity, air temperature, relative humidity, and characteristic dimension of the product is also noted.
- The moisture content data obtained in the above step is non-dimensionalized using equation (3.80).
- The dimensionless moisture content distribution and drying time is regressed in the exponential form of equation (3.79). Thus lag factor (G) and drying coefficient (S) are determined.

- The values of the characteristic roots ( $\mu_1$ ) are estimated from the equations (3.82) through (3.84) depending upon the geometry of the product.
- The moisture diffusivity values are determined using equation (3.81).
- The Biot number ( $Bi_m$ ) is determined from equation (3.86).
- The moisture transfer coefficients are determined using equation (3.85).
- Dimensionless numbers are determined using their definitions as

$$\text{Reynolds number is defined as: } Re = 2UY/\nu \quad (3.87)$$

$$\text{Dincer number is defined as: } Di = U/SY \quad (3.88)$$

$$\text{Biot number is defined as: } Bi_m = h_m Y/D \quad (3.89)$$

- By studying the nature of data and applying regression in power form, we have obtained the following new drying correlations:

- 1) Biot-Reynolds ( $Bi_m$ -Re) Correlation ( $Bi_m = a Re^{-b}$ )

- 2) Biot-Dincer ( $Bi_m$ -Di) Correlation ( $Bi_m = c Di^{-d}$ )

- 3) Biot-Lag Factor ( $Bi_m$ -G) Correlation ( $\ln Bi_m = e \ln G - f$ )

- 4) Biot-Drying Coefficient ( $Bi_m$ -S) Correlation ( $Bi_m = g S^h$ )

The procedure employed to determine the moisture transfer parameters and dimensionless moisture distribution is as follows:

1. Lag factor (G) and drying coefficient (S) are determined by regressing the experimental dimensionless moisture content values against the drying time using the least square curve fitting method.
2. Reynolds number (Re) and Dincer number (Di) are calculated using equation (3.87) and (3.88)

3. Using the developed correlations Biot numbers are estimated for slab, cylinder and sphere.
4. The characteristic roots are then evaluated using the relations in equations (3.82) through (3.84) for three different objects.
5. The moisture diffusivities are then calculated using the equation (3.81).
6. The moisture transfer coefficients are calculated using equation (3.85).
7. Finally the dimensionless moisture distribution is obtained as: (Dincer and Dost, 1996)

$$\Phi = A_1 B_1 \quad (3.87)$$

where for slab:

$$A_1 = \exp((0.2533Bi_m)/(1.3 + Bi_m)) \quad (3.88a)$$

for cylinder:

$$A_1 = \exp((0.5066Bi_m)/(1.7 + Bi_m)) \quad (3.88b)$$

for sphere:

$$A_1 = \exp((0.7599Bi_m)/(2.1 + Bi_m)) \quad (3.88c)$$

and for all objects

$$B_1 = \exp(-\mu_1^2 Fo_m) \quad (3.89)$$

where

$$Fo_m = Dt / Y^2 \quad (3.90)$$



## **CHAPTER 4**

### **RESULTS AND DISCUSSION**

In this chapter, results of analytical and numerical analysis of heat and moisture transfer during drying of regular shaped objects are presented. In the first part, analytical results of heat and moisture transfer during drying of regular objects such as slab, cylinder and sphere are presented. The results obtained from the two-dimensional numerical analysis of heat and moisture transfer during drying are presented for the three regular shaped objects. Finally, new developed drying correlations are presented for drying applications. And at the end of each subsection a comparison has been made between the results obtained from the present study and experimental data available in the literature to validate the present models.

#### **4.1. Results of Analytical Heat and Moisture Transfer Analyses**

##### **4.1.1. 1-D Slab Object**

Convective drying of the rectangular slab is formulated analytically using a Laplace transformation method and a closed form solution for the conduction and diffusion equations are obtained to determine the temperature and moisture content variation in time and coordinate. Table 4.1 gives the drying conditions and properties of a slab object used in the simulation.

**Table 4.1: Drying conditions and properties of apple slab used in the simulation**

Shape	Slab
$T_i$	298 K
$T_d$	323 K
$k$	0.219 W/m K *
$\rho$	856.0 kg/m <sup>3</sup> *
$c_p$	851.0 J/kg K *

[\*Source: Dincer, 1997]

Figure 4.1 shows the temperature variation at different locations inside the slab. Temperature rises rapidly in the early heating period due to convective boundary condition at the surface. This is more pronounced in the surface vicinity of the slab. This can also be seen from Figure 4.2, in which the time derivative of temperature profiles is shown with time. The rapid rise of the temperature at the surface of the slab is because of the internal heat gain in this region.

Figure 4.3 shows the temperature profiles inside the slab, as heating period is variable. Temperature reduces sharply in the slab in the early heating period and attains almost constant slope. This can be seen from Figure 4.4, in which temperature gradient is shown. The sharp variation in temperature gradient in the early heating period is because of the energy transport mechanism. In this case, convective heating situation at the surface results in internal heat gain of the slab in this region. This results in significantly high temperature gradient in the surface region.

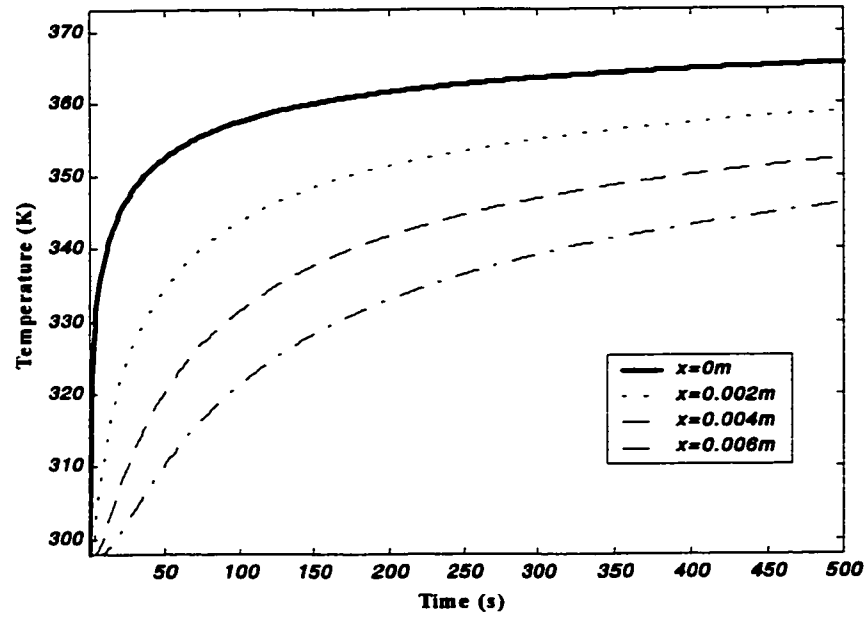


Figure 4.1: Temperature distribution within a slab object at different locations

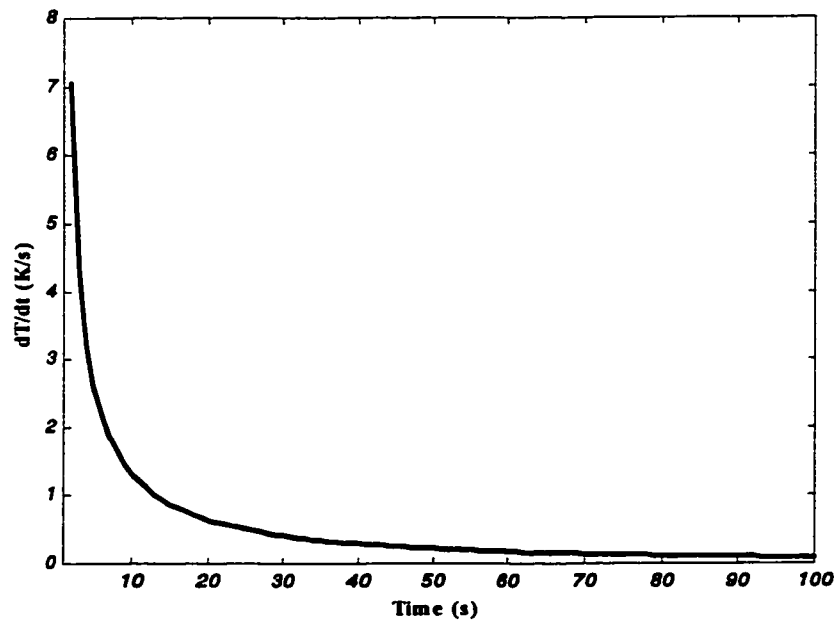


Figure 4.2: Temperature gradient with respect to time in a slab object

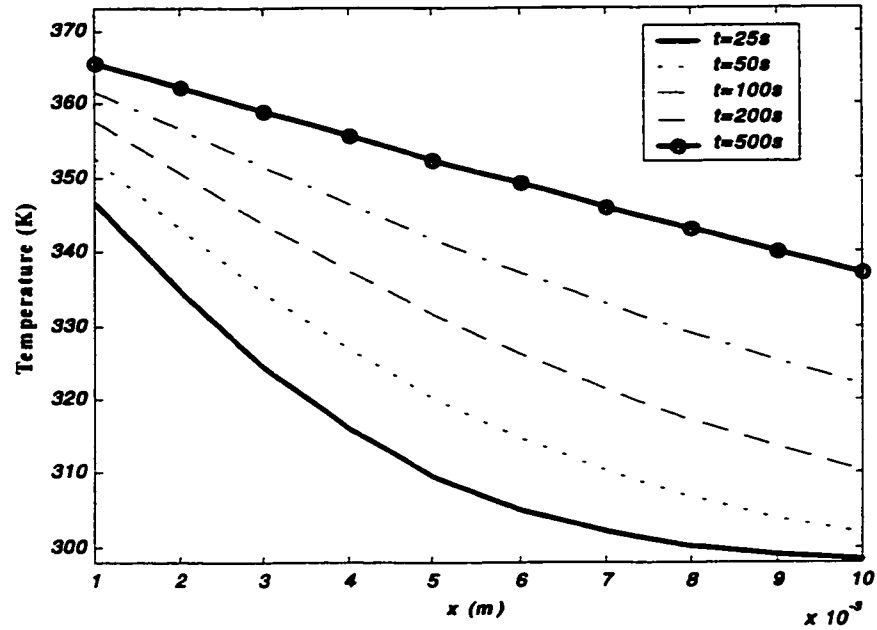


Figure 4.3: Temperature distributions inside a slab object at different drying periods

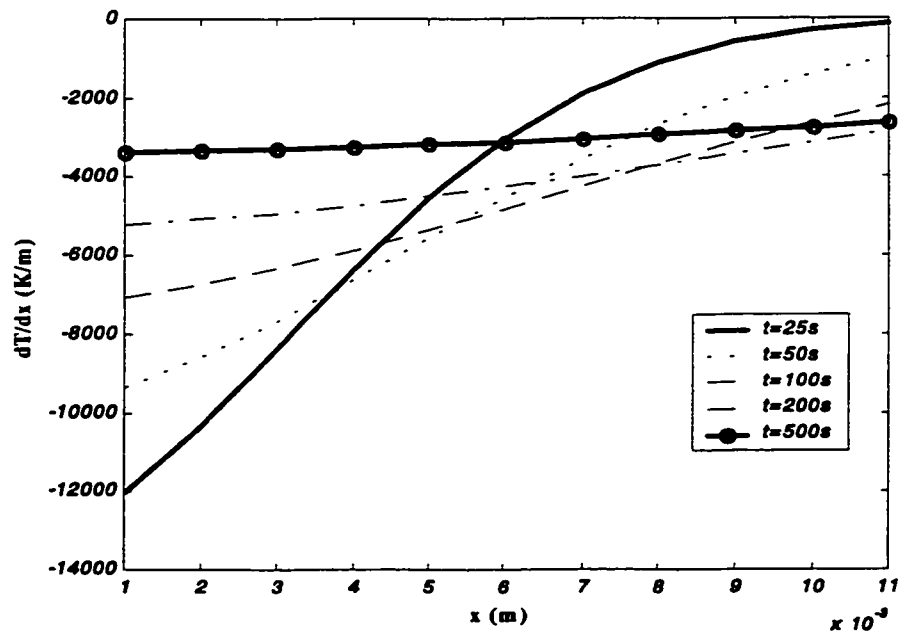


Figure 4.4: Temperature gradient inside a slab object at different drying periods

The temporal variation of moisture content at different depths inside the slab is shown in Figure 4.5. The moisture content reduces as the time period progresses for all depths. The reduction rate of moisture content in the surface region is higher as compared to those corresponding to other depths below the surface. Moreover, in the early heating period moisture content reduces rapidly and as the heating period progresses, the rate of reduction of moisture content becomes less, i.e., it reduces almost steady with progressing heating period. This can also be seen from Figure 4.6.

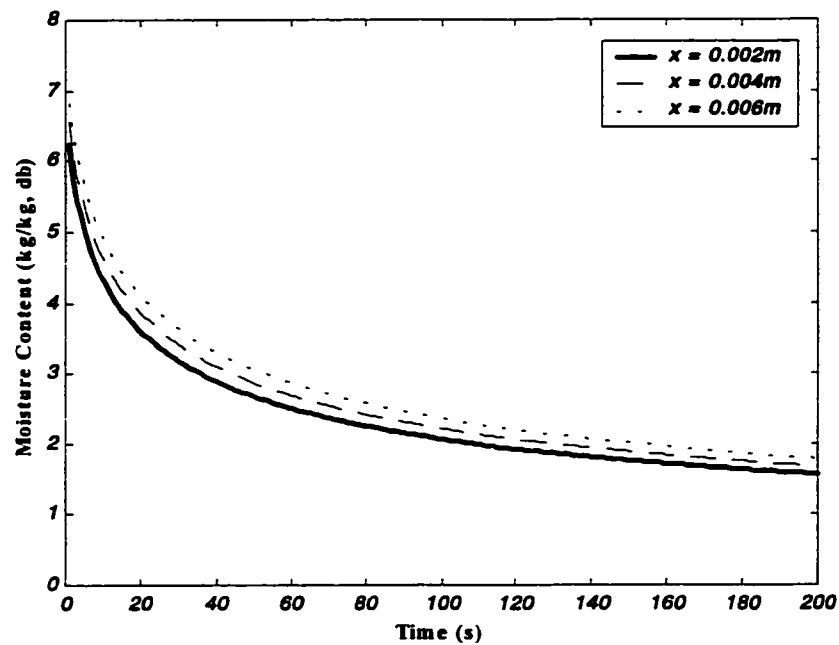


Figure 4.5: Moisture content distribution within a slab object at different locations

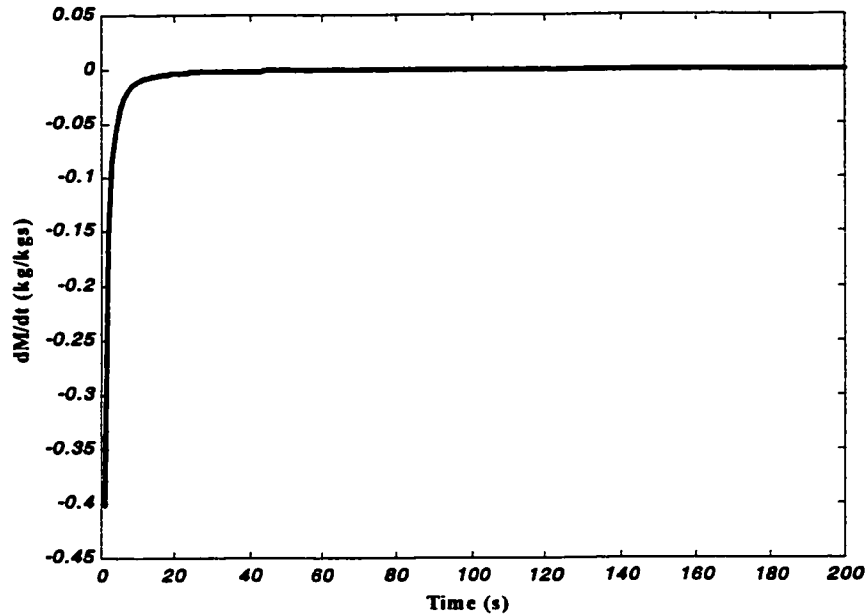


Figure 4.6: Moisture gradient with respect to time in a slab object

#### 4.1.2. 1-D Cylindrical Object

Figure 4.7 shows the dimensionless temperature distribution inside a cylindrical object of different radii subjected to drying. The temperature inside the object increases with the increase in time period and attains steady with advancing time period. As the radius of the cylindrical object increases, the time taken to attain steady temperature increases and consequently, drying time increases.

Figure 4.8 shows the dimensionless moisture distribution inside a cylindrical object of different radii subjected to drying. The moisture content inside the object reduces as the time period progresses and becomes steady with advancing time. As the radius of the cylindrical object increases time taken to attain equilibrium moisture content increases, thereby, drying time increases.

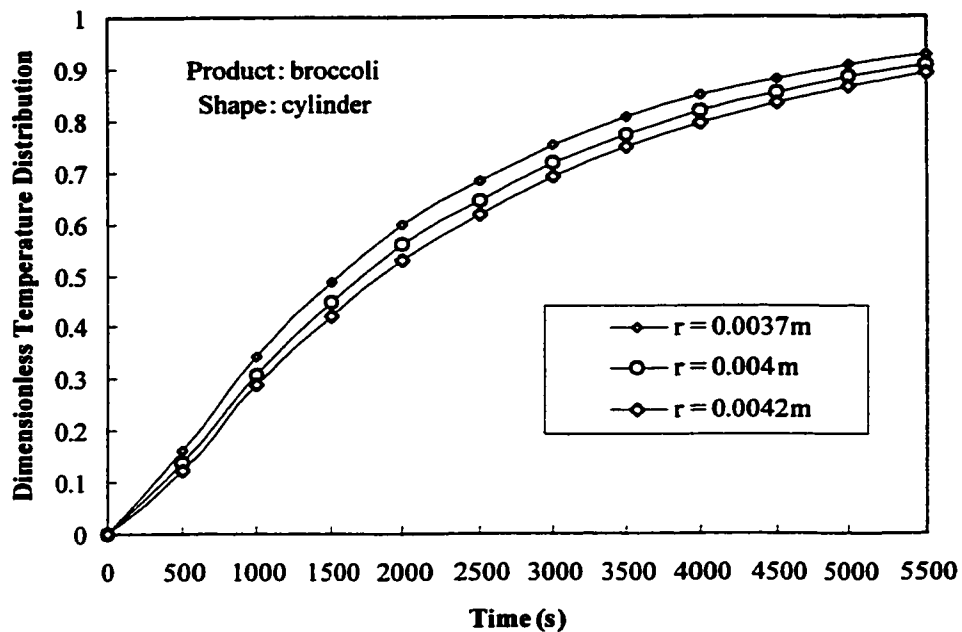


Figure 4.7: Dimensionless temperature distribution inside the cylindrical object of different radii

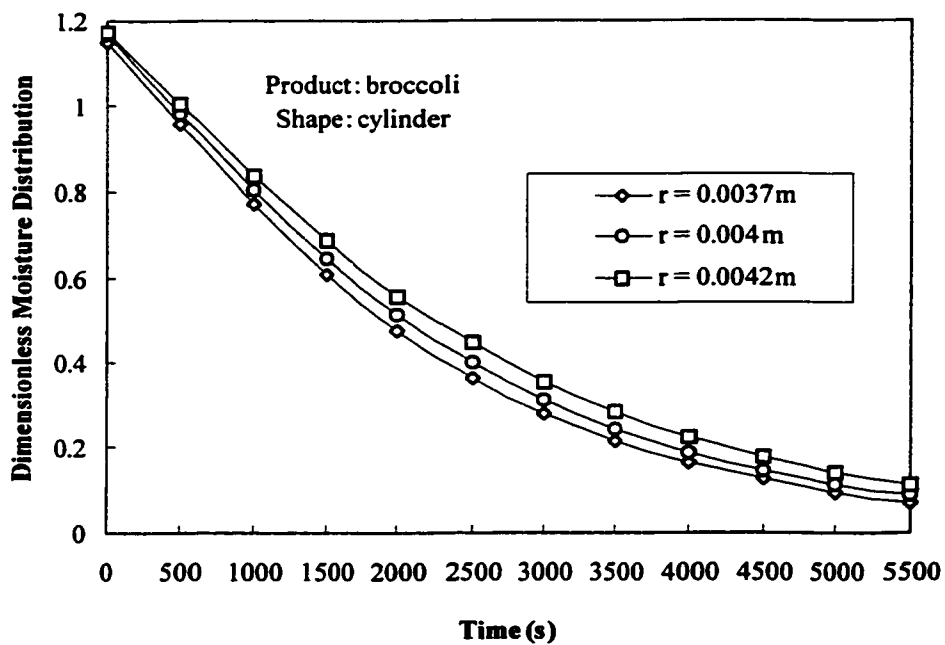


Figure 4.8: Dimensionless moisture distribution inside the cylindrical object of different radii

### 4.1.3. 1-D Spherical Object

The dimensionless temperature distribution inside the spherical object of different radii is shown in Figure 4.9. The temperature in the sphere increases with time and attains steady as the time period progresses. The time taken by the sphere of small diameter to reach the steady temperature is less than the sphere of larger diameters and consequently requires less drying time.

Figure 4.10 shows the dimensionless moisture distribution inside the spherical object of different radii. The moisture content inside the object reduces with increasing time period and the time required to attain the equilibrium moisture content is less for sphere of small diameter than large diameter spheres.

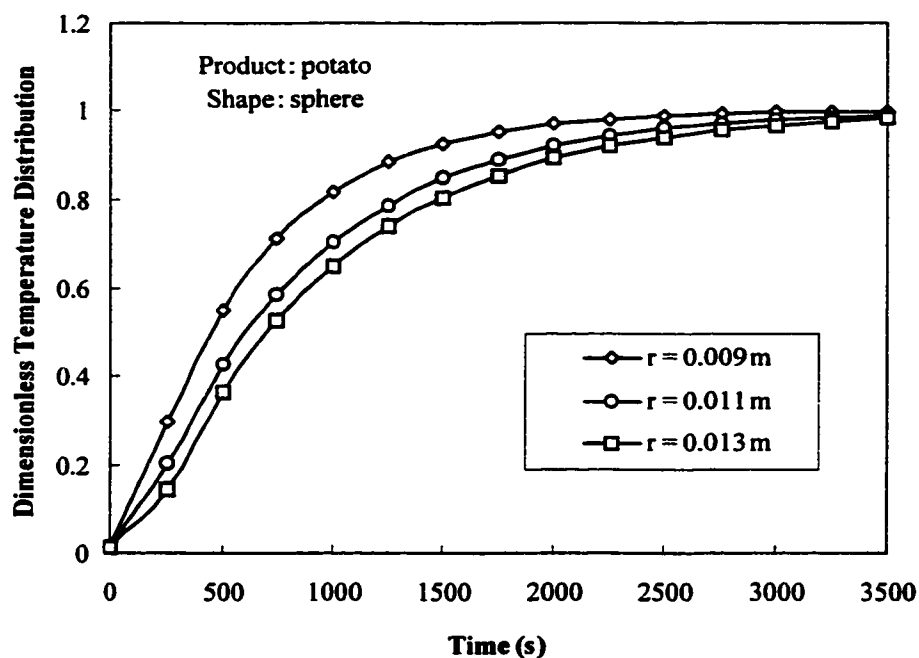


Figure 4.9: Dimensionless temperature distribution inside the spherical object of different radii



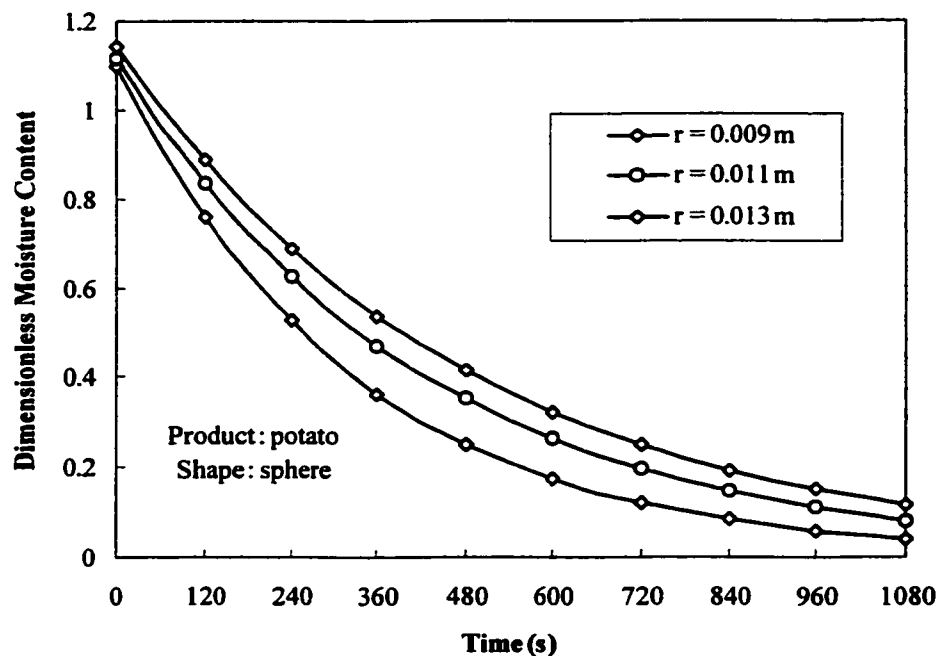


Figure 4.10: Dimensionless moisture distribution inside the spherical object of different radii

In the present section, a closed form (analytical) solutions for temperature and moisture distribution inside the regular objects are presented for drying applications. It is found that temperature rises rapidly in the early heating period and as the heating period progresses, the rise of temperature attains almost steady with advancing heating period. The moisture gradient is higher in the early heating period and as heating progresses, the moisture gradient remains almost steady.

## 4.2. Results of Numerical Heat and Moisture Transfer Analyses

### 4.2.1. 2-D Slab Object

This sub-section presents the temperature and moisture distribution inside the slab of dimension  $0.03 \times 0.02$  m. The product considered in the simulation was apple. In order to investigate the effect of heat transfer coefficient on the temperature distribution inside the slab, five different heat transfer coefficients are considered ranging from 25-250  $W/m^2K$ . Thermophysical properties and the drying conditions used in the simulation are listed in Table 4.2.

Table 4.2: Thermophysical properties and drying conditions used in the simulation

K	0.576W/mK (*)
$\rho$	856 kg/m <sup>3</sup> (*)
$c_p$	1929.72J/kgK (*)
H	25-250W/m <sup>2</sup> K
$h_m$	0.0001m/s
$T_i$	298K
$T_d$	323K
$M_i$	7.196kg/kg(db)
RH	0.196kg/kg(db)

[\*Source: Dincer, 1997]

Figures 4.11-4.16 show the temperature distribution in the slab for different time periods. Temperature in the slab increases as the time period progresses. This is because of the higher ambient temperature than the slab temperature. The temperature contours in

the slab is elliptic profiles due to the rectangular shape of the drying product. Moreover, temperature distribution inside the slab is non-uniform, giving an indication that the temperature dependent moisture diffusivity varies in the slab, which in turn affects the rate of moisture diffusion in the slab.

The variation of reduced center temperature and reduced surface temperature for different heat transfer coefficients are shown in Figures 4.17 and 4.18 respectively. Reduced center temperature and surface temperature increases with the increase in heat transfer coefficient. The time required to reach the maximum limit (unity) is minimum for the maximum heat transfer coefficient. This is clear that increasing the heat transfer coefficient will enhance the heat transfer rate. The optimal heat transfer coefficient in the drying application depends on the nature of drying, initial temperature of the product to be dried, type of the product and its moisture content.

Figures 4.19 and 4.20 show the variation of reduced center temperature gradient and reduced surface temperature gradient for different heat transfer coefficients respectively. The reduced center temperature gradient initially increases and then decreases with time for all heat transfer coefficients considered here. The initial increase is due to sudden increase of temperature after steady behavior of temperature for a certain period of time; also refer to as warming up of the solid. The reduced surface temperature gradient decreases with time and the maximum heat transfer coefficient has the highest gradient all the time and shows the highest heat transfer rate for the maximum heat transfer coefficient.

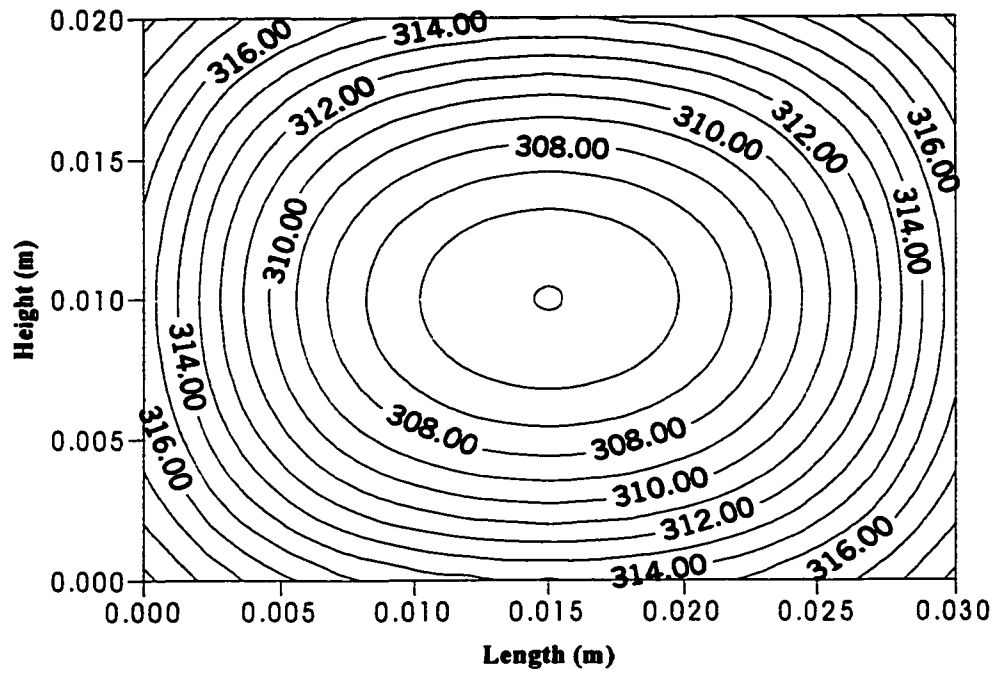


Figure 4.11: Temperature distribution inside a slab object after 100 s

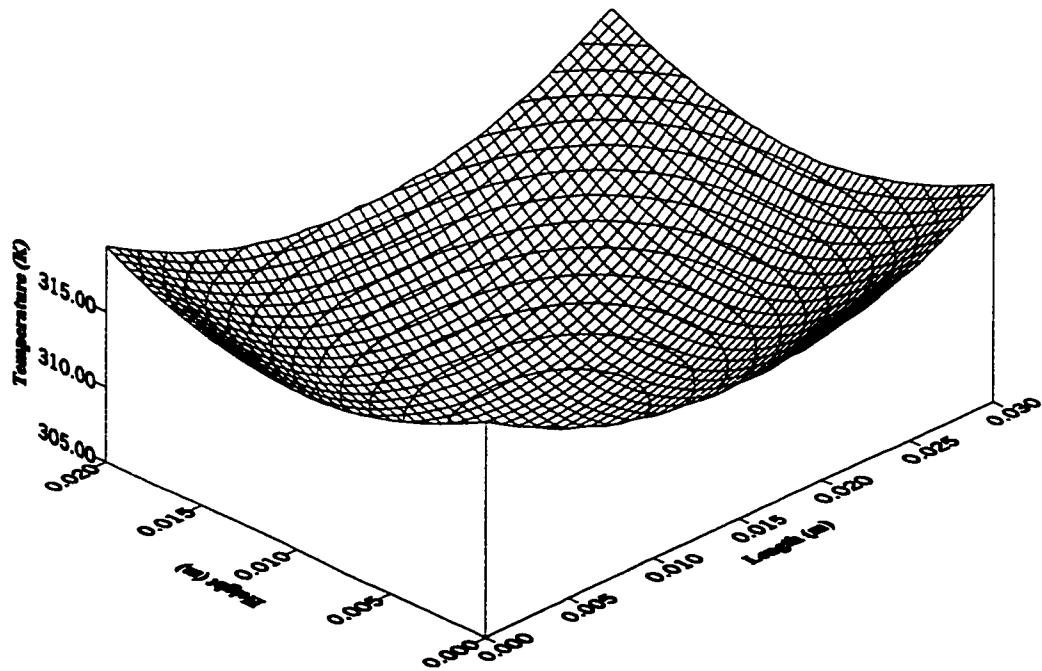


Figure 4.12: 3-D plot showing temperature distribution inside a slab object after 100 s

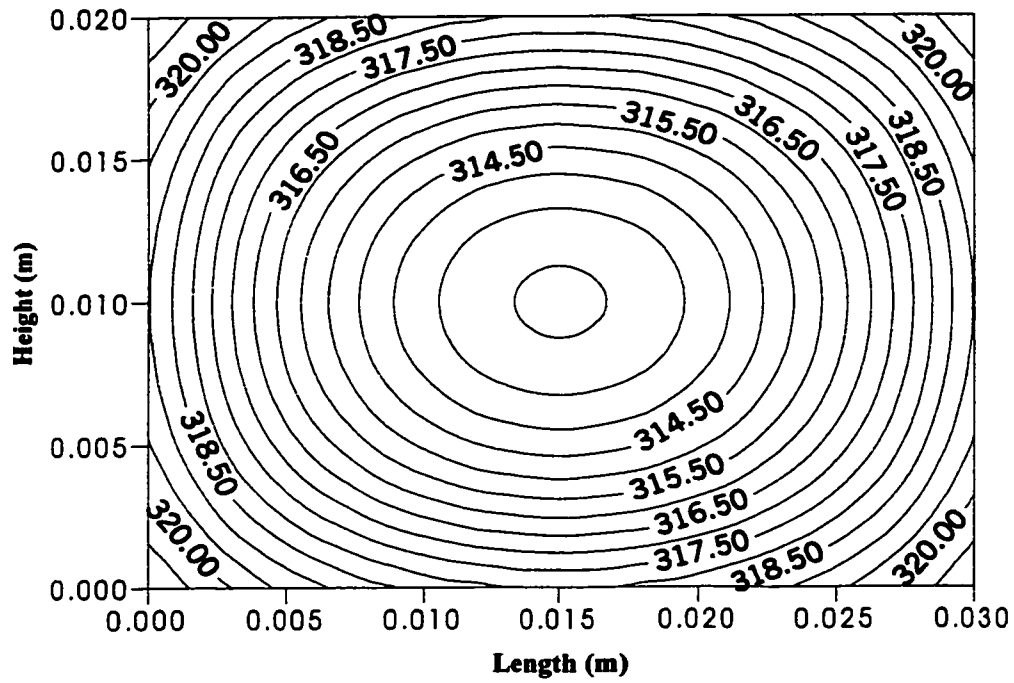


Figure 4.13: Temperature distribution inside a slab object after 200 s

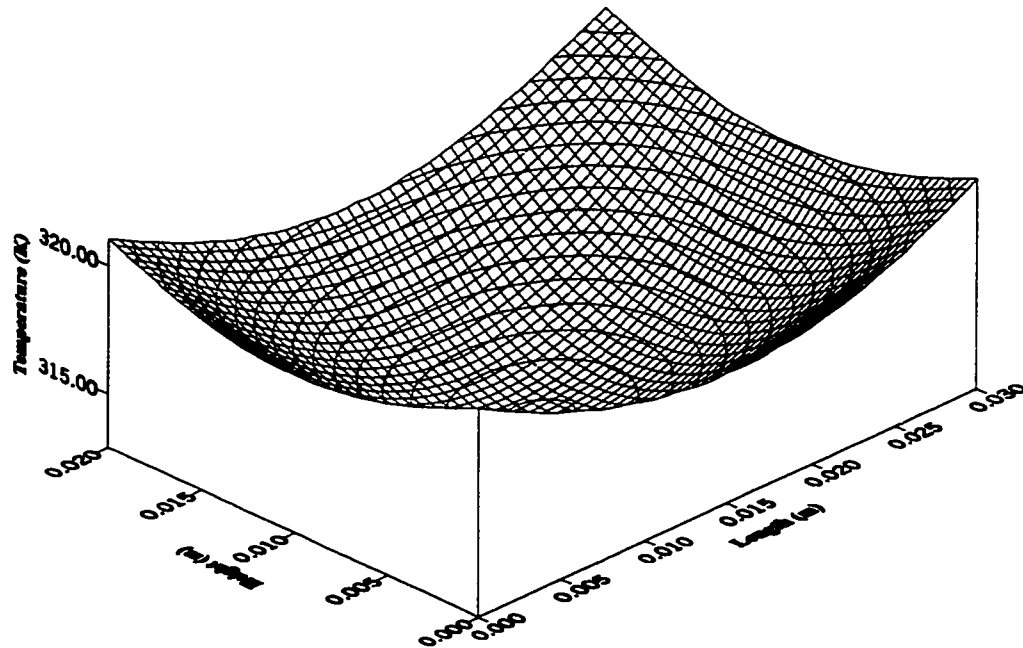


Figure 4.14: 3-D plot showing temperature distribution inside a slab object after 200 s

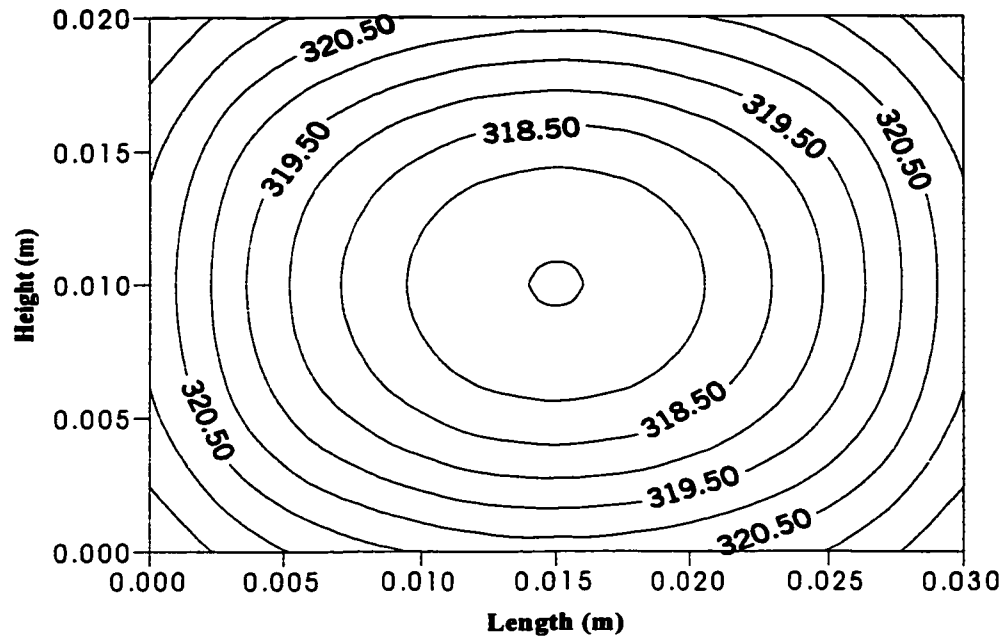


Figure 4.15: Temperature distribution inside a slab object after 300 s

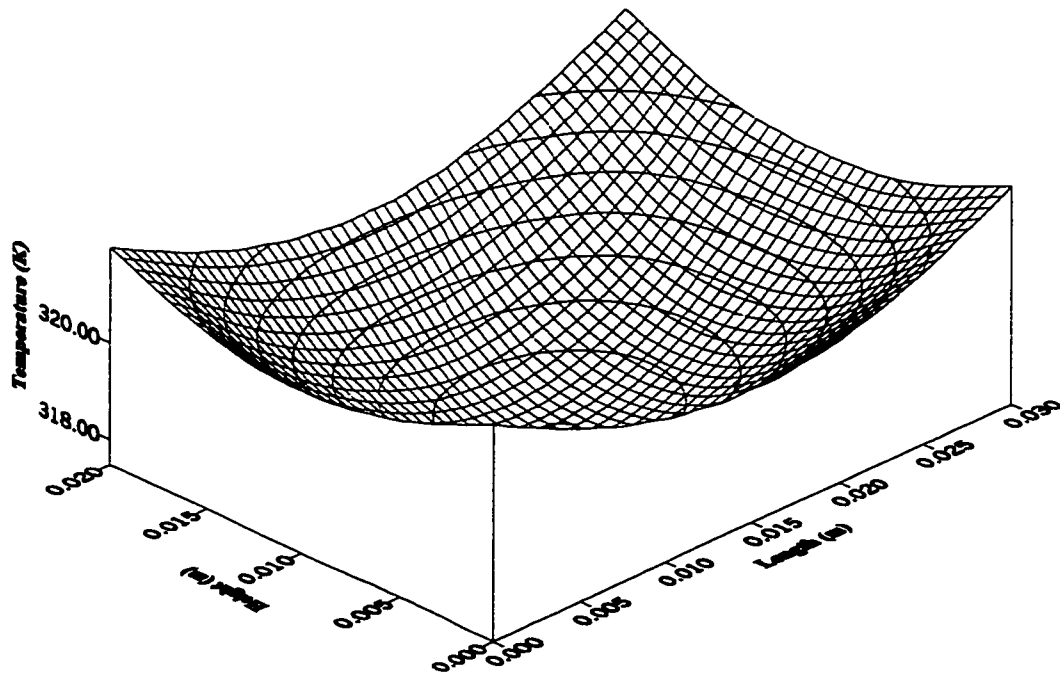


Figure 4.16: 3-D plot showing temperature distribution inside a slab object after 300 s

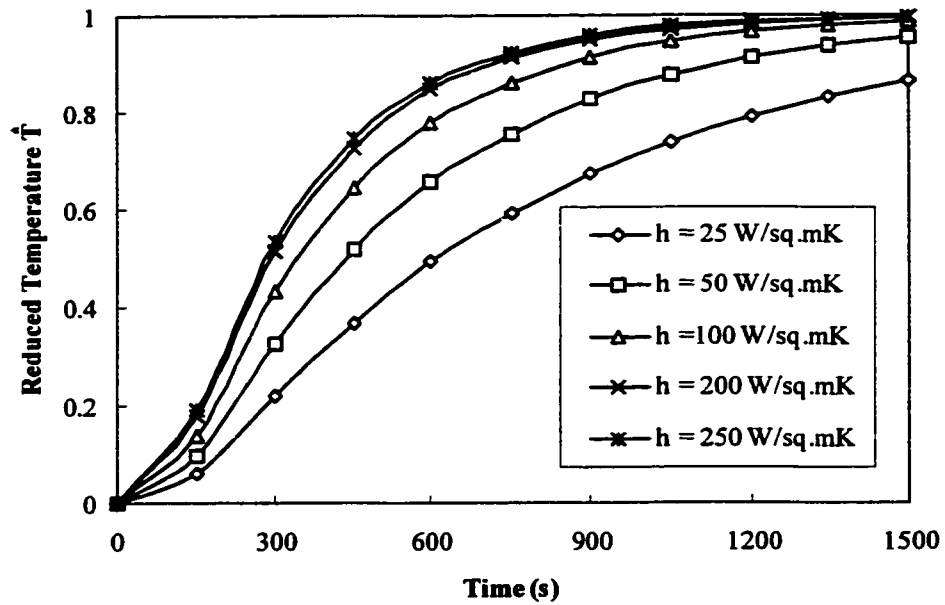


Figure 4.17: Variation of reduced center temperature in a slab object for different heat transfer coefficients

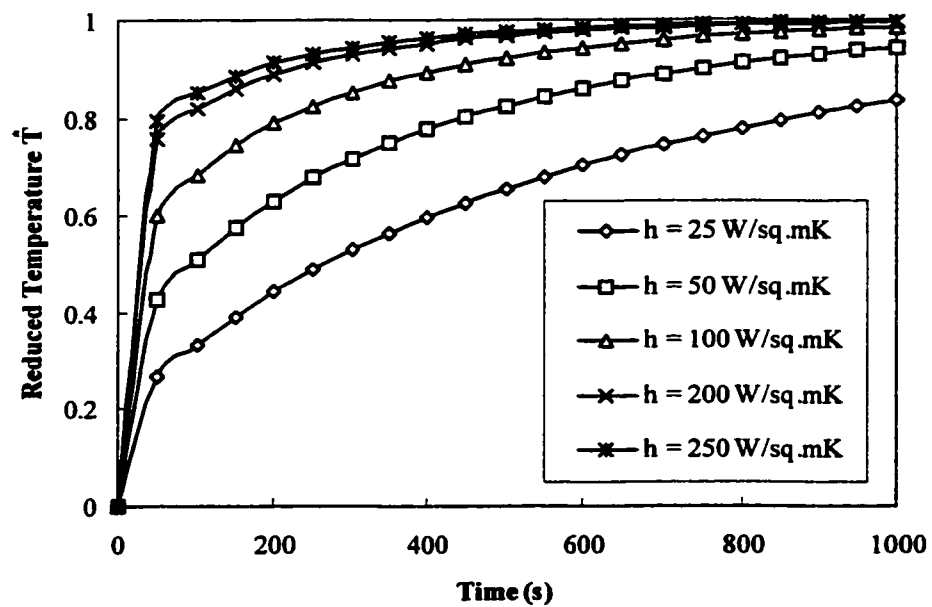


Figure 4.18: Variation of reduced surface temperature in a slab object for different heat transfer coefficients

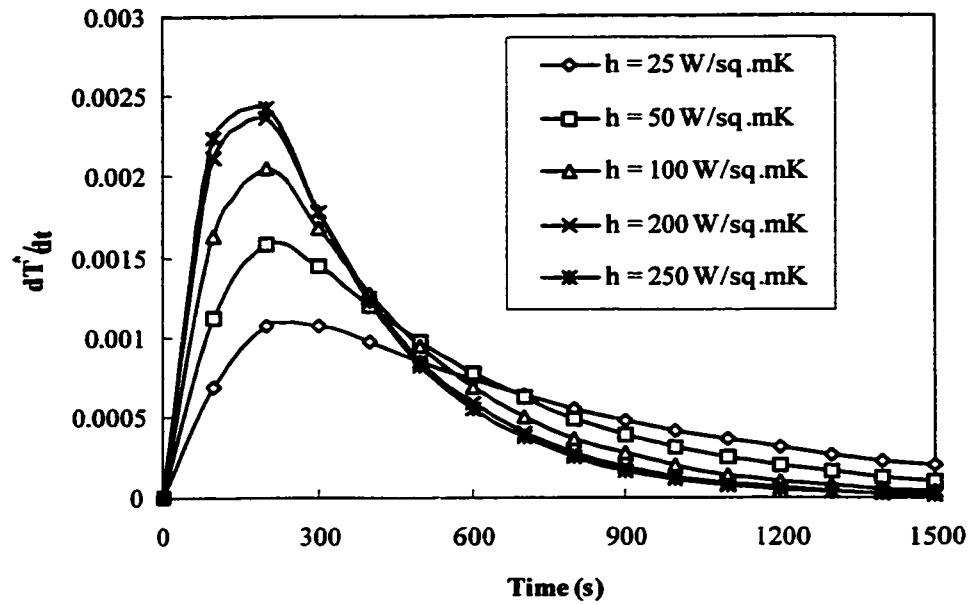


Figure 4.19: Variation of reduced center temperature gradient in a slab object for different heat transfer coefficients

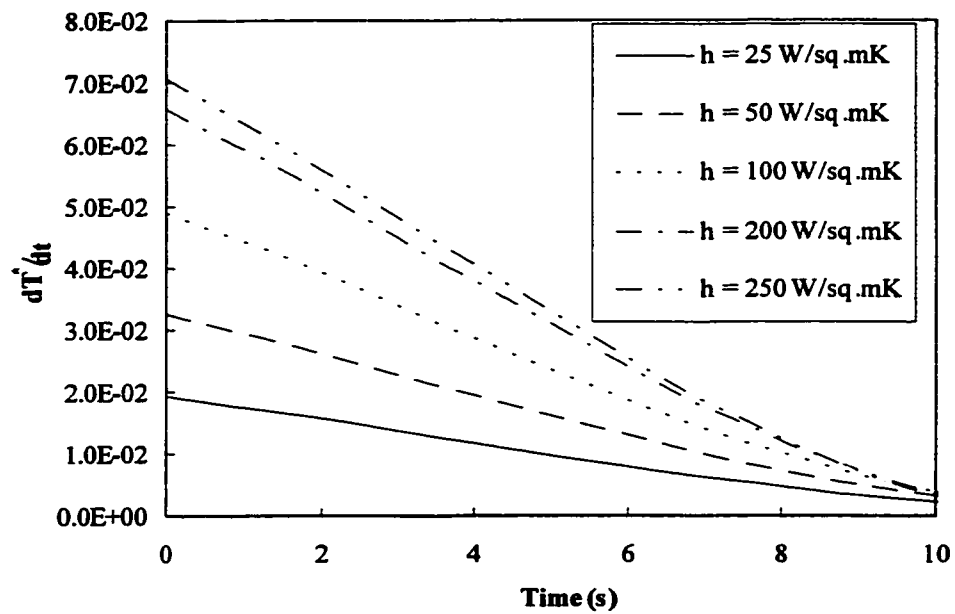


Figure 4.20: Variation of reduced surface temperature gradient in a slab object for different heat transfer coefficients



The moisture distribution in a rectangular slab for different time periods is shown in Figures 4.21- 4.26. The moisture in the slab reduces as the time period progresses. The initial moisture content reduces to half of its initial value at the center of the slab after the time period of 300 s. Since the slab is rectangular, the resulting contours are in elliptic shape. The moisture distribution inside the slab is not uniform, therefore the time required to reduce the moisture content to half of its initial value varies at each location in the rectangular slab.

Figure 4.27 shows the variation reduced center and surface moisture content with time. The reduced moisture content at the surface and at the center reduces as the time period progresses. Both profiles have the same trend but the reduction of moisture content is faster at the surface than that corresponding to the center.

Figure 4.28 shows the rate of drying with time. It exhibits the general trend in which rate of drying takes place in two periods. First it is constant for some period of time representing the constant rate period and then starts decreasing as the time period progresses expressing the falling rate period.

The comparison of center temperature and moisture distributions inside the slab, calculated from the present analytical and numerical models, and obtained from the experimental data available in the literature are shown in Figures 4.29 and 4.30. Experimental drying conditions and product properties are listed in Table 4.3. A good agreement has been found between the calculated and measured results. The difference between the calculated and experimental values may be due to the errors in the experimental measurement and the assumptions made in the present analysis as indicated earlier.

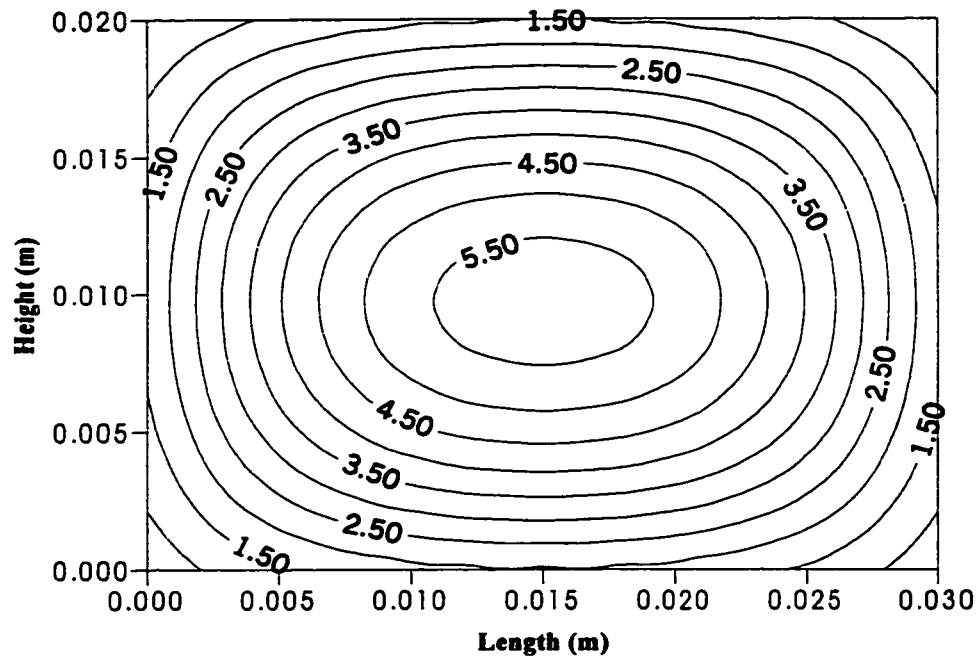


Figure 4.21: Moisture distribution inside a slab object after 100 s

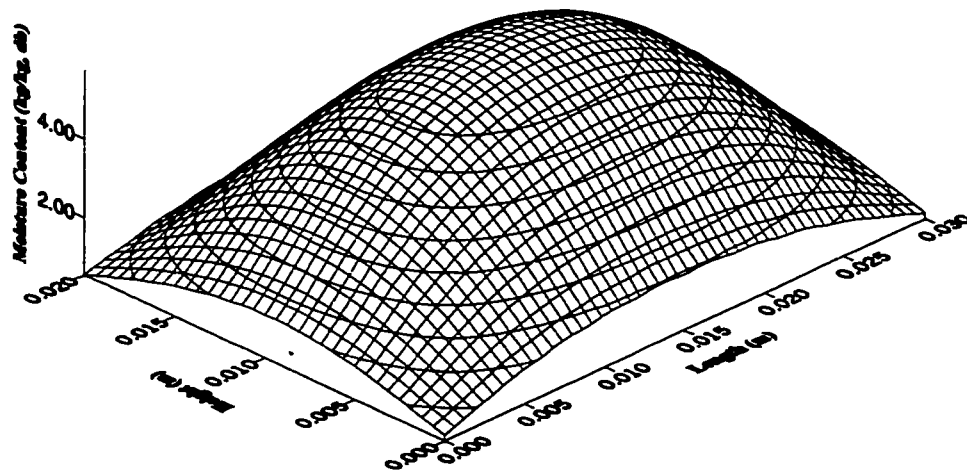


Figure 4.22: 3-D plot showing moisture distribution inside a slab object after 100 s

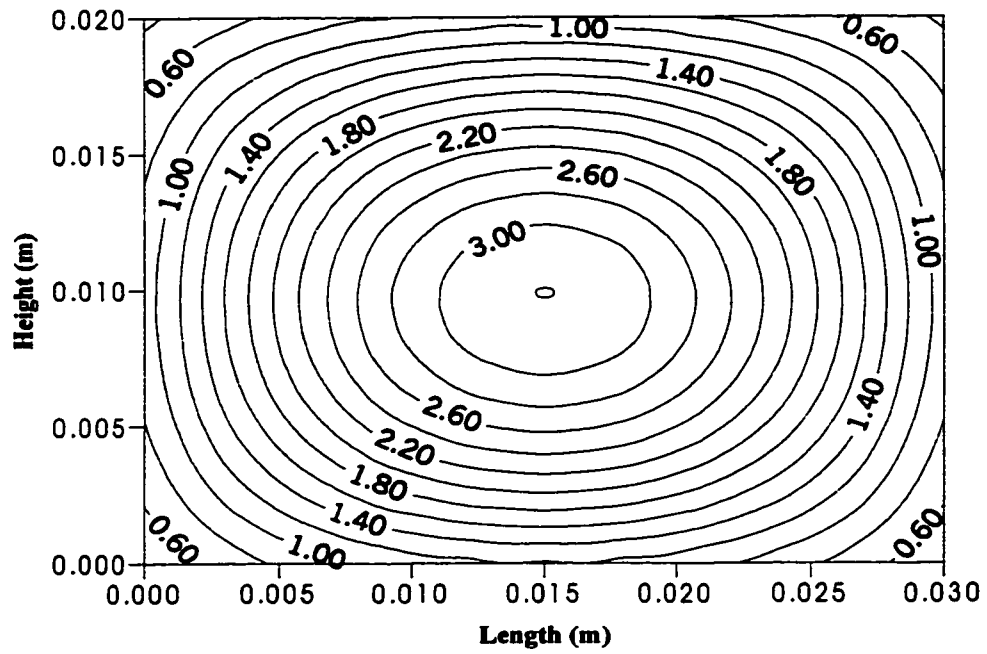


Figure 4.23: Moisture distribution inside a slab object after 200 s

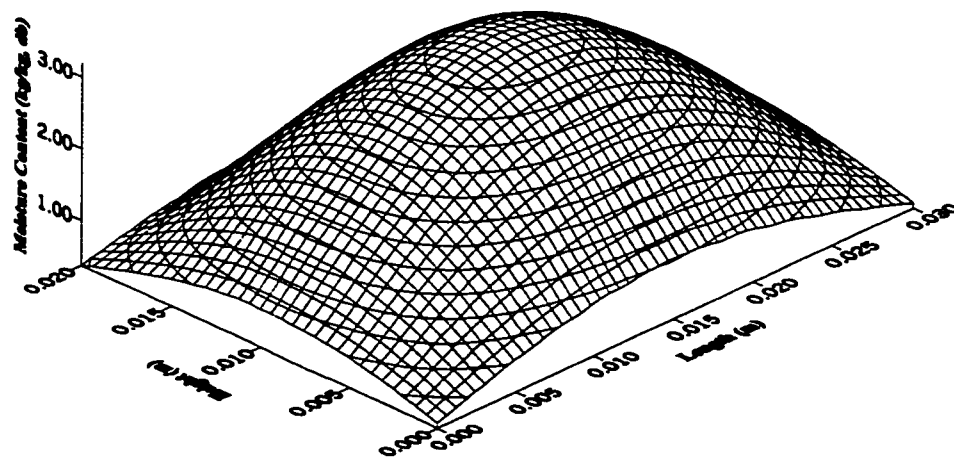


Figure 4.24: 3-D plot showing moisture distribution inside a slab object after 200 s

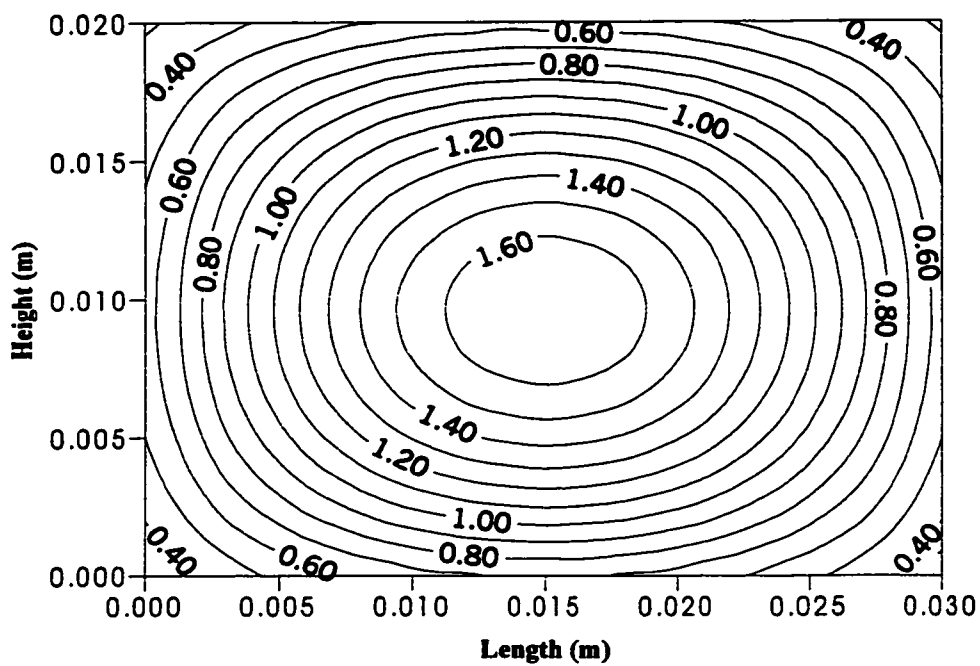


Figure 4.25: Moisture distribution inside a slab object after 300 s

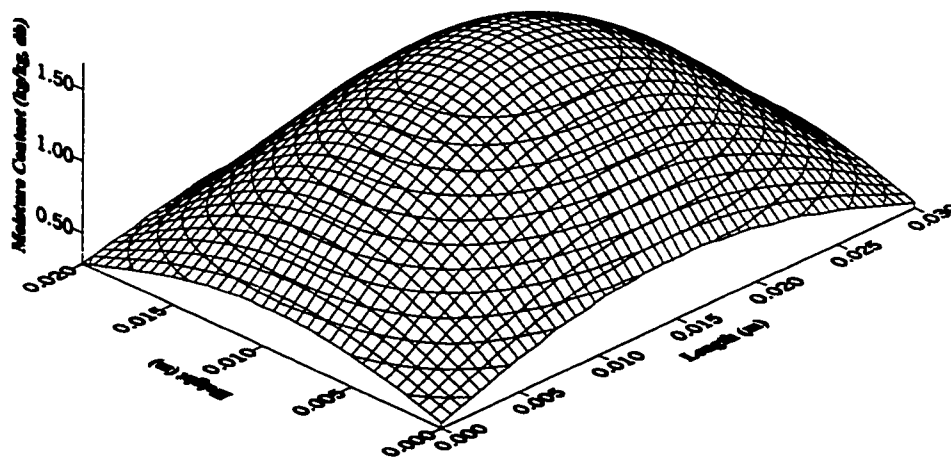


Figure 4.26: 3-D plot showing moisture distribution inside a slab object after 300 s

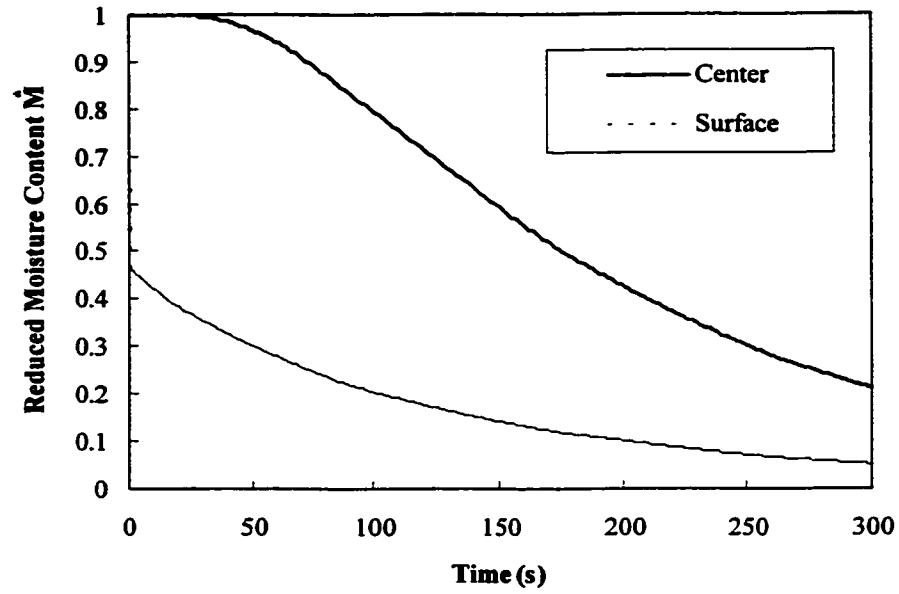


Figure 4.27: Variation of reduced center and surface moisture content in a slab object with respect to time

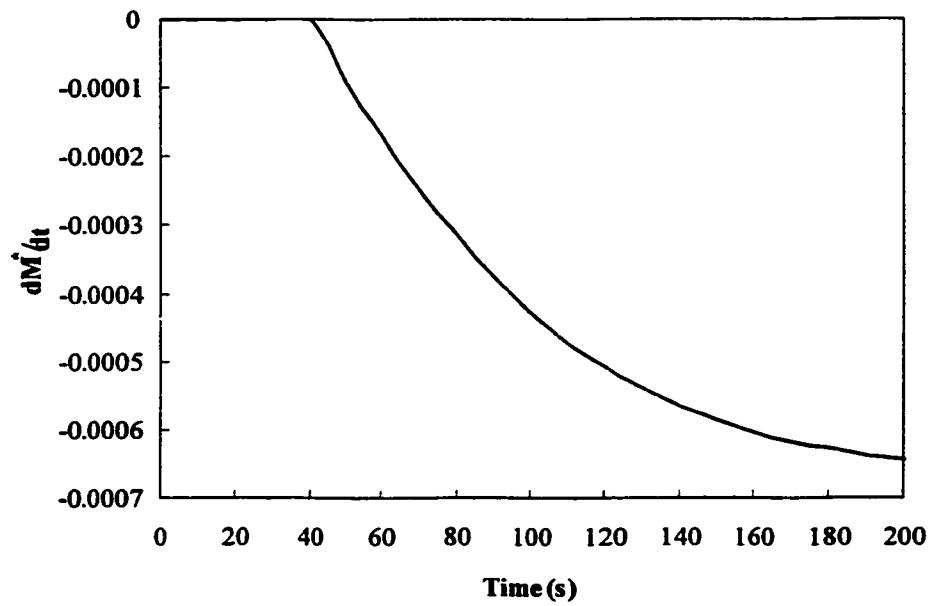


Figure 4.28: Drying rate variation with time in a slab object

Table 4.3: Experimental drying conditions and product properties

Product	Slab shaped apple
Size	4.8×4.9×2.0 cm
$T_i$	303 K
$T_d$	354 K
$M_i$	87 %
RH	12 %
$k$	$0.148+0.493 \times M_i$ (W/mK)*
$\rho$	856.0 kg/m <sup>3</sup> *
$c_p$	$(1.4+3.22 \times M_i) \times 1000$ (J/kgK)*
Reference	Chiang and Petersen (1987)

[\*Source: Dincer, 1997]

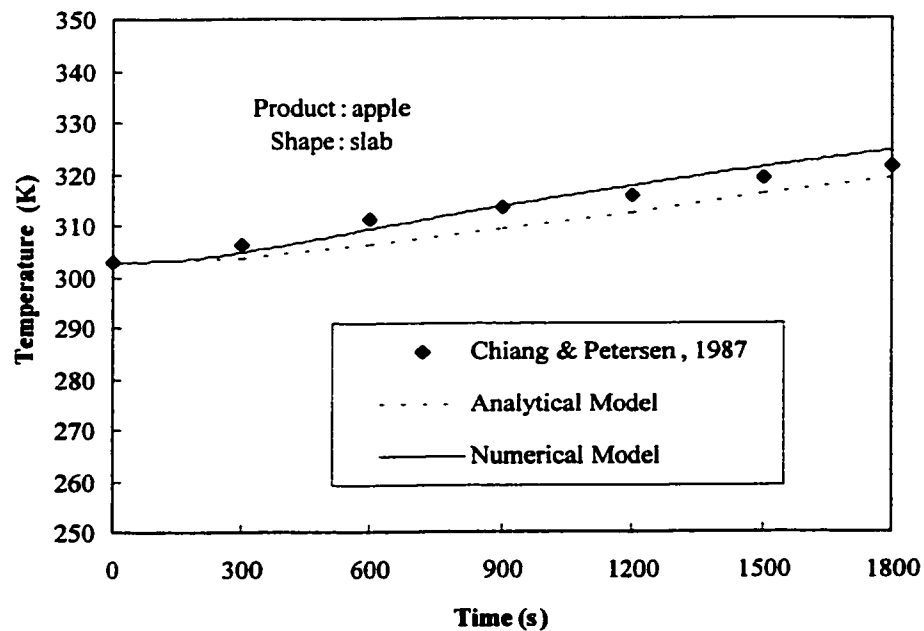


Figure 4.29: Measured and calculated center temperature distribution in a slab object

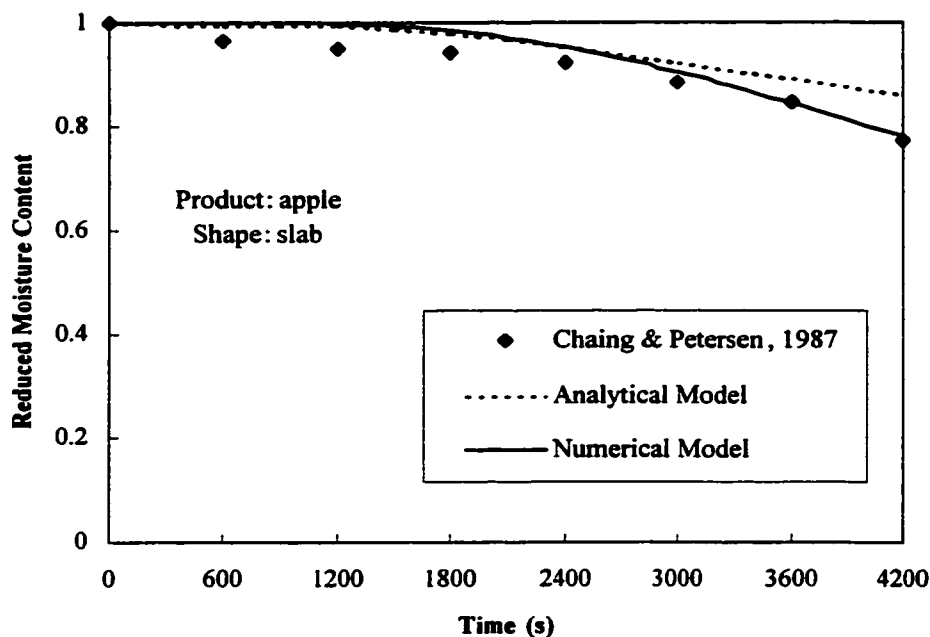


Figure 4.30: Measured and calculated center moisture content distribution in a slab object

#### 4.2.2. 2-D Cylindrical Object

In this sub-section temperature and moisture profiles obtained for the cylindrical object at different time periods are presented. The product considered in the simulation was broccoli of diameter 0.007 m and length 0.02 m. The heat transfer coefficient was varied between 25-250 W/m<sup>2</sup>K. This case enables to investigate the effect of heat transfer coefficient on temperature distribution. Thermophysical properties and the drying conditions used in the simulation are listed in Table 4.4.

Table 4.4: Thermophysical properties and drying conditions used in the simulation

$k$	0.148+0.493M W/mK (*)
$\rho$	2195.27 kg/m <sup>3</sup> (*)
$c_p$	(0.837+1.256M)×1000J/kgK (*)
$h$	25-250W/m <sup>2</sup> K
$h_m$	0.0001m/s
$T_i$	298K
$T_d$	333K
$M_i$	9.57kg/kg(db)
RH	1.18kg/kg(db)

[\* Source: Dincer, 1997]

Figures 4.31-4.36 show the temperature distribution in the cylindrical object for different time periods. Temperature in the cylinder increases as the time period progresses. This is because of the higher ambient temperature than the temperature of the object. Moreover, temperature in the cylinder is non-uniform, maximum at the surfaces and minimum at the center.

The variations of reduced temperature at the center and at the surface for different heat transfer coefficients are shown in Figures 4.37 and 4.38. The reduced center and surface temperatures increase with increasing heat transfer coefficient. The reduced center and surface temperatures attain the maximum limit (unity) for highest heat transfer coefficient considered here. The reduced surface temperature rises sharply during the first time step and then increases in a parabolic fashion. The rapid rise of the temperature in



the surface vicinity of the object is because of the internal energy gain in this region, which is due to convective heating of the surface.

The variations of reduced center temperature gradient and reduced surface temperature gradient with time are shown in Figures 4.39 and 4.40 respectively. The reduced center temperature gradient initially increases for a certain period of time and it decreases continuously after reaching a peak value. The increase is because of considerably small change of temperature during early stages of heating and temperature increases rapidly due to gain in internal energy as the heating period progresses. The reduced surface temperature gradient decreases sharply at the initial time step and then becomes almost constant as the time period progresses. This is again due to convective heating of the surface, which dominates over the conduction losses from the surface vicinity to the bulk of the solid object.

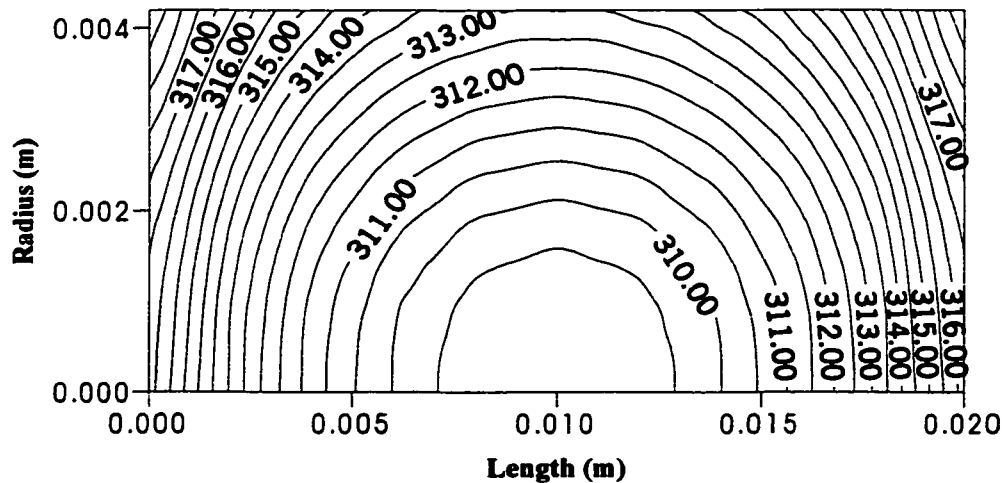


Figure 4.31: Temperature distribution inside a cylindrical object after 100 s

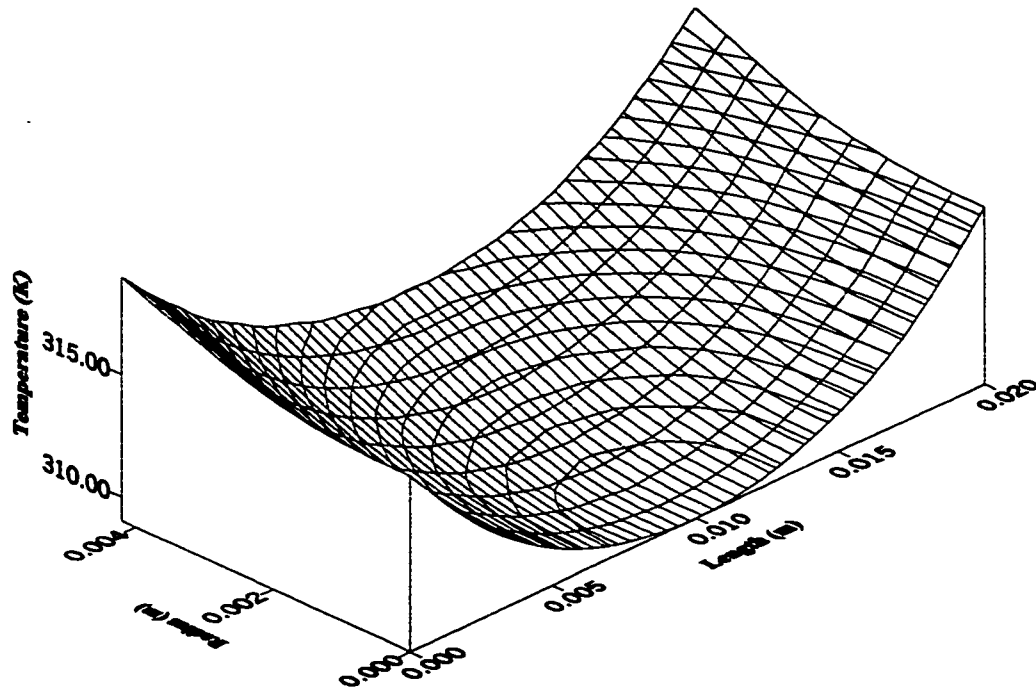


Figure 4.32: 3-D plot showing temperature distribution inside a cylindrical object after 100 s

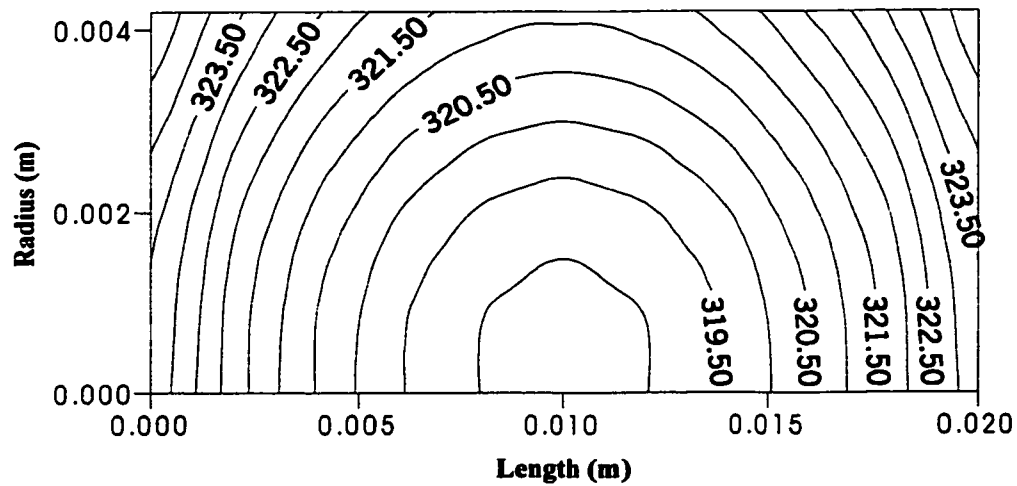


Figure 4.33: Temperature distribution inside a cylindrical object after 200 s

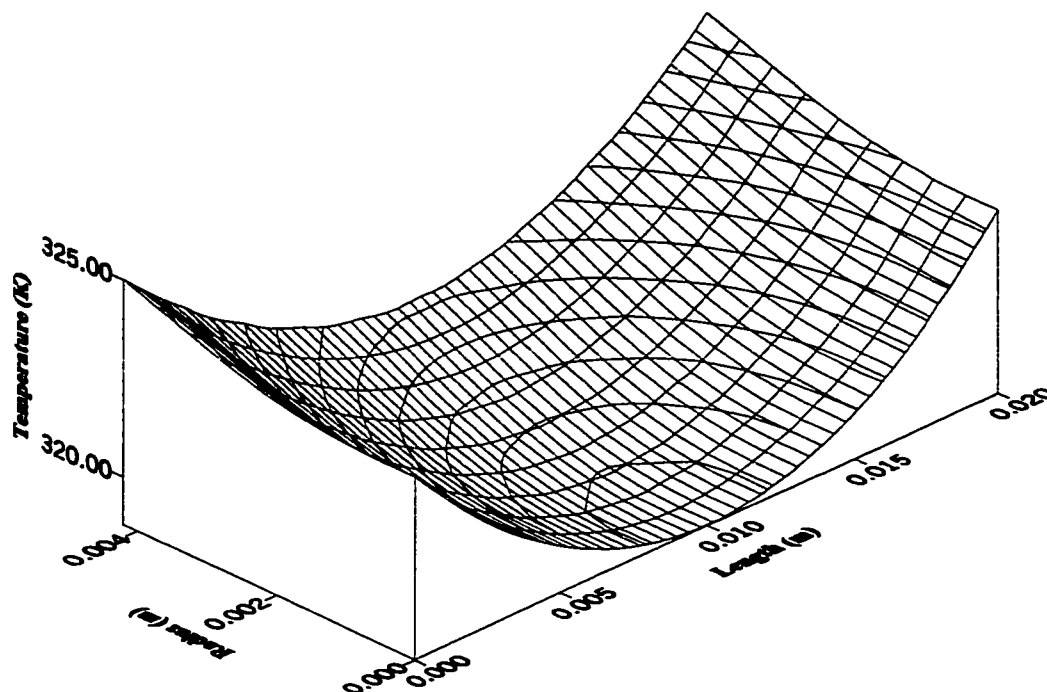


Figure 4.34: 3-D plot showing temperature distribution inside a cylindrical object after 200 s

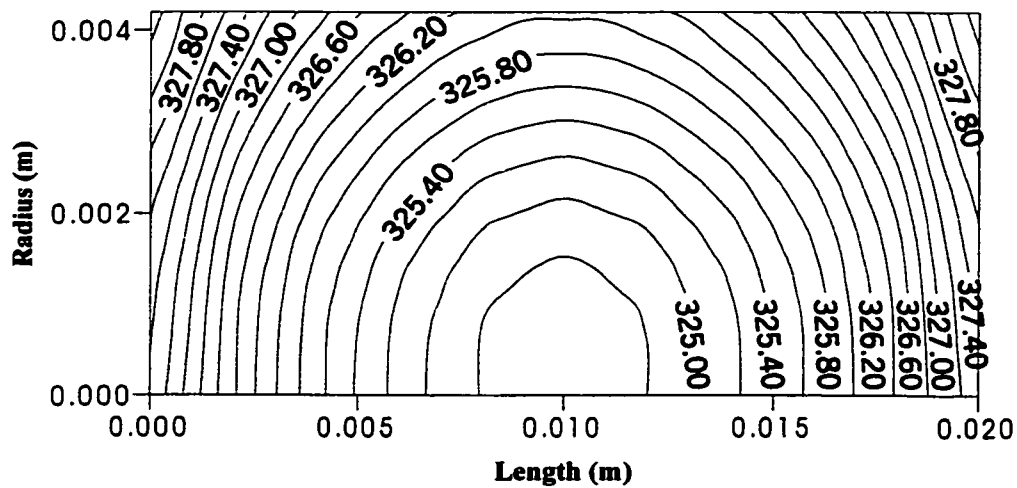


Figure 4.35: Temperature distribution inside a cylindrical object after 300 s

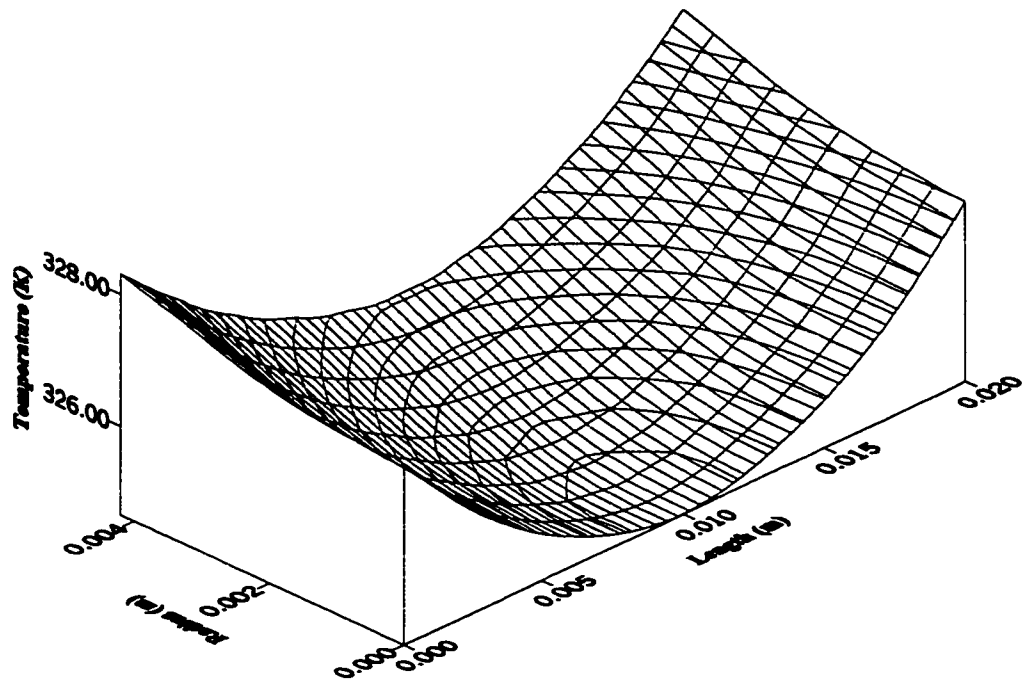


Figure 4.36: Surface plot showing temperature distribution inside a cylindrical object after 300 s

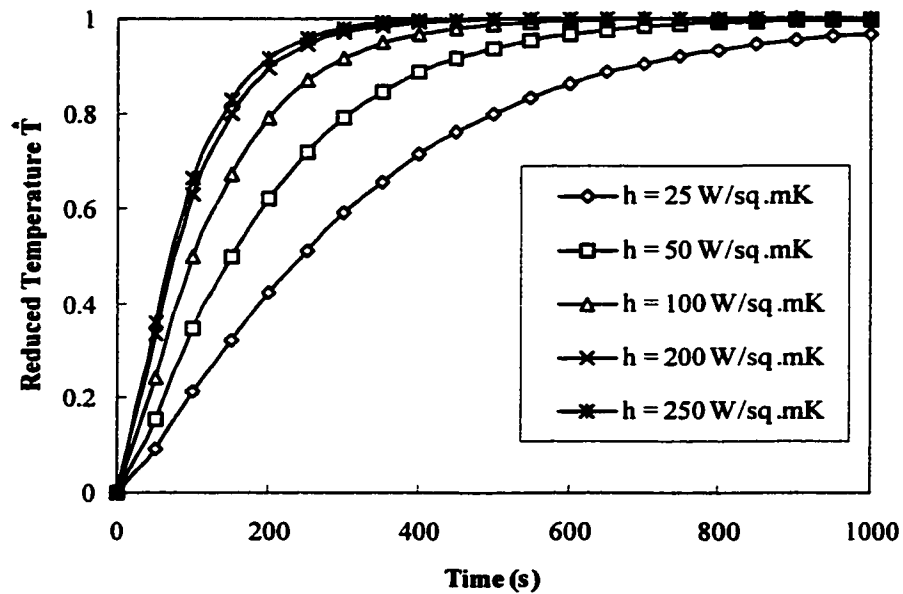


Figure 4.37: Variation of reduced center temperature in a cylindrical object for different heat transfer coefficients

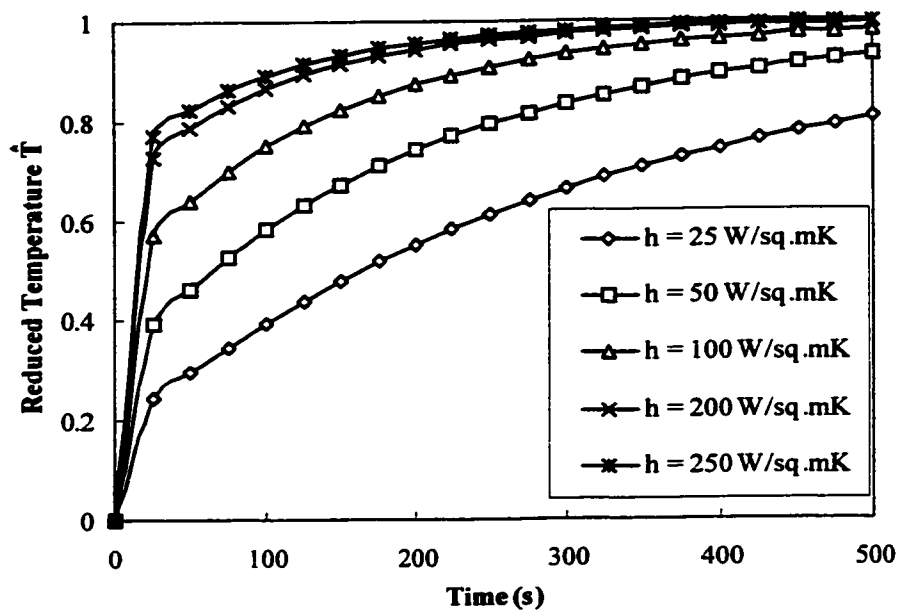


Figure 4.38: Variation of reduced surface temperature in a cylindrical object for different heat transfer coefficients

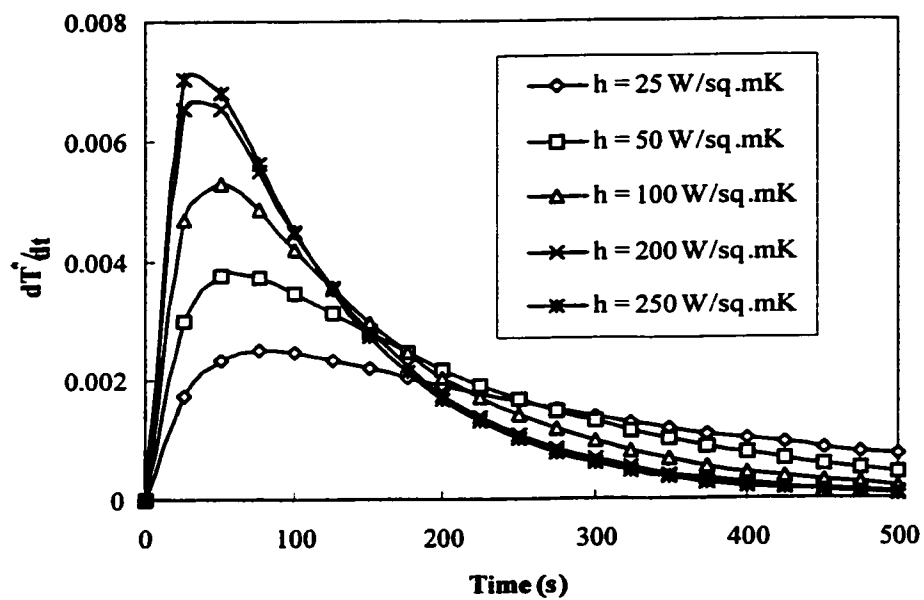


Figure 4.39: Variation of reduced center temperature gradient in a cylindrical object for different heat transfer coefficients

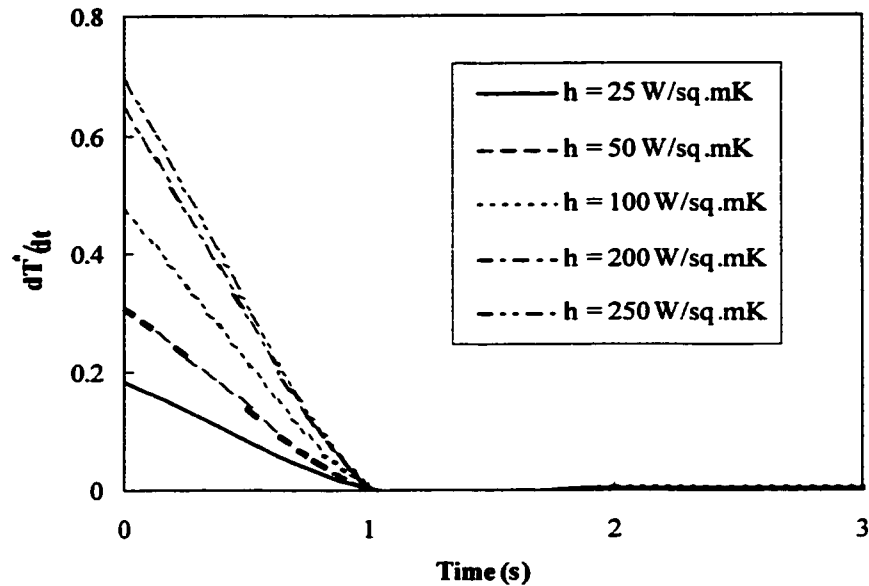


Figure 4.40: Variation of reduced surface temperature gradient in a cylindrical object for different heat transfer coefficients.

Figures 4.41-4.43 show the moisture distribution in a cylindrical object for different time periods. The moisture content inside the cylinder reduces as the time period increases. The reduction rate of moisture content in the surface region is higher as compared to the interior of the object. Moreover, in the early heating period moisture content reduces rapidly and as the heating period progresses the rate of reduction of moisture content becomes less, i.e., it reduces almost steady with progressing heating period. This is more pronounced in the surface vicinity. The rapid drop of moisture content in the early heating period is because of the high moisture gradient in this region, which in turn derives considerable diffusion rates from inside to the surface.

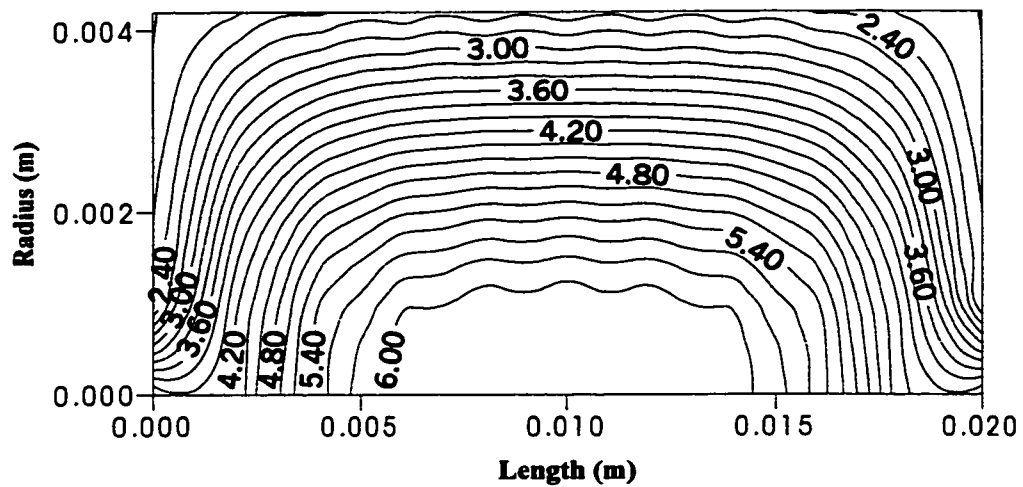


Figure 4.41: Moisture distribution inside a cylindrical object after 100 s

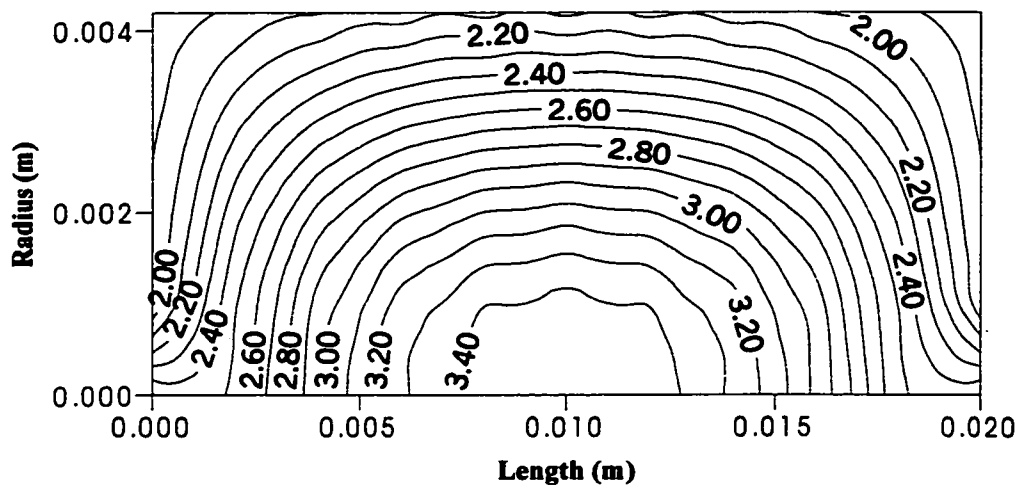


Figure 4.42: Moisture distribution inside a cylindrical object after 200 s

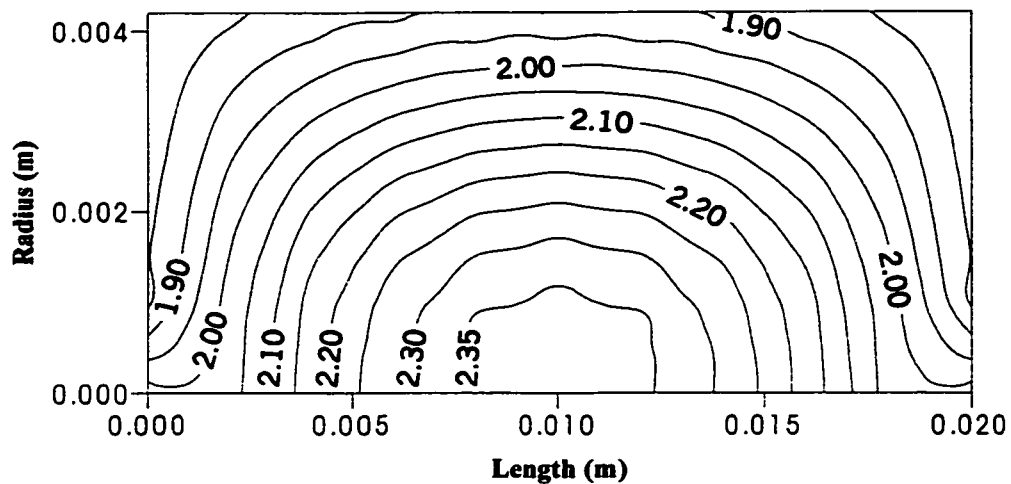


Figure 4.43: Moisture distribution inside a cylindrical object after 300 s

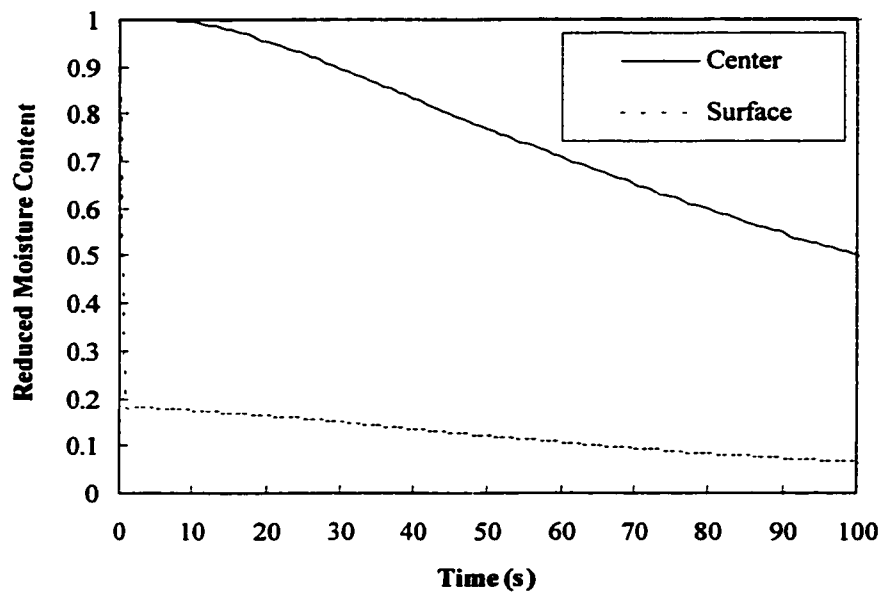


Figure 4.44: Variation of reduced center and surface moisture content in a cylindrical object with time



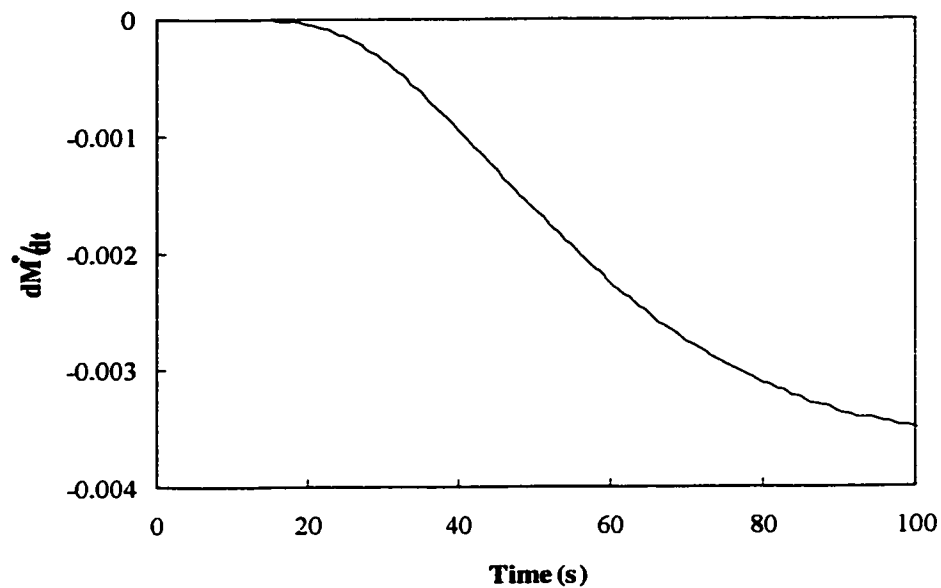


Figure 4.45: Drying rate variation with time in a cylindrical object

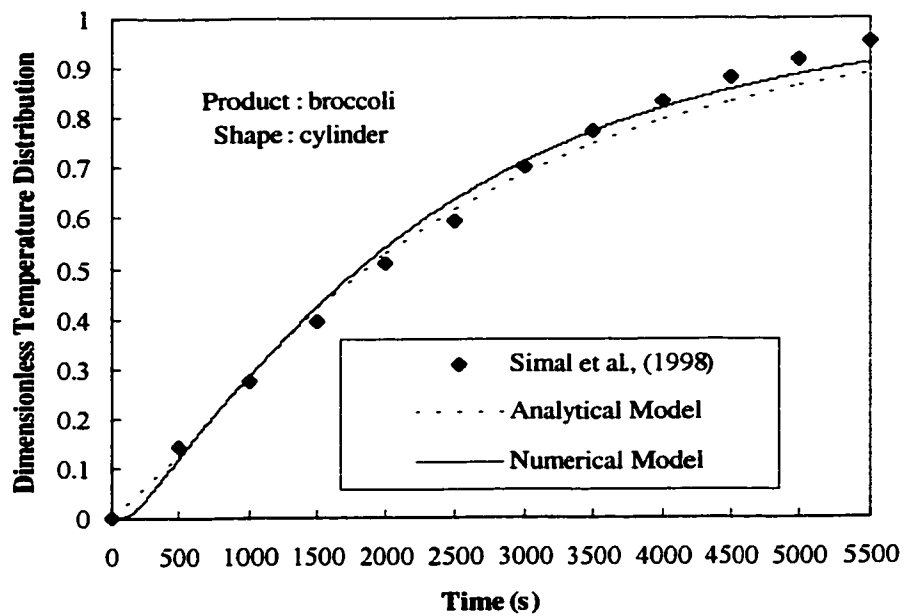


Figure 4.46: Comparison between the measured and calculated dimensionless temperature distribution in a cylindrical object

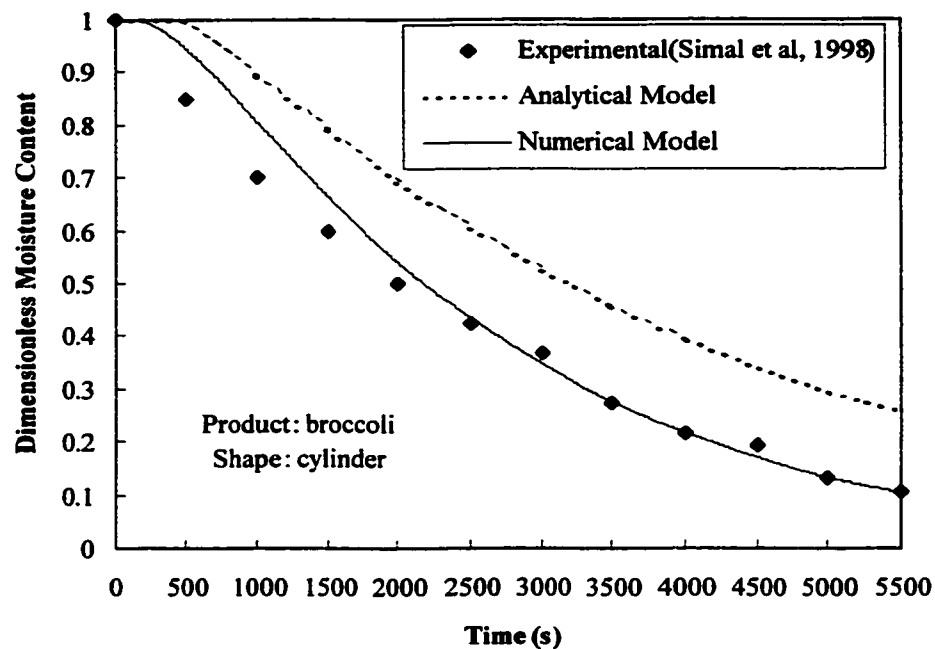


Figure 4.47: Comparison between the measured and calculated dimensionless moisture content in a cylindrical object

The variation of reduced center moisture content and reduced surface moisture content with time is shown in Figure 4.44. The reduction of moisture content is high in the early heating period and as the heating period progresses, it reduces gradually until equilibrium moisture content is attained. The attainment of high moisture gradient in the early period is because of the diffusion process. The reduction of moisture content is more pronounced at the surface and as the heating progresses it becomes constant. The rate of drying with time is shown in Figure 4.45. It is clear from the figure that drying takes place in two periods, first during the constant rate period in which rate of moisture reduction is constant which appears in the figure as straight line parallel to x-axis then the rate of moisture gradually reduces exhibiting falling-rate period.

Figures 4.46 and 4.47 show the comparison of center temperature and moisture distribution in a cylindrical object with the calculated and measured values taken from the literature. It is clear from the figures that the two-dimensional numerical model shows excellent agreement with the measured values of temperature and moisture content than the one-dimensional analytical model.

#### 4.2.3. 2-D Spherical Object

This sub-section deals with temperature and moisture profiles in a spherical object during drying. The product considered in the simulation was potato of diameter 0.04 m. Thermophysical properties and the drying conditions used in the simulation are listed in Table 4.5.

Table 4.5: Thermophysical properties and drying conditions used in the simulation

$\alpha$	$1.31 \times 10^{-7} \text{ m}^2/\text{s} (*)$
$h$	25-250W/m <sup>2</sup> K
$h_m$	0.0001m/s
$T_i$	296K
$T_d$	333K
$M_i$	5.25kg/kg (db)
RH	0.42kg/kg (db)

[\* Source: Dincer, 1997]

Figures 4.48 and 4.49 show the variations of reduced center temperature and reduced surface temperature for different heat transfer coefficients. The temperature rises rapidly for all the heat transfer coefficients in the early heating period due to convective boundary condition at the surface. This is more pronounced in the surface vicinity of the

object. This can also be seen from Figures 4.50 and 4.51, in which time derivative of reduced temperature profiles at the center and surface are shown. The rapid rise of the temperature in the surface vicinity of the object is because of the internal heat gain in this region.

The variation of reduced temperature along the radius for different heating periods is shown in Figure 4.52. The reduced temperature increases all the time from the center to the surface of the sphere. As the heating period progresses, the reduced temperature gradient decreases until a stage is reached, in which heat gain due to convective boundary condition balances the heat transfer through conduction energy transport.

Figure 4.53 shows the reduced moisture content at the center and at the surface of the spherical object subjected to drying. The moisture content inside the sphere reduces as the time period progresses. In the early heating period moisture content reduces rapidly and as the heating period progresses the rate of reduction of moisture content becomes less, i.e., it reduces almost steady with progressing heating period. This is more pronounced in the surface vicinity. The rapid drop of moisture content in the early heating period is because of the high moisture gradient in this region, which in turn derives considerable diffusion rates from bulk of the substrate to the surface.

The rate of drying with time is shown in Figure 4.54. It is clear from the figure that during early heating period, the rate of drying is constant, thus exhibiting constant rate period. As the time period progresses, the rate of drying continuously decreases representing falling rate period. The variation of reduced moisture along radius at different heating period is shown in Figure 4.55. The reduced moisture content decreases both at the center and at the surface as the time period progresses.

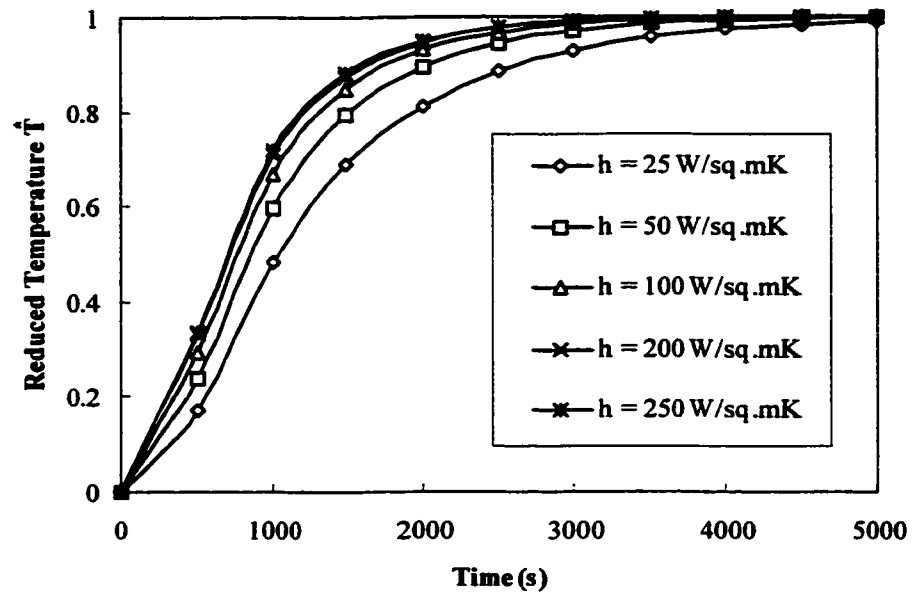


Figure 4.48: Variation of reduced center temperature in a spherical object for different heat transfer coefficients

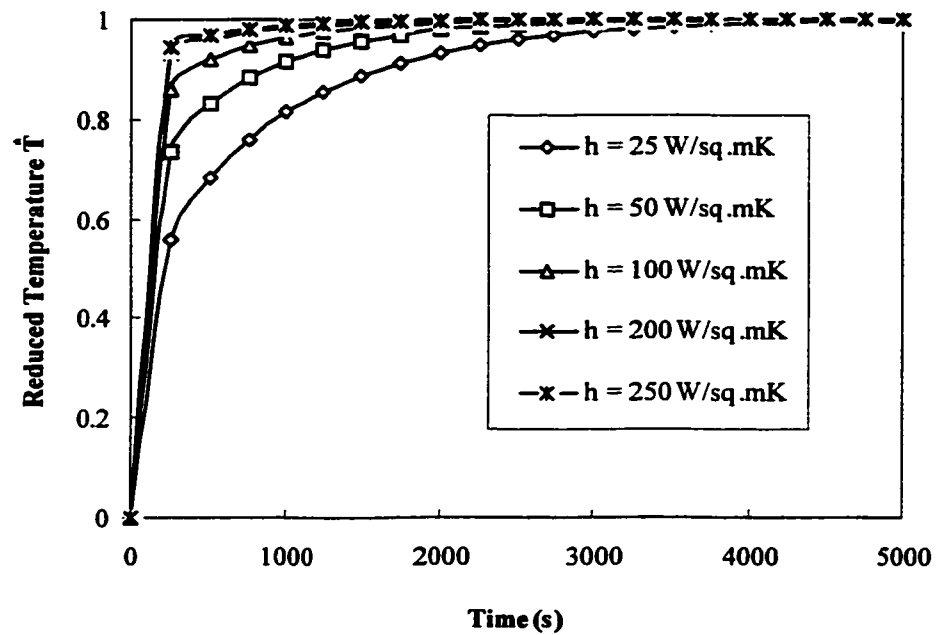


Figure 4.49: Variation of reduced surface temperature in a spherical object for different heat transfer coefficients

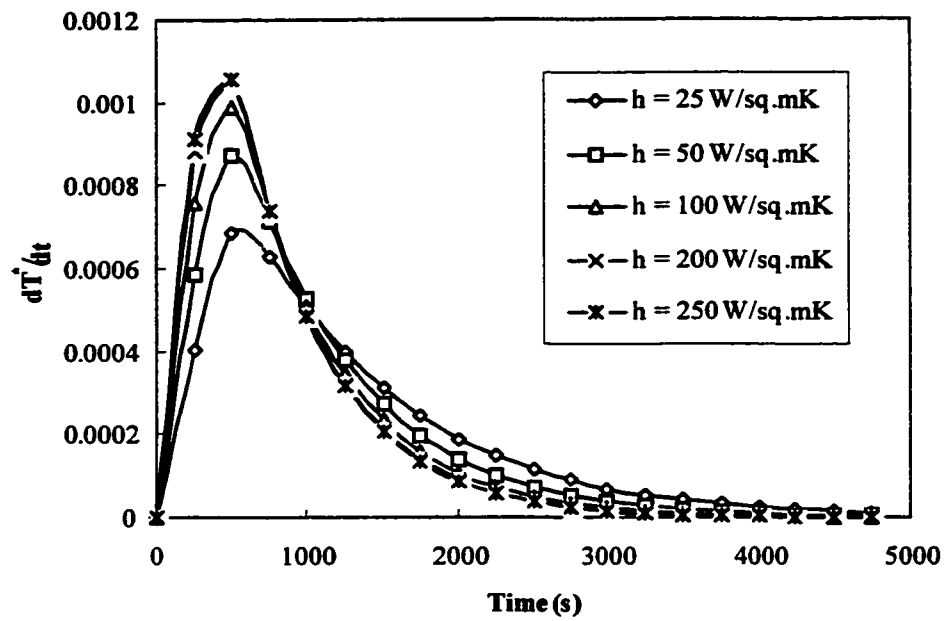


Figure 4.50: Variation of reduced center temperature gradient in a spherical object for different heat transfer coefficients

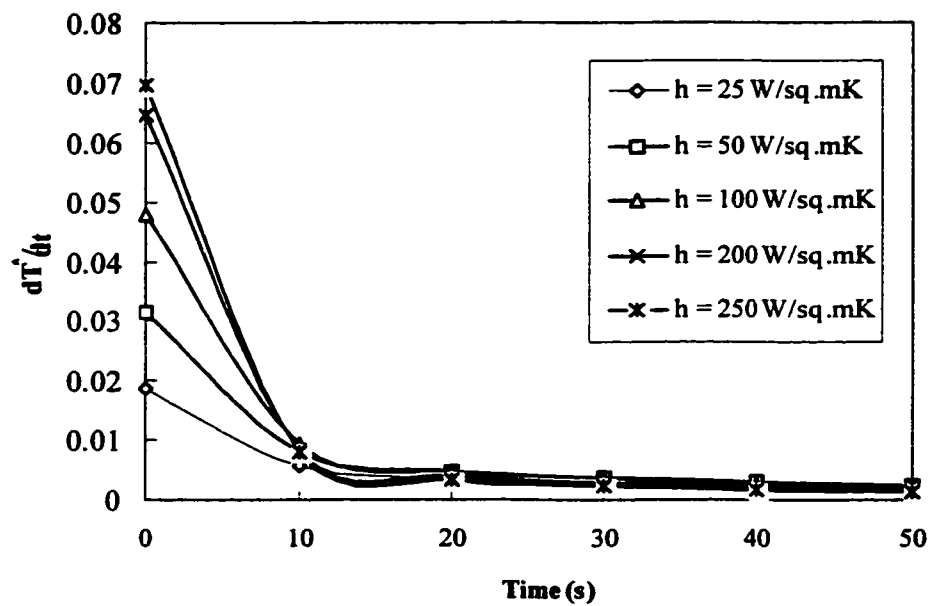


Figure 4.51: Variation of reduced surface temperature gradient in a spherical object for different heat transfer coefficients

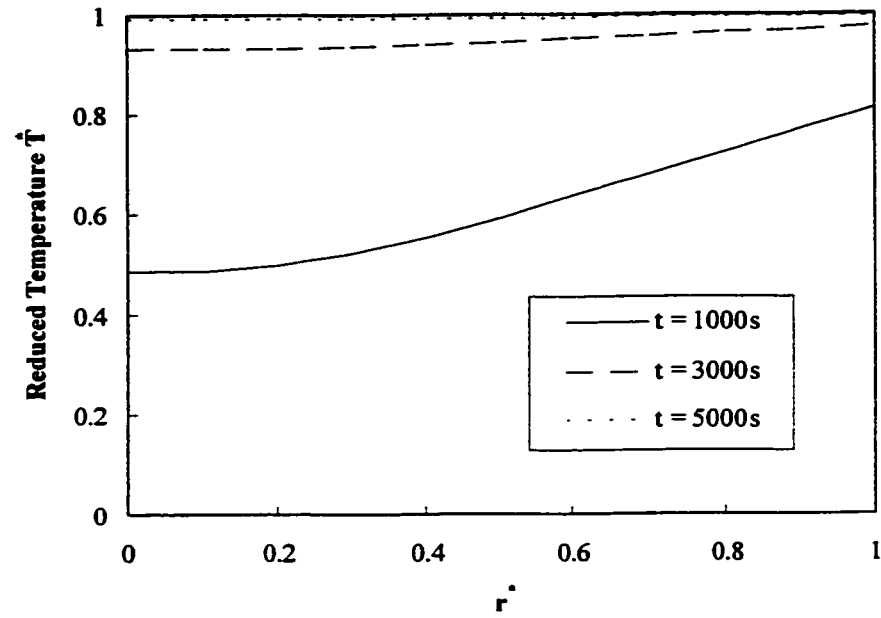


Figure 4.52: Variation of reduced temperature along radius for different drying periods

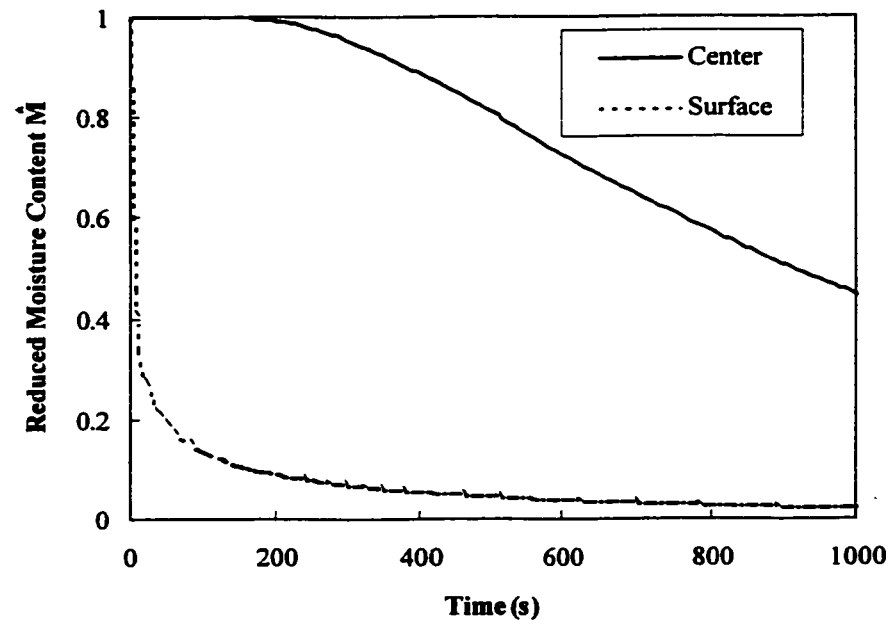


Figure 4.53: Reduced moisture distribution at the center and surface of a spherical object

The time required for the reduced moisture content to drop its half value at the center is about 1000 s. It is to be noted that the reduced moisture content is non-uniform in the sphere; consequently, half time requirement varies at each location.

Even though, we assumed the variation of temperature and moisture in the  $\Phi$ -direction in our formulation, but the results obtained proves the fact that there is no variation in that direction due to convective heating at the surface. Thus in a spherical object subjected to convective heating, the variation of temperature and moisture is only in the radial direction.

The comparison between the measured and calculated center temperature distribution and moisture content inside a spherical product are shown in Figure 4.56 and 4.57. Numerical model shows a fairly good agreement with the experimental values than the analytical model.

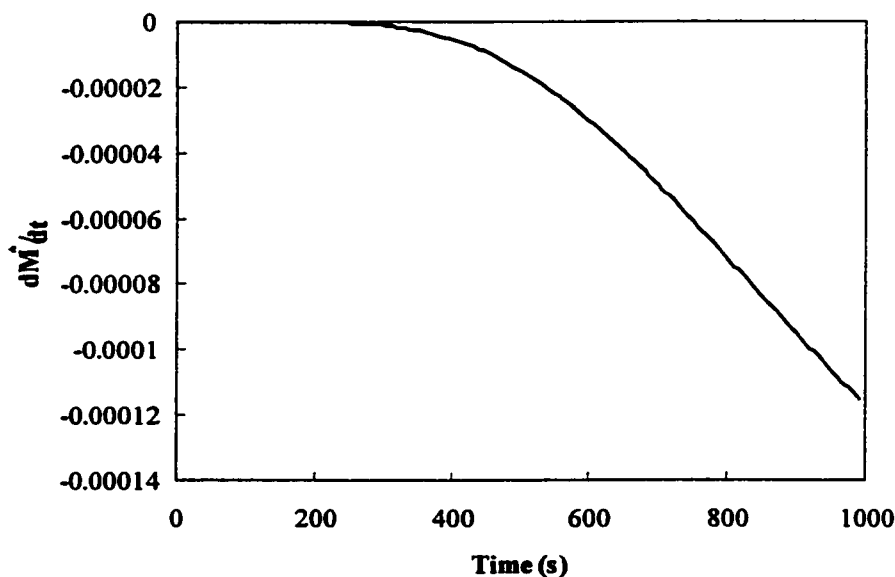


Figure 4.54: Drying rate variation with time in a spherical object



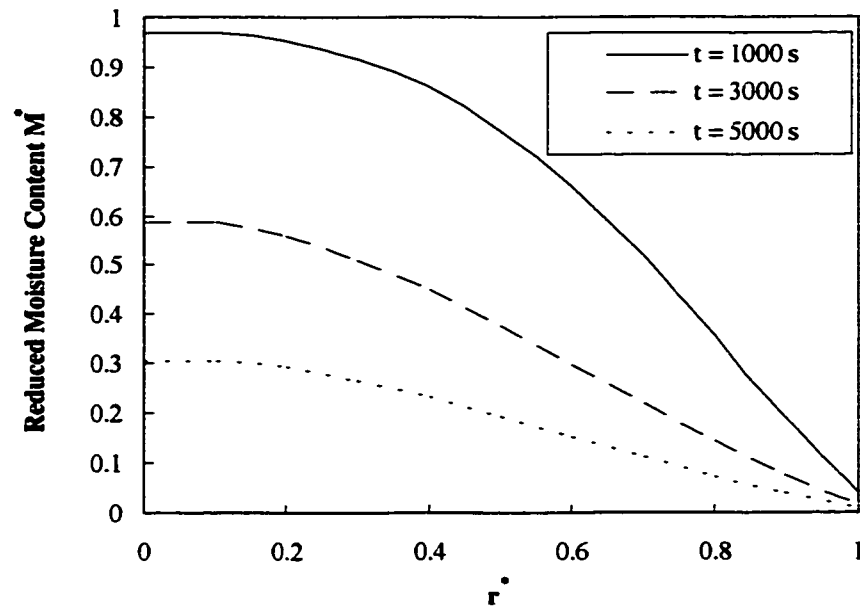


Figure 4.55: Variation of reduced moisture content along radius at different time periods

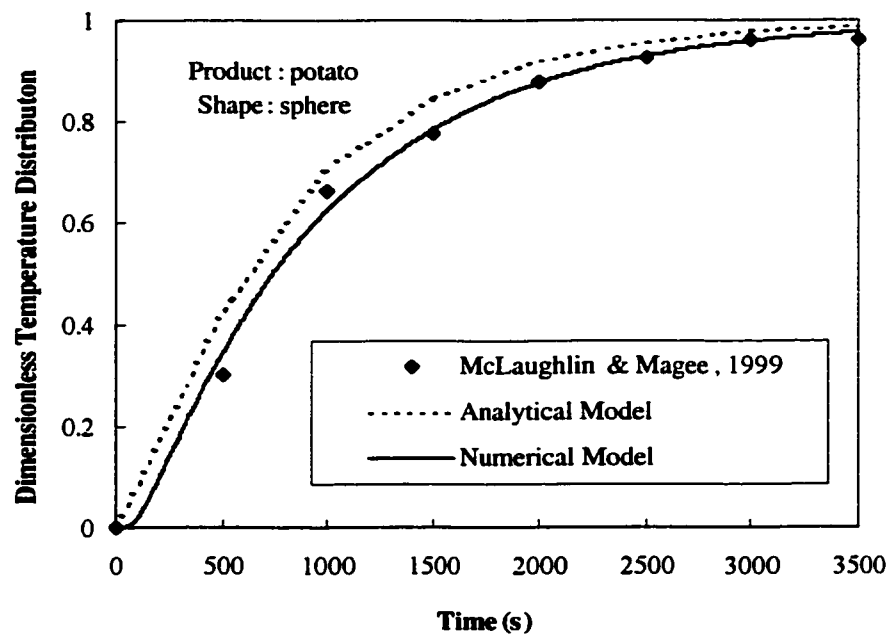


Figure 4.56: Comparison between the calculated and measured dimensionless temperature distribution in a spherical object

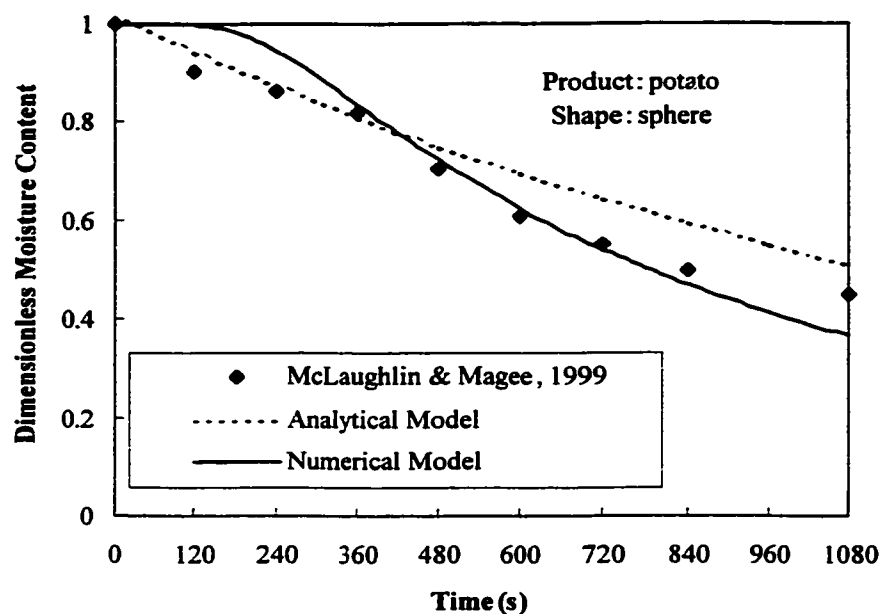


Figure 4.57: Comparison between the calculated and measured dimensionless moisture content in a spherical object

Thus in this section, the numerical solution for the temperature and moisture distribution inside the regular objects (i.e., slab, cylinder & sphere), due to convective boundary conditions at the surface is presented for drying applications. It is found that the temperature rises rapidly in the early heating period and as the heating period progresses, the rise of temperature attains almost steady with advancing heating period. The moisture gradient is higher in the early heating period and as heating progresses, the moisture gradient remains almost steady. Further, the effect of heat transfer coefficient on the temperature distribution inside the objects is also been investigated. The temperature inside the objects increases as the heat transfer coefficient increases and the time required to reach the steady temperature is less for the maximum heat transfer coefficient. Moreover, validation of the results obtained from the present analysis is performed with the experimental data available in the literature. A fairly good agreement has been found

between the calculated and measured values for the temperature and moisture distributions inside the objects.

### 4.3. Results of New Drying Correlations

#### 4.3.1. Biot Number-Reynolds Number ( $Bi_m$ -Re) Correlation

Because of the thermophysical properties and velocity of the drying fluid, it is known to have relation between Biot number and Reynolds number. Using the procedure explained in chapter 3, we have obtained the Bi-Re correlation (Figure 4.58) for several food products subjected to drying with the correlation coefficient as high as 0.72.

$$Bi_m = 22.552 Re^{-0.5897} \quad (4.1)$$

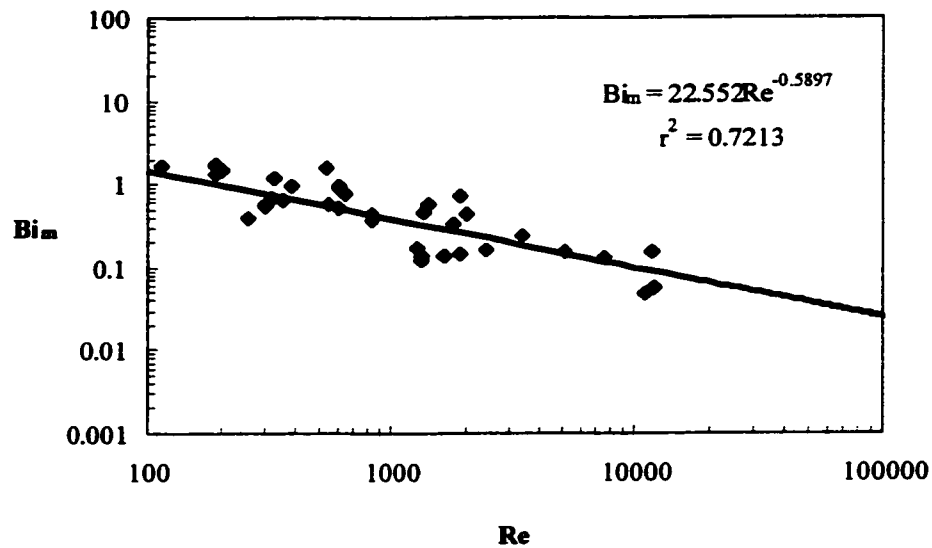


Figure 4.58:  $Bi_m$ -Re diagram for food products subjected to drying

#### 4.3.2. Verification of Biot Number-Reynolds Number ( $Bi_m$ -Re) Correlation

This sub-section presents the validation of the Biot-Reynolds ( $Bi_m$ -Re) correlation with the experimental data taken from the literature and shows application for determining the moisture transfer parameters for three regular shaped products namely slab, cylinder and

sphere. The experimental drying conditions and references are listed in Table 4.6. Drying process and moisture transfer parameters obtained in the  $Bi_m$ -Re correlation are listed in Table 4.7.

Table 4.6: Drying conditions of the experiments used for validation in  $Bi_m$ -Re correlation

Thermo physical property	Slab	Cylinder	Sphere
T (°C)	60	60	40
v (m/s)	3.5	1	1
Y (m)	0.0025	0.0135	0.009
References	Tsami and Katsioti, 2000	McMinn and Magee, 1996	McLaughlin and Magee, 1999

Table 4.7: Obtained drying process and moisture transfer parameters for the objects used in  $Bi_m$ -Re correlation

Object			
Process Parameters	Slab	Cylinder	Sphere
S (1/s)	0.0003	$7 \times 10^{-5}$	0.0009
G (-)	1.0037	1.032	1.0074
Re (-)	910.9933	1405.5325	1046.6455
Bi (-)	0.4054	0.3139	0.3736
$\mu_1$ (-)	0.1674	0.4358	0.2781
D (m <sup>2</sup> /s)	$6.6905 \times 10^{-8}$	$6.7172 \times 10^{-8}$	$9.4198 \times 10^{-7}$
$h_m$ (m/s)	$1.0849 \times 10^{-5}$	$1.5618 \times 10^{-6}$	$3.9102 \times 10^{-5}$

Figures 4.59 to 4.61 show the measured and predicted dimensionless moisture distributions using developed  $Bi_m$ - $Re$  correlation for three regular shaped products namely slab, cylinder and sphere respectively. The predicted moisture profiles using the  $Bi_m$ - $Re$  correlation are in good agreement with the measured values. The average percentage error between the predicted and measured moisture profiles for slab, cylinder and sphere were found to be  $-14.51$ ,  $\pm 2.76$  and  $-10.62$  respectively.

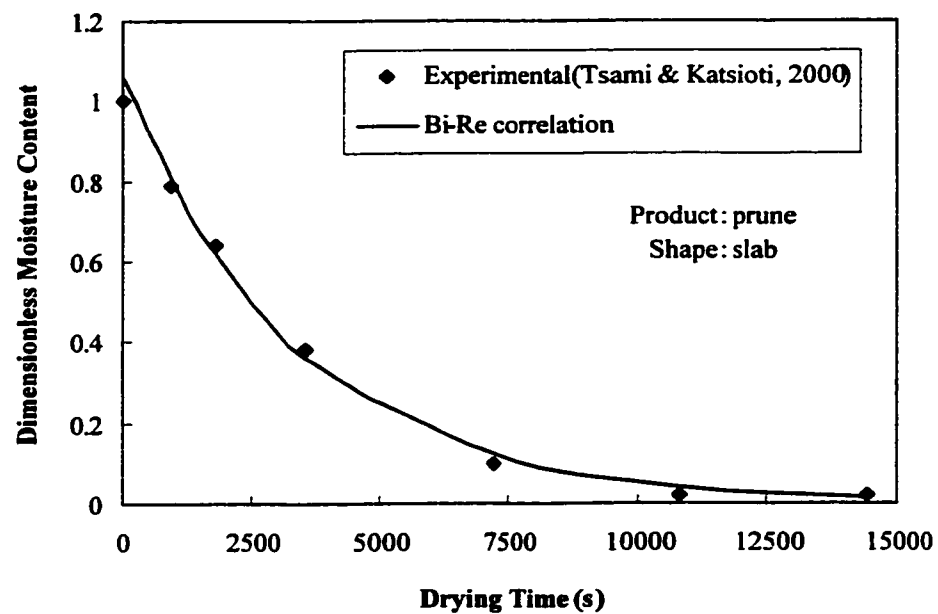


Figure 4.59: Measured and predicted dimensionless moisture distribution using  $Bi_m$ - $Re$  correlation for a slab object

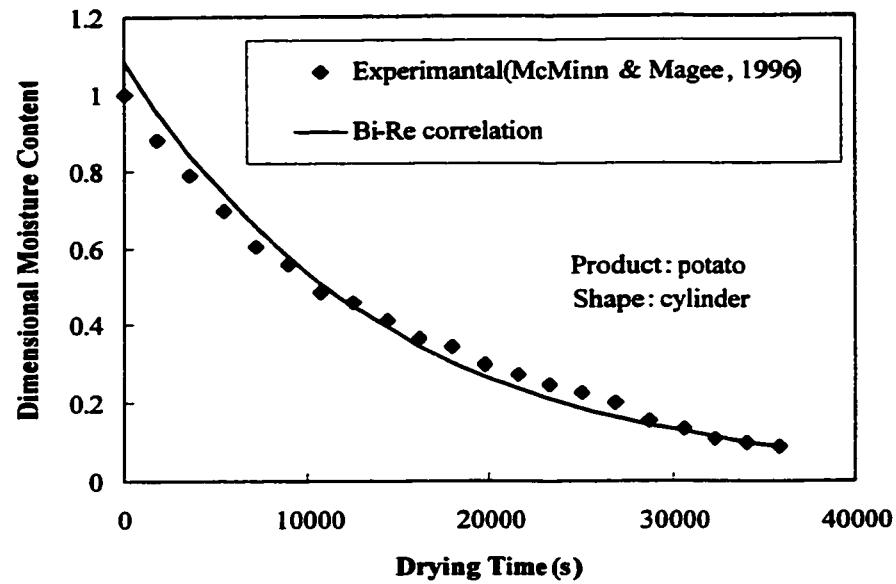


Figure 4.60: Measured and predicted dimensionless moisture distributions using  $Bi_m$ -Re correlation for cylindrical object

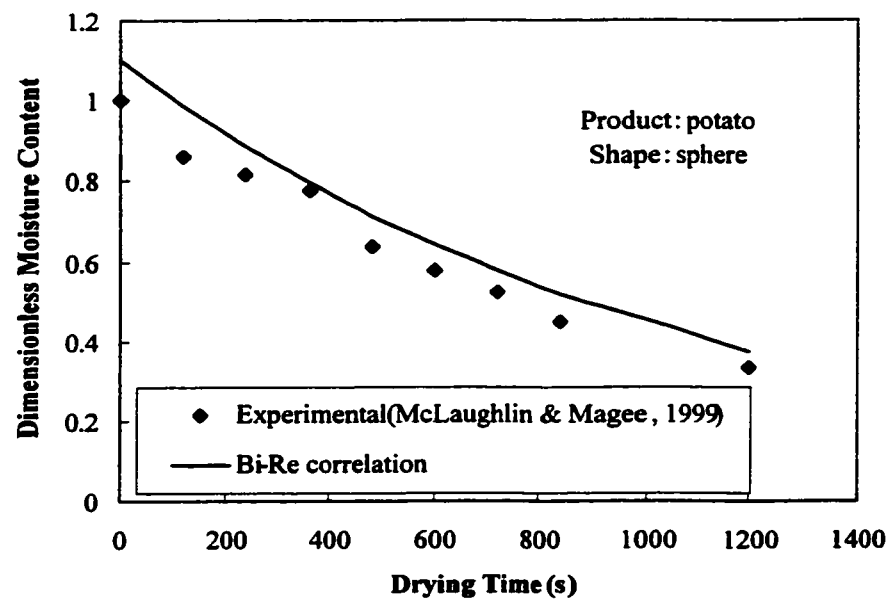


Figure 4.61: Measured and predicted dimensionless moisture distributions using  $Bi_m$ -Re correlation for spherical object

### 4.3.3. Biot Number-Dincer Number ( $Bi_m$ - $Di$ ) Correlation

In cooling, Dincer number ( $Di$ ) expresses the effect of flow velocity of the cooling fluid on the cooling coefficient (cooling process parameter) of food products subjected to cooling (Dincer, 1996). Similarly in drying, it represents the effect of flow velocity of drying air on the drying coefficient (drying process parameter) of the products subjected to drying. Using the similar approach as mentioned in the previous sections, we have found  $Bi_m$ - $Di$  correlation for several food products dried in a medium of air (Figure 4.62), with the correlation coefficient of 0.8, as:

$$Bi_m = 24.848Di^{-0.3734} \quad (4.2)$$

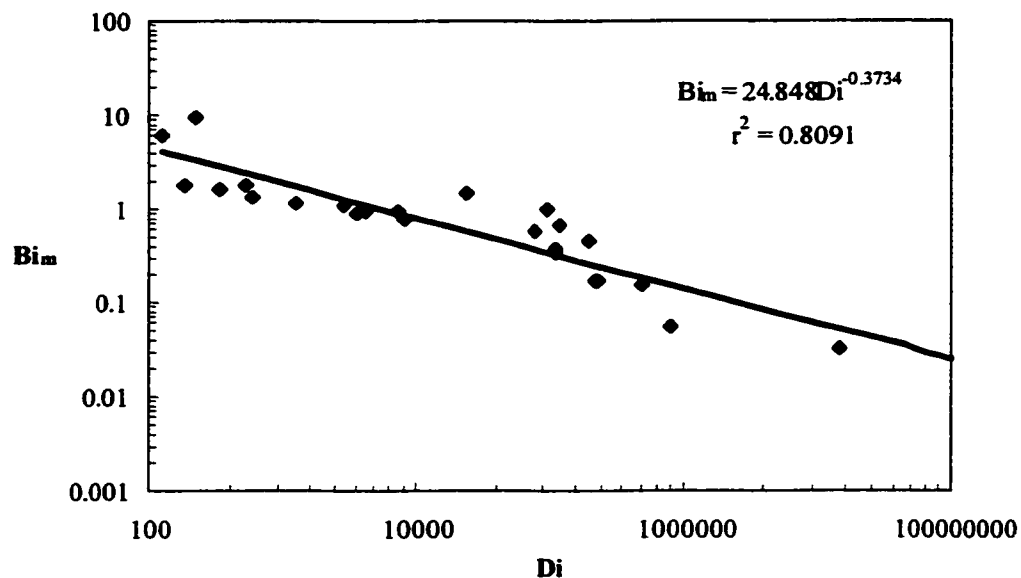


Figure 4.62:  $Bi_m$ - $Di$  diagram for food products subjected to drying

#### 4.3.4. Verification of Biot Number-Dincer Number ( $Bi_m$ -Di) Correlation

In this sub section validation and application of  $Bi_m$ -Di correlation for determining the moisture transfer parameters is presented. Drying conditions of the experiments with references are listed in Table 4.8. Obtained drying process and moisture transfer parameters for the objects used in the correlation are listed in Table 4.9.

Figures 4.63 to 4.65 show the moisture content profiles for slab, cylindrical and spherical objects subjected to drying. The obtained moisture content profiles using  $Bi_m$ -Di correlation are in good agreement with the experimental data taken from the literature. The average percentage error between predicted and measured moisture content values for slab, cylinder and sphere were found to be -3.38%, -24.84% and -1.31% with respect to measured values respectively.

Table 4.8: Drying conditions of the experiments used for validation in  $Bi_m$ -Di correlation.

Thermo physical property	Slab	Cylinder	Sphere
T (°C)	60	80	40
v (m/s)	3	1.2	1
Y (m)	0.0075	0.003	0.009
References	Tsami & Katsioti, 2000	Gogus & Maskan, 1999	Mclaughlin & Magee, 1999



Table 4.9: Obtained drying process and moisture transfer parameters for the objects used in  $Bi_m$ - $Di$  correlation

Object			
Process Parameters	Slab	Cylinder	Sphere
$S$ (1/s)	$7 \times 10^{-5}$	0.0001	0.0009
$G$ (-)	1.0016	1.1981	1.0074
$Di$ (-)	5714285.714	4000000	123456.79
$Bi$ (-)	0.0745	0.0851	0.3119
$\mu_1$ (-)	0.1407	1.2593	0.2781
$D$ ( $m^2/s$ )	$1.9889 \times 10^{-7}$	$5.6752 \times 10^{-10}$	$9.4259 \times 10^{-7}$
$h_m$ (m/s)	$1.9756 \times 10^{-6}$	$1.6098 \times 10^{-8}$	$3.2665 \times 10^{-5}$

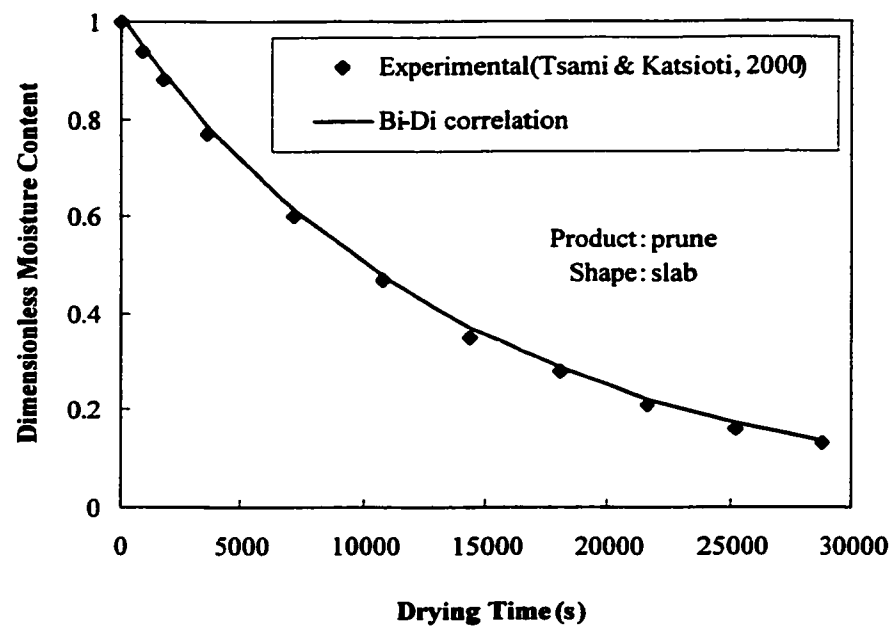


Figure 4.63: Measured and predicted dimensionless moisture distributions using  $Bi_m$ - $Di$  correlation for slab object

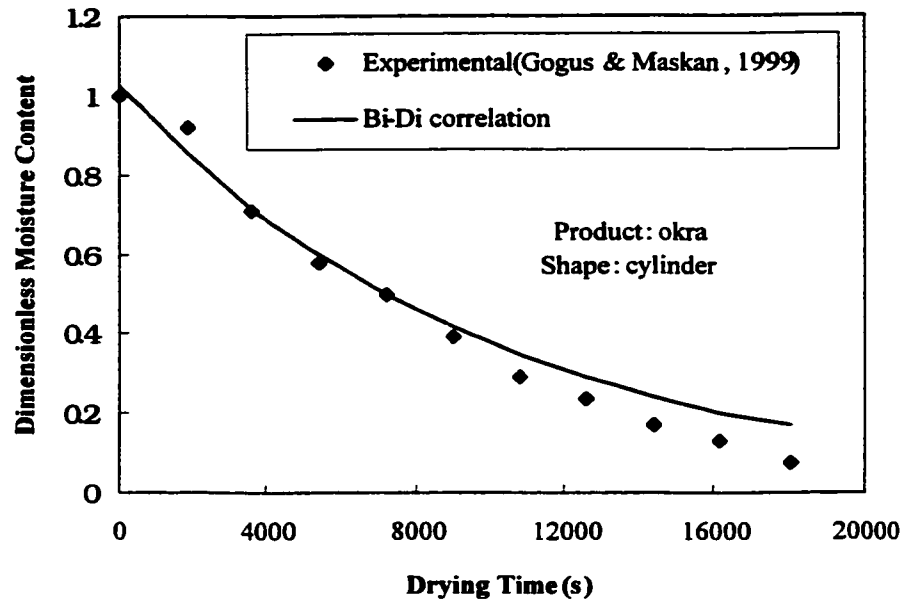


Figure 4.64: Measured and predicted dimensionless moisture distributions using  $Bi_m$ -Di correlation for cylindrical object

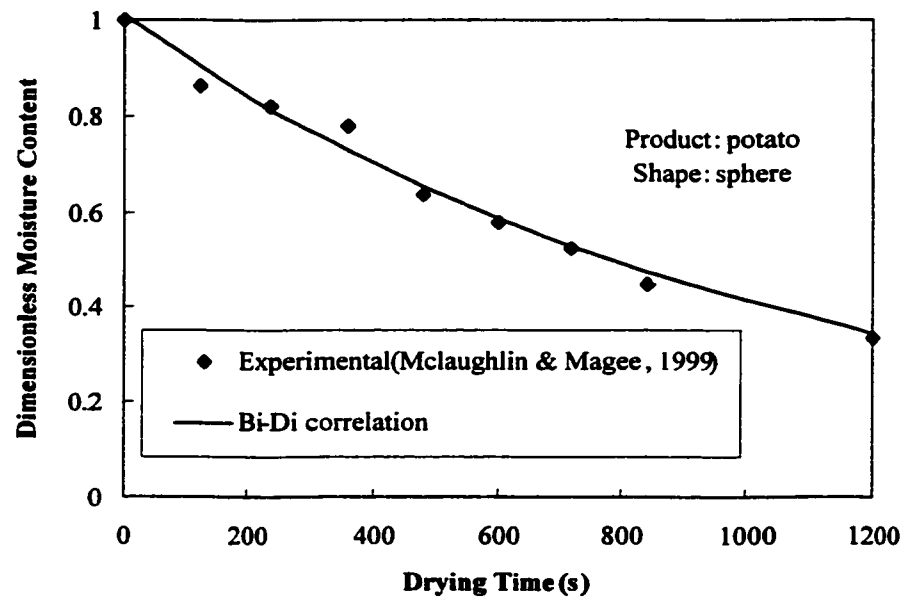


Figure 4.65: Measured and predicted dimensionless moisture distributions using  $Bi_m$ -Di correlation for spherical object

#### 4.3.5. Biot Number-Lag Factor ( $Bi_m$ - $G$ ) Correlation

As stated earlier, lag factor ( $G$ ) represents the magnitude of internal resistance to the moisture transfer from the product. And Biot number ( $Bi_m$ ) by its definition represents the ratio of the internal moisture transfer resistance to the surface moisture transfer resistance. Hence there is an intimate relation between the two (shown in Figure 4.66), which we have found with the correlation coefficient over 0.9 as

$$\ln Bi_m = 26.7 \ln G - 2.8535 \quad (4.3)$$

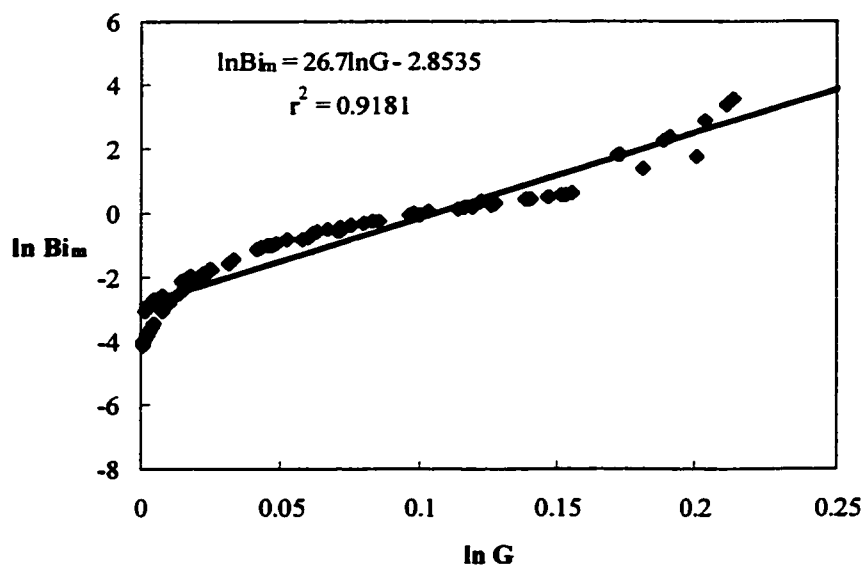


Figure 4.66: Bi-G diagram for food products subjected to drying

#### 4.3.6. Verification of Biot Number-Lag Factor ( $Bi_m$ - $G$ ) Correlation

This sub-section is devoted for the validation and calculation of moisture transfer parameters using developed Biot-lag factor ( $Bi_m$ - $G$ ) correlation. Knowing the lag factor ( $G$ ) from the regression analysis, Biot number ( $Bi_m$ ) is calculated directly from the developed correlation given by equation (4.3). Drying conditions of the experiments used

in the validation are given in Table 4.10. Obtained drying process and moisture transfer parameters for the objects used in  $Bi_m$ -G correlation are listed in Table 4.11.

Table 4.10: Drying conditions of the experiments used for validation in  $Bi_m$ -G correlation

Thermo physical property	Slab	Cylinder	Sphere
T (°C)	50	62	105
v (m/s)	0.5	2	-
Y (m)	0.0025	0.005	0.03
References	Sawhney et al., 1999	Akiyama et al., 1997	Lu et al., 1998

Table 4.11: Obtained drying process and moisture transfer parameters for the objects used in  $Bi_m$ -G correlation

Object			
Process Parameters	Slab	Cylinder	Sphere
S (1/s)	0.0002	0.0006	0.0046
G (-)	1.1503	1.0181	1.2864
Bi (-)	2.4214	0.0929	47.9471
$\mu_1$ (-)	0.9951	0.3398	1.6552
D (m <sup>2</sup> /s)	$1.2623 \times 10^{-9}$	$1.2991 \times 10^{-7}$	$1.511 \times 10^{-6}$
$h_m$ (m/s)	$1.2226 \times 10^{-6}$	$2.4137 \times 10^{-7}$	$2.4151 \times 10^{-3}$

The dimensionless moisture content profiles for slab, cylindrical and spherical objects subjected to drying are shown in Figures 4.67 to 4.69. The obtained moisture content profiles using the  $Bi_m$ -G correlation are in good agreement with the measured values taken from the literature. The average percentage error between predicted and measured moisture content values for slab, cylinder and sphere were found to be +21.53, +1.98 and +0.17 respectively.

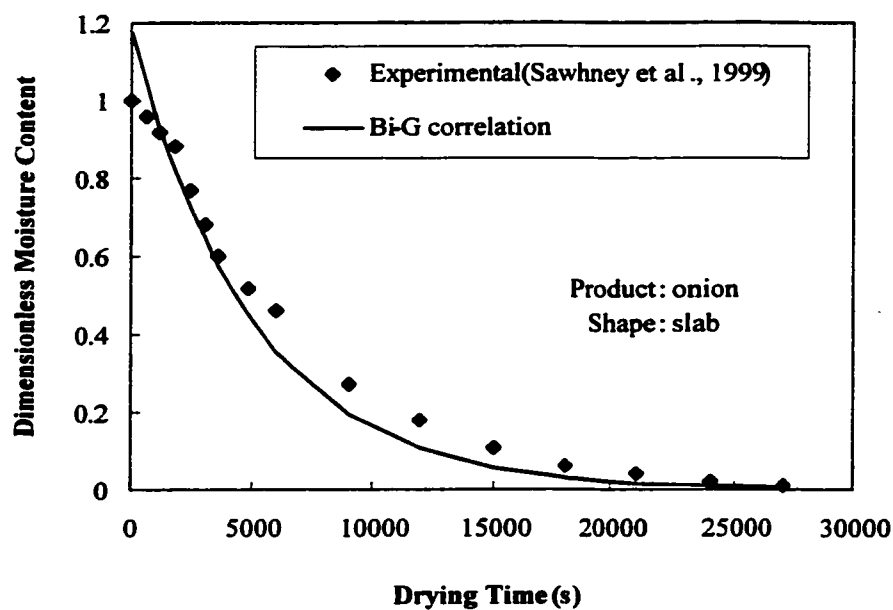


Figure 4.67: Measured and predicted dimensionless moisture distributions using  $Bi_m$ -G correlation for slab object

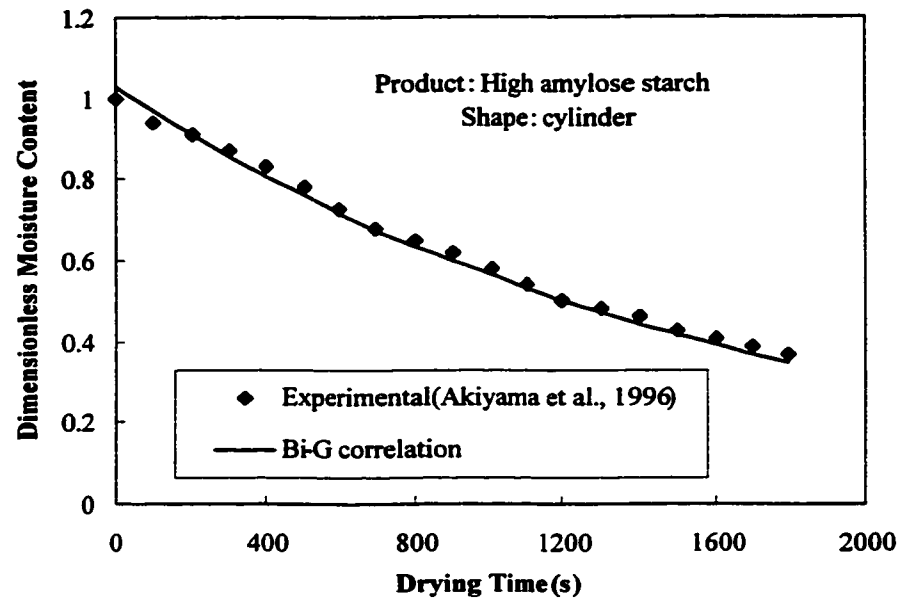


Figure 4.68: Measured and predicted dimensionless moisture distributions using  $Bi_m$ -G correlation for cylindrical object

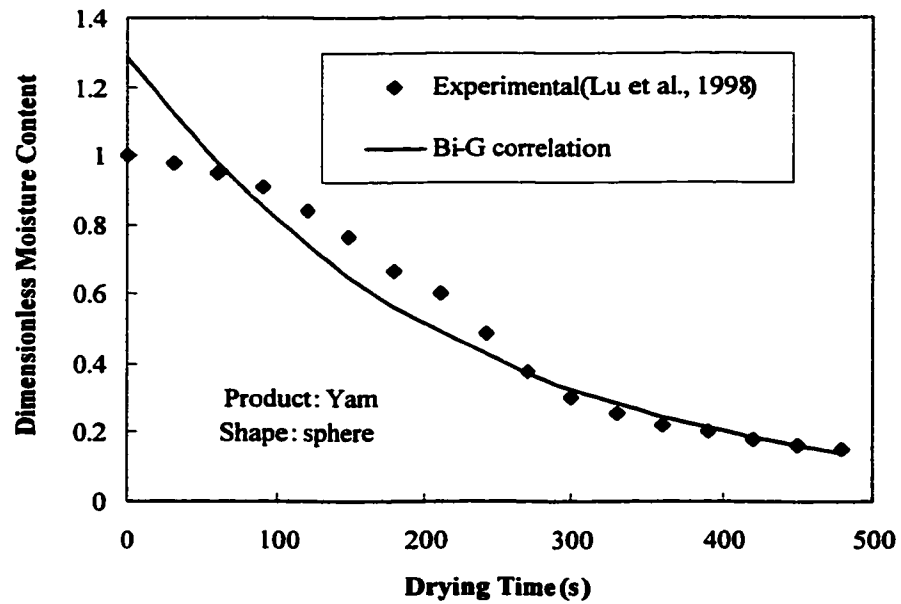


Figure 4.69: Measured and predicted dimensionless moisture distributions using  $Bi_m$ -G correlation for spherical object

#### 4.3.7. Biot Number-Drying Coefficient ( $Bi_m$ -S) Correlation

As introduced in the previous chapter, drying coefficient (S) is a drying process parameter representing the drying capability of the product exposed to drying. And Biot number ( $Bi_m$ ) is the ratio of internal moisture transfer resistance to the surface moisture transfer resistance. Thus there is a clear linkage between the Biot number and drying coefficient because of their definitions.

Using the experimental processed data as mentioned in the previous section, we have deduced  $Bi_m$ -S correlation (Figure 4.70) for different kinds of food products being dried in a medium of air with correlation coefficient over 0.8 as

$$Bi_m = 1.687S^{0.4075} \quad (4.4)$$

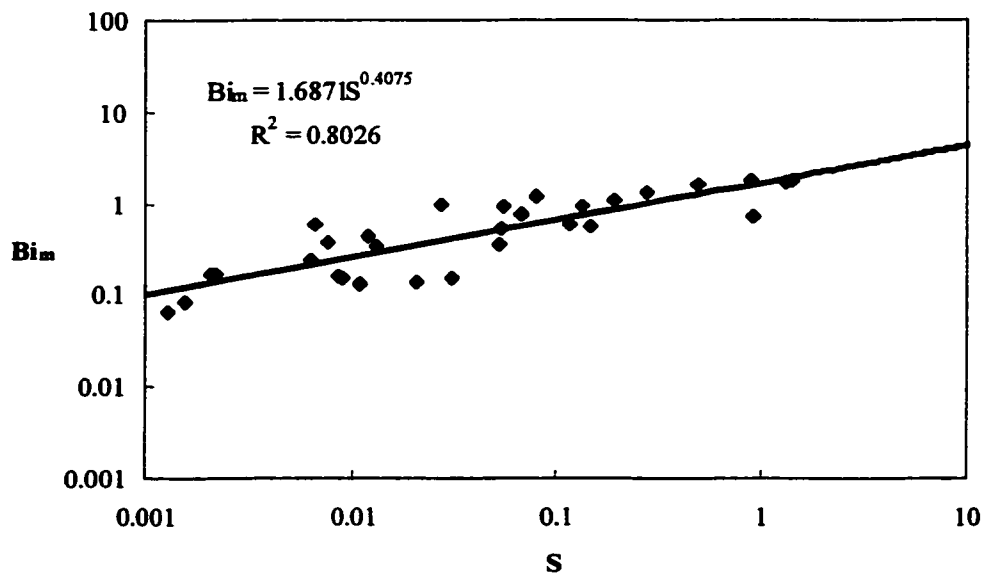


Figure 4.70:  $Bi_m$ -S diagram for food products subjected to drying

#### 4.3.8. Verification of Biot Number-Drying Coefficient ( $Bi_m$ -S) Correlation

The present sub-section deals with the verification of Biot –Drying Coefficient ( $Bi_m$ -S) correlation and calculation of moisture transfer parameters involved in the drying process. Knowing the drying coefficient (S), we can determine the Biot number ( $Bi_m$ ) from the developed ( $Bi_m$ -S) correlation. Experimental conditions of drying used in the validation with references are listed in table 4.12. The drying process and moisture transfer parameters obtained for the objects used in the  $Bi_m$ -S correlation are listed in Table 4.13.

Figures 4.71.to 4.73 show the moisture profiles for slab, cylinder and spherical objects subjected to drying. The obtained moisture profiles using the  $Bi_m$ -S correlation are in good agreement with the experimental data taken from the literature. The average percentage error between predicted and measured values for slab, cylinder and sphere were found to be -10.03, +14.23 and -4.59 respectively.

Table 4.12: Drying conditions of the experiments used for validation in  $Bi_m$ -S correlation

Thermo physical property	Slab	Cylinder	Sphere
T (°C)	105	60	40
v (m/s)	6.71	0.5	1
Y (m)	0.0015	0.0009	0.009
References	Blasco et al., 1998	Sawhney et al., 1999	McLaughlin & Magee, 1999



Table 4.13: Obtained drying process and moisture transfer parameters for the samples used in  $Bi_m$ -S correlation

Object			
Process Parameters	Slab	Cylinder	Sphere
S (1/s)	0.0004	$4 \times 10^{-5}$	0.0009
G (-)	1.0047	1.101	1.0074
Bi (-)	0.0972	0.046	0.1266
$\mu_1$ (-)	0.1798	0.8446	0.27819
D ( $m^2/s$ )	$1.6363 \times 10^{-8}$	$4.5419 \times 10^{-11}$	$9.4198 \times 10^{-7}$
$h_m$ (m/s)	$1.0603 \times 10^{-6}$	$2.3214 \times 10^{-9}$	$1.325 \times 10^{-5}$

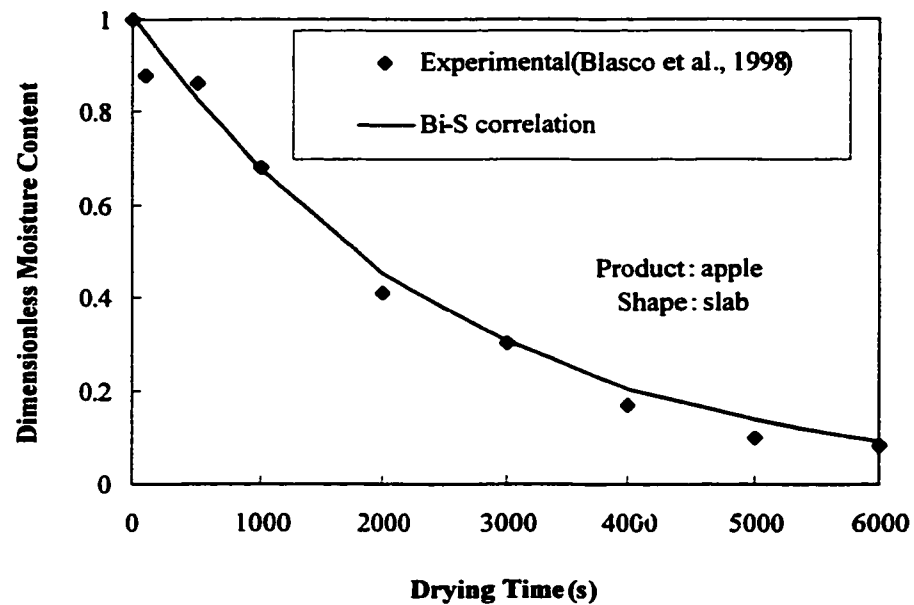


Figure 4.71: Measured and predicted dimensionless moisture distributions using  $Bi_m$ -S correlation for slab object

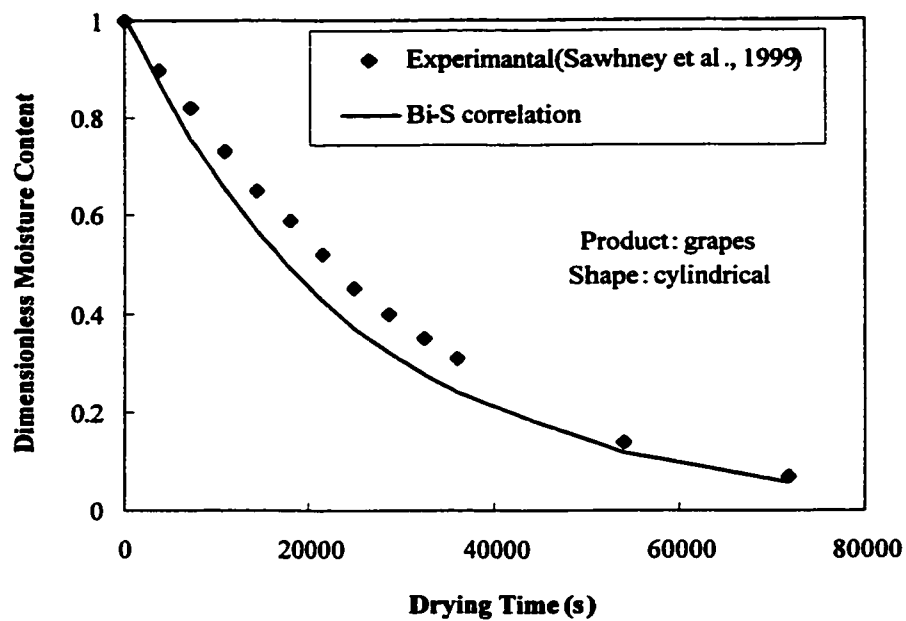


Figure 4.72: Measured and predicted dimensionless moisture distributions using  $Bi_m$ -S correlation for cylindrical object

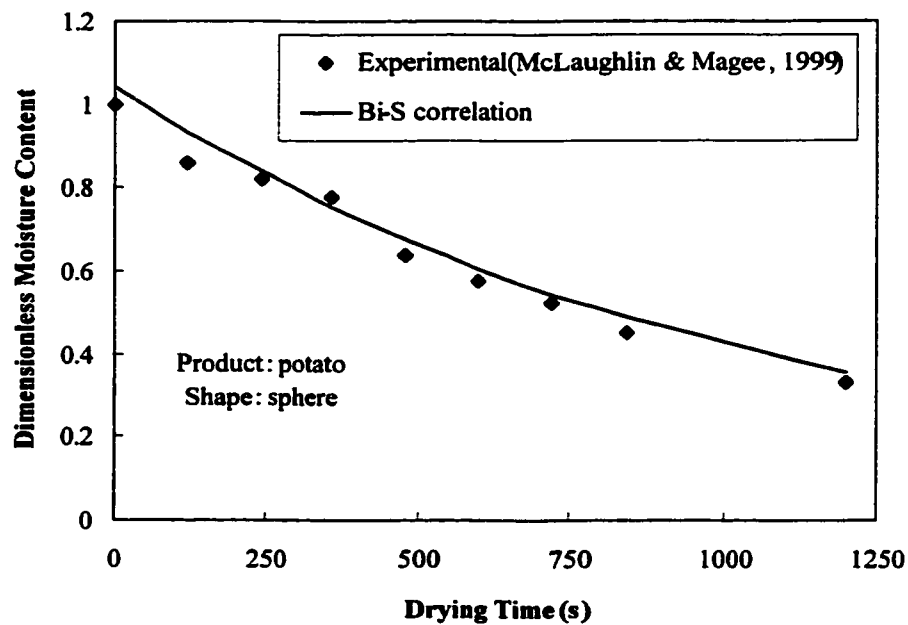


Figure 4.73: Measured and predicted dimensionless moisture distributions using  $Bi_m$ -S correlation for spherical object

Thus in this chapter, the results of analytical and numerical heat and moisture transfer analysis are presented for drying applications. In addition, new developed drying correlations are presented for determining the moisture transfer parameters in terms of moisture diffusivity and moisture transfer coefficient. Moreover results obtained from the analytical and numerical analysis of heat and moisture transfer during drying of regular shaped objects are compared with the experimental data found in the literature. The developed correlations are also validated by comparing the dimensionless moisture content values taken from the experimental results available in the literature and those calculated using the correlations. The predicted temperature and moisture histories during drying of regular objects using the two-dimensional numerical model shows excellent agreement with the measured values taken from the literature as compared to one-dimensional analytical model, hence justifies the variation of temperature and moisture in two dimensions. A good agreement has also been found between the measured and predicted moisture content values using the newly developed correlations. Hence, it is believed that these correlations are beneficial to those working in design and manufacturing in the drying industries to calculate the most important moisture transfer parameters in a simple and accurate manner and suggests design improvements.

## **CHAPTER 5**

### **CONCLUSIONS AND RECOMMENDATIONS**

#### **5.1. Conclusions**

In the analytical part of heat and moisture transfer analysis, a closed form solution for the temperature and moisture distribution inside the slab due to convective boundary condition is presented for drying applications. Moisture diffusivity ( $D$ ) dependence on temperature considered in the analysis is of the form of Arr-henius equation, which changes with time and location. It is found that the temperature rises rapidly in the early heating period and as the heating period progresses, the rise of temperature attains almost steady state with advancing heating period. The temperature gradient becomes high in the surface region with the increase of time, which in turn, enhances the conduction energy transport from the surface to the inside of the slab. The moisture gradient is higher in the early heating period and as heating progresses, the moisture gradient remains almost steady. A comparison between the calculated temperature and moisture distribution with the data available in the literature was carried out and found to be in good agreement with those values.

In the numerical heat and moisture transfer analysis, finite difference scheme have been used to discretize the governing equations of heat conduction and moisture diffusion. The resulting difference equations are then used to solve for temperature and moisture distributions inside the regular shaped objects such as rectangular slab, cylinder and

sphere. Moisture diffusivity, which is considered as a function of temperature, varies with time and location. The effect of heat transfer coefficient on temperature distribution inside the objects has also been investigated. The obtained results show that with the increase of time temperature in the objects increases and attains a steady value with advancing time period. Moreover, increasing the heat transfer coefficient decreases the time period to attain a steady temperature inside the objects but has negligible effect on the rate of moisture reduction for the range studied here. The temperature distribution inside the objects is non-uniform, indicating that the temperature dependent moisture diffusivity varies in the objects, which in turn affects the rate of moisture diffusion in the objects. The moisture content inside the objects reduces as the time period progresses and the moisture gradients are higher in the early heating period and as heating progresses, the moisture gradient remains almost steady. A verification of the results obtained from the present analysis has been carried out for all the three objects with the experimental data available in the literature and a good agreement is found between the present analysis and the measures values.

In the final part of the present study, simple and accurate new drying correlations has been developed and successfully used to calculate the moisture transfer parameters for the products subjected to drying. Illustrative examples have been presented to show the application of the developed correlations. Moreover, the developed correlations are verified by calculating the moisture distribution using the correlations and comparing with the experimental data found in the literature. A good agreement is obtained between the predicted and measured values. Thus these correlations will be beneficial to the design engineers and researchers working in the drying industries in calculating the moisture

transfer parameters in a fairly simple and accurate manner and suggest design improvements.

## **5.2. Recommendations for Future Work**

The present work can be extended to:

1. Objects with irregular geometries.
2. Account for variation of temperature and moisture in the third coordinate of the coordinate system.
3. Account for variable properties such as  $k$ ,  $\rho$ ,  $\alpha$  etc. New values of these quantities that change with temperature may be computed at each time step.
4. Account for internal heat generation within the object.
5. Fluid flow analysis of drying chambers in order to investigate the effect of velocity of the drying air on the drying rate of the objects.

## REFERENCES

**Acharyaviriya, S., Sophonronarit, & S., Terdyothin, A.,** (2000), 'Diffusion models of papaya and mango glaze drying', *Drying Technology*, Vol. 18 (7), 1605-1615.

**Akiyama, T., Liu, H. & Hayakawa, K.,** (1997), 'Hygrostress multi-crack formation and propagation in cylindrical viscoelastic food undergoing heat and moisture transfer processes', *Int. J. Heat & Mass Transfer*, Vol. 40, no. 7, pp. 1601-1609.

**Blasco, R., Diaz, G. & Reyes, A.,** (1998), 'Pneumatic suspension drying: modeling and computational simulation', *Drying Technology*, Vol. 16, no. 1&2, pp. 199-215.

**Chiang, W-C., and Petersen, J. N.,** (1987), 'Experimental measurement of temperature and moisture profiles during apple drying', *Drying Technology*, 5(1), 25-49.

**Chiang, W. C.,** (1988), 'Analysis of temperature and moisture profiles during apple drying', *Dissertation Abstracts International B* 48 (8), 2393.

**Chung, D. S. and Chung, D. I.,** (1982) 'Principles of food dehydration', *Journal of Food Protection*, 45 (5), 475-478.

**Cunningham, J. G.,** (1982), 'Practical applications of food dehydration: a review', *Journal of Food Protection*, 45 (5), 479-483.

**Dincer, I. and Dost, S.** (1996). 'A modeling study for moisture diffusivities and moisture transfer coefficients in drying of solid objects', *Int. J. Energy Research* 20, 531-539.

**Dincer, I.** (1996). 'Development of a new number (the Dincer number) of forced-convection heat transfer in heating and cooling applications', *Int. J. Energy Research* 20 (5), 419-422.

**Dincer, I.** (1997). '*Heat Transfer in Food Cooling Applications*', Taylor & Francis, Washington, DC.

**Dincer, I.** (1998), 'Moisture loss from wood products during drying-part I: moisture diffusivities and moisture transfer coefficients', *Energy Sources*, 20, 67-75.

**Estrada, J. A. and Litchfield, J. B.** (1993). 'High humidity of corn: effect on drying rate and product quality', *Drying Technology*, 11(1), 65-84.

**Garg, H. P., Rakesh Kumar and Datta, G.** (1998) 'Simulation model of the thermal performance of a natural convection-type solar tunnel dryer', *International Journal of Energy Research*, 22, 1165-1177.

**Gogus, F., Maskan, M.,** (1999), 'Water adsorption and drying characteristics of okra (*Hibiscus Esculenuts L.*)', *Drying Technology*, 17(4&5), 883-894.

**Hansmann, C. F. and Van Noort, G.** (1992). 'An experimental fruit dehydration system', *Drying Technology*, 10(2), 491-508.

**Holdsworth, S. D.** (1971), 'Dehydration of food products –a review', *Journal of Food Technology*, 6, 331-370.

**Jia, C-C, Sun, D-W. and Cao, C-W.** (2000), 'Mathematical simulation of temperature and moisture fields within a grain kernel during drying', *Drying Technology* 18, 1305-1325.

**Jumah, R. Y. and Mujumdar, A. S.** (1996). 'Batch drying kinetics of corn in a novel rotating jet spouted bed', *The Canadian Journal of Chemical Engineering*, volume 74, 479-486.



- Kechaou, N. and Maalej, M.**, (2000), 'A simplified model for determination of moisture diffusivity of date from experimental drying curve', *Drying Technology*, 18(4&5), 1109-1125.
- Khattab, N. M.** (1997), 'Novel design of an agricultural dryer', *Energy Sources*, 19, 417-426.
- King, C. J.**, (1977), 'Heat and mass transfer fundamentals applied to food engineering', *Journal of Food Proc. Eng.*, 1, 3-14.
- Kiranoudis, C. T., Maroulis, Z. B. and Marinos-kouris, D.** (1992). "Drying kinetics of onion and green pepper", *Drying Technology*, 10(4), 995-1011.
- Krokida, M. K., Kiranoudis, C.T., Maroulis, Z. B., and Marinos-Kouris, D.**, (2000), 'Drying related properties of apple', *Drying Technology*, 18 (6), 1251-1267.
- Lu, L., Tang, J. and Liang, L.** (1998), 'Moisture distribution in spherical foods in microwave drying', *Drying Technology*, 16(3-5), 503-524.
- Luikov, A. V.** (1973), 'Systems of differential equation of heat and mass transfer in capillary porous', *Int. Journal of Heat and Mass Transfer*, 18, 1-14.
- McLaughlin, C.P. and Magee, T.R.A.** (1999). 'The effects of air temperature, sphere diameter and puffing with CO<sub>2</sub> on the drying of potato spheres', *Drying Technology* 17, 119-136.
- McMinn, W. A. M. and Magee, T. R. A.** (1996). 'Air drying kinetics of potato cylinders', *Drying Technology*, 14(9), 2025-2040.
- Mujumdar, A.S.**, (1987), '*Handbook of Industrial Drying*', Marcel Dekker, New York.
- Mujumdar, A. S.**, (1999), 'Energy and environment aspects in industrial drying', *The International Symposium on Energy & Environment*, Yokohama and Hakone, Japan.

- Patankar, S. V.**, (1980), 'Numerical Heat Transfer and Fluid Flow', hemisphere publishing corporation,
- Perera, C. O., and Shafiur Rahman, M.** (1997). 'Heat pump dehumidifier drying of food', *Trends in Food Science & Technology*, vol. 8, 75-78.
- Piotrowski, D. and Lenart, A.** (1998). 'The influence of constant and variable conditions on the drying kinetics of apples', *Drying Technology*, 16 (3-5), 761-768.
- Rizvi, S. S. H.**, (1986), 'Thermodynamic properties of foods in dehydration, 133-214, In: Rao, M. A. and Rizvi, S. S. H., (ed). '*Engineering properties of foods*' Marcel Dekker Inc., New York.
- Ruiz-Cabrera, M. A., Salgado-Cervantes, M. A., Waliszewski-Kubiak, K. N. and y Garcia-Alvarado, M. A.** (1997). 'The effect of path diffusion on the effective moisture diffusivity in carrot slabs', *Drying Technology*, 15(1), 169-181.
- Sawhney, R.L., Pangavhane, D.R., & Sarsavadia, P.N.**, (1999), 'Drying Kinetics of single layer thompson seedless grapes under heated ambient air conditions', *Drying Technology*, Vol. 17, no. 1&2, 215-236.
- Sawhney, R.L., Sarsavadia, P.N., Pangavhane, D.R., & Singh, S.P.**, (1999), 'Determination of drying constants and their dependence on drying air parameters for thin layer onion drying', *Drying Technology*, Vol. 17, no. 1&2, pp. 299-315
- Schirmer, P., Janjai, S., Esper, A., Smitabhindu and Muhlbauer, W.**, (1996) 'Experimental investigation of the performance of the solar tunnel dryer for drying bananas', *Renewable Energy*, Vol. 7, No. 2, pp. 119-129.
- Simal, S., Rosello, C., Berna, A., and Mulet, A.**, (1998), 'Drying of shrinking cylinder-shaped bodies', *Journal of Food Engineering*, 37, 423-435

**Smith, G. D.**, '*Numerical Solutions of Partial Differential Equations*', third edition, clarendon press, oxford.

**Tiris, C., Ozbalta, N., Tiris, M. and Dincer, I.** (1995). 'Experimental testing of a new solar dryer', *International Journal of Energy Research*, Vol. 18, 483-490.

**Tsami, E., and Katsioti, M.**, (2000), 'Drying kinetics for some fruits: Predicting of porosity and color during drying', *Drying Technology*, 18(7), 559-1581.

**Vagenas, G. K. and Marinos-Kouris, D.**, (1991), 'Drying kinetics of apricots', *Drying Technology*, 9 (3), 735-752.

**Zhao, Y. S., and Poulsenk, P.**, (1988), 'Diffusion in potato drying', *Journal of Food Eng.* 7 (4), 249-262.

## **Vita**

- **Mohammed Mujtaba Hussain**
- **Born in Hyderabad, Andhra Pradesh, India on August 8, 1977**
- **Received Bachelor's degree in Mechanical Engineering with Specialization in Production Engineering from Osmania University, Hyderabad, India in July, 1998.**
- **Completed Master's degree requirements at King Fahd University of Petroleum and Minerals, Dhahran, Saudi Arabia in May, 2001.**
- **Research areas include Heat & Mass transfer, Computational fluid dynamics, Refrigeration and air-conditioning.**